
Louisiana Transportation Research Center

Final Report 621

Assessment of Environmental, Seasonal, and Regional Variations in Pavement Base and Subgrade Properties

by

Kevin Gaspard
Zhongjie Zhang
Gavin Gautreau
Murad Abufarsakh
Mark Martinez

LTRC



4101 Gourrier Avenue | Baton Rouge, Louisiana 70808
(225) 767-9131 | (225) 767-9108 fax | www.ltrc.lsu.edu

TECHNICAL REPORT STANDARD PAGE

1. Report No. FHWA/LA.18/621		2. Government Accession No.	3. Recipient's Catalog No.
4. Title and Subtitle Assessment of Environmental, Seasonal, and Regional Variations in Pavement Base and Subgrade Properties		5. Report Date January 2020	
		6. Performing Organization Code LTRC Project Number: 12-2P SIO Number: 30000425	
7. Author(s) Kevin Gaspard, Zhongjie Zhang, Gavin Gautreau, Murad Abufarsakh, Claudia Zapata, and Mark Martinez		8. Performing Organization Report No. 12-2P	
9. Performing Organization Name and Address Department of Civil and Environmental Engineering Louisiana State University Baton Rouge, LA 70803		10. Work Unit No.	
		11. Contract or Grant No.	
12. Sponsoring Agency Name and Address Louisiana Department of Transportation and Development P.O. Box 94245 Baton Rouge, LA 70804-9245		13. Type of Report and Period Covered [Final Report] [December 2015 to December 2018]	
		14. Sponsoring Agency Code	
15. Supplementary Notes Conducted in Cooperation with the U.S. Department of Transportation, Federal Highway Administration			
16. Abstract LTRC has conducted an extensive research project to determine the seasonal variation in the subgrade M_R from 14 sites throughout Louisiana. The study (1) conducted FWD testing on the 14 sites seasonal for a period of at least 3 years; (2) developed an online web application to determine the soil types throughout Louisiana based upon NCHRP soil units; (3) obtained Shelby tube samples from seven of the 14 sites and conducted soil classifications on the samples; and (4) conducted an assessment of the 14 sites with PavementME using soil data from both Shelby tube samples and NCHRP soil units. FWD tests were grouped together based upon the predominate soil type at each site: A-4, A-6, and A-7. The corresponding equations for the A-4, A-6, and A-7 soil types had r^2 values of 0.2067, 0.1243, and 0.0709, respectively Software was developed to interface with NCHRP soil units for Louisiana with DOTD databases, allowing the user to determine the soil type for any DOTD roadway. Comparisons were made between samples taken from Shelby tubes and the NCHRP soil unit database. In the first and second soil strata, 43 percent of sites had similar soil types while the third strata 67 percent similar soil types. The overall average of the similar soil types in the strata were 50 percent. Considering the high variability in soil types that can be found in anyone location, the soil types from the NCHRP soil unit samples may be considered to provide a reasonable estimate of the soils present for the purpose of pavement design. PavementME was used to conduct an analysis of the seasonal changes in the subgrade M_R from the 14 sites using soils data from both the NCHRP soil units, Shelby tube samples and FWD tests. Based upon the results, 43 percent of the PavementME results where the soil types and depths were taken from the NCHRP soil units and Shelby tube data were similar to the results from FWD testing. Comparisons of the subgrade M_R values produced by PavementME for the Shelby tube and NCHRP soil unit data indicated that they were similar 86 percent of the time. Therefore, based upon the comparisons in this research, it is reasonable to use NCHRP soil unit data as a substitute for Shelby tube samples when Shelby tube samples are not available.			
17. Key Words		18. Distribution Statement Unrestricted. This document is available through the National Technical Information Service, Springfield, VA 21161.	
19. Security Classif. (of this report)	20. Security Classif. (of this page)	21. No. of Pages	22. Price

Project Review Committee

Each research project will have an advisory committee appointed by the LTRC Director. The Project Review Committee is responsible for assisting the LTRC Administrator or Manager in the development of acceptable research problem statements, requests for proposals, review of research proposals, oversight of approved research projects, and implementation of findings.

LTRC appreciates the dedication of the following Project Review Committee Members in guiding this research study to fruition.

LTRC Administrator

Zhongjie Zhang

Pavement and Geotechnical Research Administrator

Members

Jonathan Lachney

Matthew Ziecker

Ken Free

Mark Chenevert

Jeff Lambert

Hallie Dozier

Scott Nelson

Directorate Implementation Sponsor

Christopher P. Knotts, P.E.

DOTD Chief Engineer

Assessment of Environmental, Seasonal, and Regional Variations in Pavement Base and Subgrade Properties

by

Kevin Gaspard, Zhongjie Zhang, Gavin Gautreau, Murad Abufarsakh, and Mark Martinez

Louisiana Transportation Research Center

4101 Gourrier Ave.

Baton Rouge, LA 70808

LTRC Project No. 12-2P

SIO No. 30000425

conducted for

Louisiana Department of Transportation and Development

Louisiana Transportation Research Center

The contents of this report reflect the views of the author/principal investigator who is responsible for the facts and the accuracy of the data presented herein. The contents do not necessarily reflect the views or policies of the Louisiana Department of Transportation and Development the Federal Highway Administration or the Louisiana Transportation Research Center. This report does not constitute a standard, specification, or regulation.

January 2020

ABSTRACT

LTRC has conducted an extensive research project to determine the seasonal variation in the subgrade M_R from 14 sites throughout Louisiana. The study (1) conducted FWD testing on the 14 sites seasonal for a period of at least 3 years; (2) developed an online web application to determine the soil types throughout Louisiana based upon NCHRP soil units; (3) obtained Shelby tube samples from seven of the 14 sites and conducted soil classifications on the samples; and (4) conducted an assessment of the 14 sites with PavementME using soil data from both Shelby tube samples and NCHRP soil units.

FWD tests were grouped together based upon the predominate soil type at each site: A-4, A-6, and A-7. The corresponding equations for the A-4, A-6, and A-7 soil types had r^2 values of 0.2067, 0.1243, and 0.0709, respectively

Software was developed to interface with NCHRP soil units for Louisiana with DOTD databases, allowing the user to determine the soil type for any DOTD roadway. Comparisons were made between samples taken from Shelby tubes and the NCHRP soil unit database. In the first and second soil strata, 43 percent of sites had similar soil types while the third strata 67 percent similar soil types. The overall average of the similar soil types in the strata were 50 percent. Considering the high variability in soil types that can be found in anyone location, the soil types from the NCHRP soil unit samples may be considered to provide a reasonable estimate of the soils present for the purpose of pavement design.

PavementME was used to conduct an analysis of the seasonal changes in the subgrade M_R from the 14 sites using soils data from both the NCHRP soil units, Shelby tube samples and FWD tests. Based upon the results, 43 percent of the PavementME results where the soil types and depths were taken from the NCHRP soil units and Shelby tube data were similar to the results from FWD testing. Comparisons of the subgrade M_R values produced by PavementME for the Shelby tube and NCHRP soil unit data indicated that they were similar 86 percent of the time. Therefore, based upon the comparisons in this research, it is reasonable to use NCHRP soil unit data as a substitute for Shelby tube samples when Shelby tube samples are not available.

ACKNOWLEDGMENTS

Significant contributions to this study were performed by Mitch Terrell, Terrell Gorham, Benjamin Key, Renee Crosse, Preston Causey, and Hend Alyousey.

IMPLEMENTATION STATEMENT

Based upon testing with the FWD, Shelby tube sampling, NCHRP soil unit data, subgrade resilient modulus testing, and PavementME assessments, the soil data obtained from NCHRP soil units can generally be used whenever soil samples are unavailable from Shelby tube sampling or subgrade soil surveys. The equations developed from FWD testing representing seasonal changes in the subgrade resilient modulus may be used for soils with A-4 or A-6 classifications.

TABLE OF CONTENTS

ABSTRACT.....	III
ACKNOWLEDGMENTS	V
IMPLEMENTATION STATEMENT	VII
TABLE OF CONTENTS.....	IX
LIST OF TABLES	XI
LIST OF FIGURES	XIII
INTRODUCTION	1
Literature Review.....	2
Background on the Environmental Effects Incorporation into the Pavement Design	2
EICM for the MEPDG.....	5
Inputs Required to Model Thermal and Moisture Conditions	6
General Information.....	7
Weather Information.....	7
Groundwater Table Depth.....	8
Pavement Structure – Layer Thickness.....	8
AC and PCC Material Properties	8
Unbound Material Properties	9
Index Properties	9
Mass-Volume Relationships	10
Estimation of G_s	10
Estimation of $\gamma_{d\ max}$ and w_{opt}	11
Saturated Hydraulic Conductivity.....	14
Soil Water Characteristic Curve Parameters.....	15
Determination of Moisture Conditions throughout Pavement Systems	18
Soil-atmosphere Interaction Predominance over Groundwater Table Depth .	19
Fluid Flow Model	20
Environmental Effects on Resilient Modulus of Unbound Materials.....	20
Resilient Modulus as Function of Soil Moisture	21
Resilient Moduli for Frozen/Thawed Unbound Materials.....	22
Computation of Environmental Adjustment Factor, F_{env}	24
Adjustment Factors at Node Level	25
Composite Adjustment Factors, F_{env} , for Structural Layers	26
Determination of the Temperature throughout Pavement Systems	28
Heat Flux Boundary Conditions for CMS Model.....	29

Recent Efforts Aimed at Enhancing the EICM.....	32
National Database of SWCC Parameters and Selected Soil Index Properties	32
Integrating the National Database of Subgrade Properties with the MEPDG	36
Development of New Models to Estimate the SWCC Parameters for Non- Plastic Materials.....	37
Enhancement of Resilient Modulus Prediction as Function of Soil Moisture	40
Matric Suction as Fundamental Variable for the Prediction of Resilient Modulus Changes.....	43
Additional Considerations for Future Revisions of the EICM	46
Climatic Data	46
Limitations in Temperature Profile Predictions for Bound Materials	47
Effect of Soil Density on EICM Predictions.....	47
OBJECTIVES	49
SCOPE	51
METHODOLOGY	53
Research Test Site Selection.....	53
Soil Type Identification	54
Resilient Modulus Testing in the Laboratory	56
FWD Tests	56
PavementME Site Assessment.....	57
DISCUSSION OF RESULTS	59
Soil Type Identification	59
Resilient Modulus Laboratory Testing	63
Seasonal Subgrade M_R Results from FWD Testing and PavementME	65
Summary of Subgrade M_R Results from FWD Testing and PavementME Analyses.....	74
Summary of FWD Test Results when Grouped by Soil Type.....	76
Comparison of FWD Subgrade M_R Data to NCHRP Subgrade M_R Data	77
CONCLUSIONS.....	79
RECOMMENDATIONS	81
ACRONYMS, ABBREVIATIONS, AND SYMBOLS	82
REFERENCES	85
APPENDIX A.....	91
APPENDIX B.....	95

LIST OF TABLES

Table 1 AC and PCC materials inputs required for EICM calculations	9
Table 2 Specific gravity of solids of selected soils.....	10
Table 3 Values of a, b, km for coarse-grained and fine-grained materials	22
Table 4 Recommended values of RF for coarse grain materials (P200 <50%).....	23
Table 5 Recommended values of RF for materials (P200>50%)	23
Table 6 Locations of the 14 research test sites	54
Table 7 Summary of soil type and soil strata comparisons	63
Table 8 Summary of comparisons between FWD and PavementME data sets.....	75
Table 9 Summary of comparisons for subgrade M _R from PavementME analyses.....	75
Table 10 Groups of sites per soil type	76
Table 11 FWD subgrade M _R versus NCHRP subgrade M _R	78
Table 12 Shelby tube soil data for LA 1; Site 1-1	91
Table 13 Shelby tube soil data for US 171; Site 1-2.....	91
Table 14 Shelby tube soil data for LA 2, Site 2-4	92
Table 15 Shelby tube soil data for US 165; Site 2-5.....	92
Table 16 Shelby tube soil data for US 84; Site 3-8.....	93
Table 17 Shelby tube soil sample from LA 13; Site 4-12.....	93
Table 18 Shelby tube soil data for US 61; Site 4-13.....	94
Table 19 NCHRP soil unit data for LA 1; Site 1-1	95
Table 20 NCHRP soil unit data for US 171; Site 1-2	96
Table 21 NCHRP soil unit data for US 171; Site 1-3.....	97
Table 22 NCHRP soil unit data for LA 2; Site 2-4.....	98
Table 23 NCHRP soil unit data for US 165; Site 2-5	99
Table 24 NCHRP soil unit data for LA 34; Site 2-6.....	100
Table 25 NCHRP soil unit data for US 65; Site 3-7	101
Table 26 NCHRP soil unit data for US 84; Site 3-8.....	102
Table 27 NCHRP soil unit data for US 71; Site 3-9.....	103
Table 28 NCHRP soil unit data for LA 1; Site 3-10.....	104
Table 29 NCHRP soil unit data for US 171; Site 4-11	105
Table 30 NCHRP soil unit data for LA 13; Site 4-12.....	106
Table 31 NCHRP soil unit data for US 61; Site 4-13	107
Table 32 NCHRP soil unit data for LA 21; Site 4-14.....	108

LIST OF FIGURES

Figure 1 Model predicted moisture contents before 1999 – ICM 2.1 – Level 3 data shown ...	4
Figure 2 Predicted moisture contents after changes to the model by ASU in 1999 – ICM version 2.6. - Level 3 data shown	4
Figure 3 Predicted moisture contents after subsequent changes to the model by ASU in 2006 – EICM in MEPDG version 0.91 – Level 1 data shown	5
Figure 4 Effect of moisture changes on the resilient modulus.....	22
Figure 5 State of Louisiana map with region grid (32).....	34
Figure 6 Region 14 for Louisiana (32)	35
Figure 7 Example of a printable report displayed in the excel interface (32).....	36
Figure 8 Searching tool main web portal (33)	38
Figure 9 Measured versus predicted degree of saturation for granular soils (34)	40
Figure 10 Data collected in the study conducted by Cary and Zapata (36).....	41
Figure 11 Variation of F_u as a function of $(S-S_{opt})$ and wPI (36).....	43
Figure 12 Using the EICM model to estimate the adjustment factor F_u (equation 35)	45
Figure 13 Using the matric suction dependent model (equation 64)	46
Figure 14 Geologic map of Louisiana with locations of 14 sites	53
Figure 15 Soil type and strata for LA 1 – Site 1-1	55
Figure 16 M_R/M_{Ropt} versus $S-S_{opt}$ example.....	56
Figure 17 Subgrade M_R seasonal variation results	57
Figure 18 Soil type and strata for US 171 – Site 1-2.....	59
Figure 19 Soil type and strata for Site 2-4; LA 2.....	60
Figure 20 Soil type and strata for Site 2-5; US 165.....	60
Figure 21 Soil type and strata for Site 3-8; US 84.....	61
Figure 22 Soil type and strata for Site 4-12; LA 13.....	61
Figure 23 Soil type and strata for Site 4-13; US 61	62
Figure 24 MEPDG EICM model with test points.....	63
Figure 25 In place moisture content – Opt. moisture content versus in place dry density – maximum dry density relationship.....	64
Figure 26 MEPDG EICM curve with refined data set.....	65
Figure 27 Seasonal variation in subgrade M_R from FWD and PavementME for Site 1-1	66
Figure 28 Seasonal variation in subgrade M_R from FWD and PavementME for Site 1-2	66
Figure 29 Seasonal variation in subgrade M_R from FWD and PavementME for Site 1-3	67
Figure 30 Seasonal variation in subgrade M_R from FWD and PavementME for Site 2-4	68
Figure 31 Seasonal variation in subgrade M_R from FWD and PavementME for Site 2-6	69
Figure 32 Seasonal variation in subgrade M_R from FWD and PavementMR for Site 3-7	69

Figure 33	Seasonal variation in subgrade M_R from FWD and PavementME for Site 3-8	70
Figure 34	Seasonal variation in subgrade M_R from FWD and PavementME for Site 3-9	71
Figure 35	Seasonal variation in subgrade M_R from FWD and PavementME for Site 3-10 ..	71
Figure 36	Seasonal variation in subgrade M_R from FWD and PavementME for Site 4-11 ..	72
Figure 37	Seasonal variation in subgrade M_R from FWD and PavementME for Site 4-12 ..	73
Figure 38	Seasonal variation in subgrade M_R from FWD and PavementME for Site 4-13 ..	73
Figure 39	Seasonal variation in subgrade M_R from FWD and PavementME for Site 4-14 ..	74
Figure 40	Subgrade M_R values for A-4 soils	76
Figure 41	Subgrade M_R values for A-6 soils	77
Figure 42	Subgrade M_R values for A-7 soils	77

INTRODUCTION

In the last decades, it has been widely recognized by the pavement engineering community that environmental conditions have a significant effect on the performance of both flexible and rigid pavements. External factors such as precipitation, temperature, wind speed, solar radiation, relative humidity, and depth to water table are environment parameters that impact pavement performance [1-3]. On the other hand, internal factors such as the susceptibility of the pavement materials to moisture and temperature changes, freeze-thaw damage, drainage of paving layers, and infiltration potential of the pavement, define the extent to which the pavement will react to the applied external environmental conditions [2-3].

In a pavement structure, moisture and temperature are the two environmentally driven variables that can significantly affect the pavement layer and subgrade properties and, hence, its load carrying capacity and stiffness [3]. The environmental conditions have a direct effect on several pavement distresses. Such effects are more detrimental in some distresses than in others. For the case of flexible pavements; the environmental conditions affect fatigue and thermal cracking, permanent deformations and the smoothness of pavement surface. In rigid pavements, distresses such as faulting and fatigue cracking, curling and warping, shrinkage, punch-out, and roughness are also affected by moisture and temperature gradients. Mechanisms of failure such as the initial crack width are also directly related to these factors.

Some of the effects of the environment on pavement materials include:

- Temperature and moisture gradients particularly in the top portland cement concrete (PCC) layer can significantly affect stresses and deflections and consequently pavement damage and distresses.
- At freezing temperatures, the resilient modulus of the unbound materials can rise to values 20 to 120 times higher than the value of the modulus before freezing.
- All other conditions being equal, the higher the moisture content the lower the modulus of unbound materials; however, moisture has two separate effects: First, it can affect the state of stress, through suction or pore water pressure. Second, it can affect the structure of the soil through destruction of the cementation between soil particles and aging effects.
- Excessive moisture can lead to stripping in asphalt mixtures or can have long-term effects on the structural integrity of cement bound materials.
- Freeze-thaw effects are experienced in the underlying layers but eventually lead to distresses in the pavement surface.

All the distresses considered in the American Association of State Highway Transportation Official's (AASHTO) Mechanistic Empirical Pavement Design Guide (MEPDG) are affected by the environmental factors to some degree. Therefore, diurnal and seasonal fluctuations in the moisture and temperature profiles in the pavement structure as a result of changes in ground water table, precipitation /infiltration, freeze-thaw cycles, and other external factors are modeled in a very comprehensive manner by a climatic model called the Enhanced Integrated Climatic Model (EICM). Note: The MEPDG has changed names several times since its inception and is now called PavementME; however, MEPDG will continue to be used in the literature review portion of this report.

Literature Review

Background on the Environmental Effects Incorporation into the Pavement Design

The Enhanced Integrated Climatic Model (EICM) is basically a one-dimensional coupled heat and moisture flow program capable of simulating changes in temperature and moisture of pavement and subgrade materials in conjunction with climatic conditions over several years of operation.

The roots of the EICM can be traced back to the early 1970s, when a computer program called the Climatic Materials Structures (CMS) model was developed at the University of Illinois [2]. The CMS incorporates climatic effects into the analysis and design of multilayered flexible pavement structures and estimates realistic temperature and moisture profiles as well as material strength properties.

The original version of the EICM, referred to as the Integrated Climatic Model (ICM), was developed for the Federal Highway Administration (FHWA) at Texas A&M University, Texas Transportation Institute in 1989 [3]. This original version consists of three major models coupled to generate an integrated environmental predictive methodology:

- The Climatic-Materials-Structural Model (CMS Model) developed at the University of Illinois [3].
- The Infiltration and Drainage Model (ID Model) developed at Texas A&M University [3].
- The Cold Regions Research and Engineering Laboratory Frost Heave and Thaw Settlement Model (CRREL Model) developed at the United States Army Cold Regions Research and Engineering Laboratory (CRREL) [4].

The original version of the ICM was then modified and released in 1997 as ICM version 2.0 [5]. The Integrated Model was originally used for heat flow applications and temperature predictions. Although reasonably good validation studies supported the models, less attention was initially given to the moisture content predictions.

Additional modifications in the model were performed between 1999 and 2006 at Arizona State University (ASU) as part of the MEPDG development {National Cooperative Highway Research Program (NCHRP) 1-37A project} to improve the moisture prediction capability of ICM version 2.1, leading to the version referred to as EICM [6]. In developing the EICM, data from the Long Term Pavement Performance (LTPP) Seasonal Monitoring Program (SMP) test sections were used. Data was also extracted from MnRoad, WesTrack, and the U.S. Geological Survey databases [6-9]. The EICM was subjected to further evaluation and calibration under the NCHRP 9-23 Project titled Environmental Effects in Pavement Mix and Structural Design Systems [10, 11], with data collected from 30 sites visited and cored throughout the continental U.S. The changes recommended under the NCHRP 9-23 project were included in the MEPDG version 0.8 released in November 2005.

The next effort to improve the models was taken over by NCHRP 1-40D project entitled Technical Assistance Project to NCHRP in the M-E Pavement Analysis System Developed under NCHRP 1-37A [12]. Based on sensitivity studies of the models, deficiencies and limitations of the program, and continuous feedback received from the project technical panel and users of the beta version of the program, two subsequent versions of the MEPDG were generated: version 0.9 released in June 2006; and version 0.91 released in September 2006. The improvement in the prediction of moisture content after the model changes done in 1999 and subsequent changes in 2006 can be judged by the information presented in Figures 1 to 3.

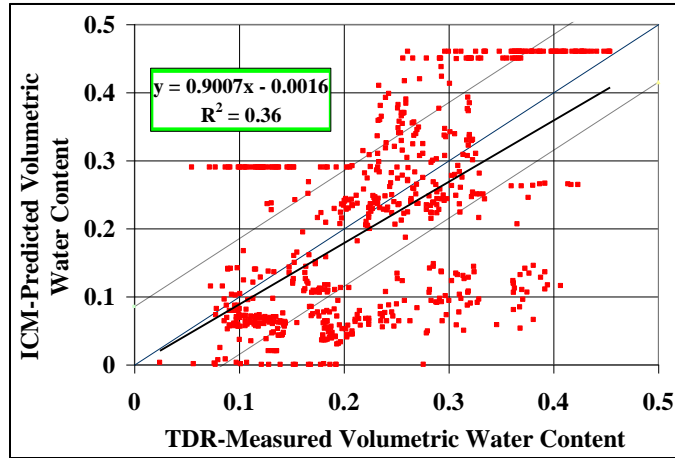


Figure 1

Model predicted moisture contents before 1999 – ICM 2.1 – Level 3 data shown

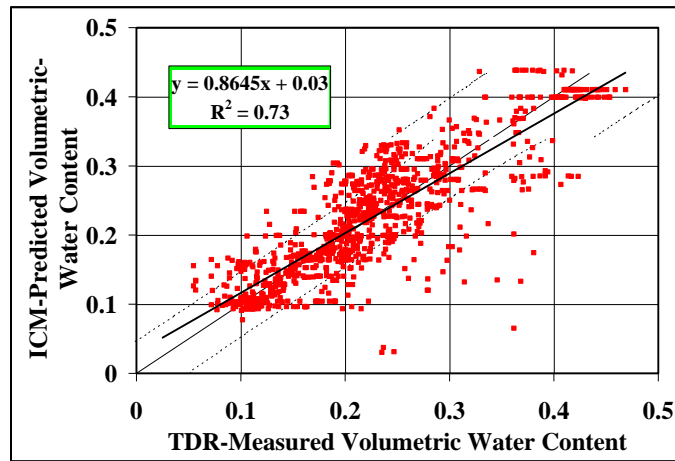


Figure 2

Predicted moisture contents after changes to the model by ASU in 1999 – ICM version 2.6. - Level 3 data shown

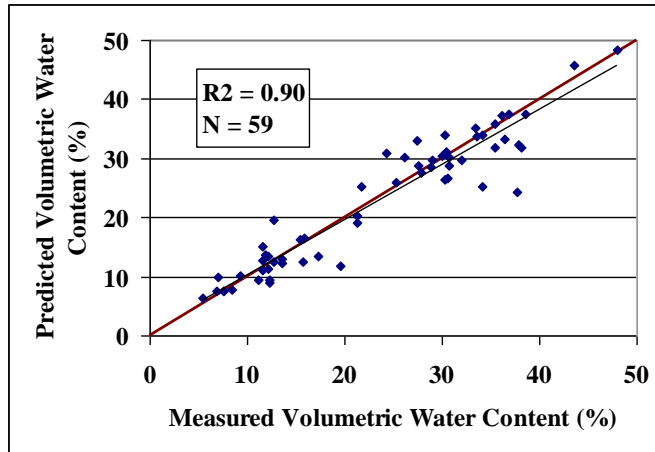


Figure 3

Predicted moisture contents after subsequent changes to the model by ASU in 2006 – EICM in MEPDG version 0.91 – Level 1 data shown

EICM for the MEPDG

The EICM software has been made an integral part of the MEPDG procedure. The user inputs to the EICM are entered through interfaces provided as part of the MEPDG software and EICM processes these inputs and feeds the processed outputs to the three major components of the Guide: materials, structural responses, and performance prediction. The EICM model can be applied to either flexible asphalt concrete (AC) or rigid Portland cement concrete (PCC) pavements.

For the case of flexible asphalt concrete pavements, the EICM records the user supplied resilient modulus (M_R) of all unbound layer materials at an initial or reference condition. Generally, this will be at or near the optimum water content (M_{Ropt}). Subsequently, the EICM computes and predicts the following information throughout the entire pavement profile:

- Evaluates the expected changes in moisture content, from the initial or reference condition, as the subgrade and unbound materials reach equilibrium moisture condition. Also evaluates the seasonal changes in moisture contents.
- Evaluates the effect of changes in soil moisture content with respect to the reference condition on the user inputted M_R .
- Estimates a set of adjustment factors for unbound material layers that account for the effects of moisture content changes, freezing, thawing, and recovery from thawing. This factor, denoted F_{env} , varies with position within the pavement structure and with time throughout the analysis period.

- Makes use of time-varying M_R values in the computation of critical pavement response parameters and damage at various points within the pavement system.
- Evaluates changes in temperature as a function of time for all asphalt bound layers.

For rigid pavements, the following additional information is generated by the EICM:

- Temperature profiles in the PCC and underlying layers used for thermal gradients in PCC; and joint and crack openings and closings.
- Effective linear temperature gradient used to model slab curvature and thermal stresses.
- Probability distribution of effective linear temperature gradients.
- Freezing index and the number of freeze-thaw cycles for the selected location.
- Mean monthly relative humidity values used in the estimation of moisture warping of the PCC slabs.

After the environmental effects are computed by EICM, another module within the MEPDG adds the effect of dynamic loading due to external forces, such as traffic, to the changes in the material properties. Finally, the MEPDG makes use of transfer functions to predict pavement performance, through empirically calibrated models.

Inputs Required to Model Thermal and Moisture Conditions

The approach for selecting or determining material inputs in the MEPDG is hierarchical in nature. This approach is based on the philosophy that the level of engineering effort exerted in the pavement design process should be consistent with the relative importance, size, and cost of the design project. Level 1 is the most current implementable procedure available, normally involving comprehensive laboratory or field tests. Note: Level 1 inputs are no longer allowed into PavementME, but will continue to be discussed in this report since it was part of the original modeling schemata. In contrast, Level 3 requires the designer to estimate the most appropriate design input value of the material property based on experience with little or no testing. Inputs at Level 2 are estimated through correlations with other material properties measured in the laboratory or in the field.

The inputs required by the climatic model fall under the following broad categories: General information; weather-related information; ground water related information; pavement structure and material properties. The specific inputs required under each of the mentioned categories and the recommended procedures to obtain them at the various hierarchical input levels are summarized below. The data presented covers both new and rehabilitation design.

General Information

In order to initialize the climatic model, the following information is required: base/subgrade construction completion date for new pavement design; existing pavement construction date for rehabilitation design; pavement construction date; traffic opening date; the type of design (new or rehabilitation) and type of pavement (AC or PCC).

Weather Information

The MEPDG damage accumulation approach requires five weather-related parameters on an hourly basis over the entire design life for the project being designed: air temperature, precipitation, wind speed, percentage sunshine, and relative humidity.

The air temperature is required by the heat balance equation in the EICM for calculations of long wave radiation and convective heat transfer. It is also used to define the frozen/thawing periods within the analysis time frame, to determine the number of freeze-thaw cycles; and to determine the Thornthwaite Moisture Index (TMI), which is a boundary condition essential in the computation of the soil suction and moisture content estimations of unbound materials. Details regarding the temperature model are briefly discussed in this document but can also be found elsewhere [13].

Precipitation is needed to compute infiltration for rehabilitated pavements and aging processes, while wind speed is required in the computations of the convection heat transfer coefficient at the pavement surface. The percentage sunshine is needed for the calculations of heat balance at the surface of the pavement and particularly the net long-wave radiation. Last, the relative humidity is used in computing the drying shrinkage of Jointed Plain Concrete Pavements (JPCP) and Continuously Reinforced Concrete Pavement (CRCP) and also in determining the crack spacing and initial crack width in CRCP.

The weather-related information is primarily obtained from weather stations located near the project site. The software accompanying the MEPDG has an available database from nearly 800 weather stations throughout the United States. Even though the MEPDG requires at least 24 months of actual weather station data for computational purposes, several of the major weather stations have approximately 10 years of climatic data at each time step (e.g., 1 hour) needed by the EICM. The climatic database can be tapped into by simply specifying the latitude, longitude, and elevation of the project site. Once the coordinates and elevation are specified, the MEPDG software will highlight the six closest weather stations to the site from which the user may select any number of stations deemed to be most representative of the

local climatic conditions. If needed, interpolation of climatic data from these stations is possible and the interpolated data is made available for storage as a virtual weather station.

Groundwater Table Depth

If shallow groundwater table is present in the site, this parameter becomes fundamental in the determination of the equilibrium suction that governs the moisture content long term condition. The groundwater table depth is intended to be either the best estimate of the annual average depth or the seasonal average depth. At input Level 1, it could be determined from profile characterization borings prior to design. At input Level 3, an estimate of the annual average value or the seasonal averages can be provided. Potential sources to obtain groundwater table depth estimates are the Long Term Pavement Performance (LTPP) database, the county soil reports produced by the National Resources Conservation Service and the web interface of the U.S. Geological Survey – National Water Information System (NWIS) [14, 15].

Pavement Structure – Layer Thickness

The layer thickness of each material in the pavement structure should correspond to layers that are more or less homogeneous. EICM internally subdivides these layers for more accurate calculations of moisture and temperature profiles.

AC and PCC Material Properties

Several bound material properties are required for the design of flexible and rigid pavements, and AC or PCC overlays. Among these properties are those that control the heat flow through the pavement system. These properties are the surface shortwave absorptivity, the thermal conductivity (K) and the heat or thermal capacity (Q) for both AC and PCC materials. The coefficient of thermal expansion is also needed for PCC materials. Surface long-wave absorptivity is not required, as the model makes use of the percent sunshine to calculate cloud cover, which is tightly related to the albedo.

The surface short wave absorptivity directly correlates with the amount of available solar energy that is absorbed by the pavement surface. Lighter and more reflective surfaces tend to have lower short wave absorptivity and vice versa. At Level 1, it is recommended that this parameter be estimated through laboratory testing. At Level 3, default values are given for various pavement materials:

- Weathered asphalt (gray): 0.80 – 0.90

- Fresh asphalt (black): 0.90 – 0.98
- Aged PCC layer: 0.70 – 0.90

Thermal conductivity (K) is the quantity of heat that flows normally across a surface of unit area per unit of time and per unit of temperature gradient; while the heat or thermal capacity is the actual amount of heat energy Q necessary to change the temperature of a unit mass by one degree. Direct measurements of both parameters are recommended under input Level 1 (ASTM E1952 and ASTM D2766, respectively). The coefficient of thermal expansion is the change in length per unit length of the material for a unit change in temperature.

For Level 3, it is recommended to use design values based upon agency historical data or from typical values shown in Table 1. Note: Since many of the parameters used in the soil mechanic models and equations used in this report contains variables in SI units, these units will be used throughout the literature review section.

Table 1
AC and PCC materials inputs required for EICM calculations

Material property	AC materials	PCC materials
Thermal conductivity, K	0.76 – 1.41 (W)(m ⁻¹)(K ⁻¹)	1.7-2.59 (W)(m ⁻¹)(K ⁻¹)
Heat Capacity, Q	921 – 1,674 (J)(kg ⁻¹)(K ⁻¹)	837 - 1172 (J)(kg ⁻¹)(K ⁻¹)

Legend: W=watts; m=meter; K= degree Kelvin; J=joule; kg=kilogram

Unbound Material Properties

The following sections describe the input parameters needed for compacted and natural unbound materials. The correlations used by the EICM to estimate mass-volume properties and saturated hydraulic conductivity, in the case one of these parameters is not provided by the user, are also presented.

Index Properties

Direct measurements of soil index properties for compacted and natural materials are required at all levels of analysis. The index properties refer to the grain-size distribution and the Atterberg limits: Liquid Limit (LL) and Plasticity Index (PI). The grain-size distribution should be obtained in accordance with AASHTO T 27; while the Atterberg limits should be obtained in accordance with AASHTO T 90.

Mass-Volume Relationships

The parameters needed in this category are the maximum dry density ($\gamma_{d\ max}$), the optimum gravimetric moisture content (w_{opt}), and the specific gravity of solids (G_s) of the compacted unbound or natural material in question. From these three inputs, all other mass-volume parameters can be computed. At Levels 1 and 2, it is required that the $\gamma_{d\ max}$, w_{opt} , and G_s be carefully measured in the laboratory in accordance with standard protocols for each unbound layer: Compaction procedure AASHTO T180 for base layers, compaction procedure AASHTO T99 for other layers; and AASHTO T100 procedure for G_s determination. If the user chooses not to measure $\gamma_{d\ max}$, w_{opt} , and G_s , then it is suggested that Level 3 inputs be adopted. At input Level 3, the user enters the gradation and the PI . From these parameters, the EICM will compute $\gamma_{d\ max}$, degree of saturation at optimum condition (S_{opt}), and w_{opt} using the correlations presented later.

Estimation of G_s

The G_s of materials is controlled by the mineral composition of the aggregates. Unless hydrometer analysis is performed to measure the exact percentage of clay content in the soil, an estimate of G_s based on simple soil properties is difficult to justify. It was therefore recommended to use G_s values provided by the user at Level 3 analysis, based on their experience with particular soils and minerals found in their own regions.

Values of specific gravity of solids for a selected group of soils are given in Table 2 [16-17].

Table 2
Specific gravity of solids of selected soils

Soil	G _s
Sand	2.65 – 2.67
Silty sand	2.67 – 2.70
Inorganic clay	2.70 – 2.80
Soil with mica or iron	2.75 – 3.00
Organic soil	1.0 - 2.60
Volcanic ash, Kansas	2.32
Kaolinite	2.61
Alluvial montmorillonitic clay	2.65
Platte River sand	2.65
Iowa loess soil	2.70
Micaceous silt, Alaska	2.76
Oxisol (Latosol), Hawaii	3.00

Estimation of $\gamma_{d \max}$ and w_{opt}

These parameters should be input at Levels 1 and 2. EICM then computes the volumetric water content (θ_{opt}), the degree of saturation at optimum condition (S_{opt}) and the porosity or saturated volumetric water content ($\theta_{sat.}$) as follows:

$$\theta_{opt} = \frac{w_{opt} \gamma_{d \max}}{\gamma_{water}} \quad (1)$$

$$S_{opt} = \frac{\theta_{opt}}{1 - \frac{\gamma_{d \max}}{\gamma_{water} G_s}} \quad (2)$$

and,

$$\theta_{sat} = \frac{\theta_{opt}}{S_{opt}} \quad (3)$$

where,

γ_{water} = unit weight of water (in consistent units)*

* From this point on, “in consistent units” means that the variables in the equation can work properly for both Imperial and SI units, but mixed units may not be used in the equations.

For Level 3 analysis, two models are used to estimate $\gamma_{d \max}$ and w_{opt} : one for granular non-plastic materials and one for plastic materials.

The following model estimates the optimum gravimetric moisture content for granular non-plastic materials:

$$w_{opt} = -120.14 - 0.06766 * P_{1.5''} + 3.7269 * D_{60} - 0.167 * P_{40} + 0.117 * P_{60} + 142.53 * \exp(-0.0389 * D_{60}) \quad (4)$$

where,

$P_{1.5''}$ = percent passing 38 mm sieve (%)

P_{40} = percent passing #40 sieve (%)

P_{60} = percent passing #60 US sieve (%)

D_{60} = diameter corresponding to 60% passing material (mm)

The saturation at optimum conditions for granular materials is then obtained:

$$S_{opt} = -100.17 + 1.4991 * P_{2''} + 0.56155 * P_{1''} - 0.36755 * P_{0.5''} \quad (5)$$

where,

$P_{2''}$ = percent passing 50.8 mm sieve (%)

$P_{1''}$ = percent passing 25.4 mm sieve (%)

$P_{0.5''}$ = percent passing 12.7 mm sieve (%)

The following model estimates the maximum dry unit weight for compacted materials:

$$\gamma_{d \max \text{compmod}} = \frac{G_s \gamma_{water}}{1 + \frac{w_{opt} G_s}{S_{opt}}} \quad (6)$$

where,

$\gamma_{d \max \text{compmod}}$ = maximum dry density by Modified proctor (in consistent units)

G_s = specific gravity of solids

γ_{water} = unit weight of water (in consistent units)

w_{opt} = optimum gravimetric moisture content by Modified proctor (%)

S_{opt} = degree of saturation at optimum condition (%)

For compacted materials, the dry unit weight is assumed to be equal to the maximum dry unit weight found above.

$$\gamma_{dry} = \gamma_{d \max \text{ comp mod}} \quad (7)$$

where,

γ_{dry} = dry unit weight (in consistent units).

For uncompacted materials, the dry unit weight is derived from the maximum dry unit weight found with the Standard proctor, using the following relationship:

$$\gamma_{dry} = 1.0156 \gamma_{d \max \text{ comp std}} - 2.464 \quad (8)$$

The gravimetric optimum moisture content for plastic materials is computed as follows:

An adjusted PI value (PI_{adj}) is first estimated:

$$PI_{adj} = e^{\frac{P_{200} + 42.13}{33.94}} \quad (9)$$

If $PI > PI_{adj}$, use PI_{adj}

If $PI \leq PI_{adj}$, then $PI_{adj} = PI$

Compute the adjusted weighted Plasticity index wPI_{adj} :

$$wPI_{adj} = \frac{PI_{adj} P_{200}}{100} \quad (10)$$

If $wPI_{adj} < 1$, $wPI_{adj} = 1$

The optimum water content is computer with the following equation:

$$w_{opt} = 8.3932 wPI_{adj}^{0.3075} \quad (11)$$

where,

w_{opt} = optimum gravimetric moisture content by Standard proctor (%).

To ensure continuity between the predicted optimum water content for low-plasticity materials (equation above) and the water content predicted for non-plastic materials, EICM performs a dual calculation for wPI_{adj} values that are less than or equal to 1 and both values are averaged. For other values of wPI_{adj} , EICM uses the corresponding results provided by the equation above.

To compute the maximum dry density, the following equation is recommended:

$$\gamma_{d \max_comp_std} = 142.115 - 1.959w_{opt} \quad (12)$$

where,

$\gamma_{d \max \text{ comp std}}$ = maximum dry density by Standard proctor (in consistent units)

Saturated Hydraulic Conductivity

Saturated Hydraulic Conductivity, k_{sat} , is required to determine the transient moisture profiles in compacted unbound materials and to compute their drainage characteristics. At Levels 1 and 2, a direct measurement using a permeability test (AASHTO T215) is recommended. At Level 3, EICM uses two models based on soil index properties.

For plastic soils, the model used relates the saturated hydraulic conductivity with three parameters: LL, PI and γ_{dry} :

$$\log k_{sat} = 7.014 - 0.0376LL - 0.361\gamma_{dry} - 7.932 \log PI + 0.249\gamma_{dry} PI^{0.105} \quad (13)$$

where,

k_{sat} = saturated hydraulic conductivity (cm/s)

LL = liquid limit (%)

PI = plasticity index (%)

γ_{dry} = dry unit weight (in consistent units).

For non-plastic soils the following model is used:

$$k_{sat} = 10^{-6} \times 10^{\left(5.3D_{10} + 0.049D_{60} + 0.0092\frac{D_{60}}{D_{10}} - 0.1P_{200} + 1.5\right)} \quad (14)$$

If $k_{sat} > 10$ cm/s, k_{sat} is set to 10 cm/s.

Soil Water Characteristic Curve Parameters

The soil water characteristic curve (SWCC) is defined as the variation of water storage capacity within the macro- and micro-pores of a soil, with respect to suction [18]. This relationship is generally plotted as the variation of the water content (gravimetric, volumetric, or degree of saturation) with soil matric suction [19]. Several studies have been conducted where the different models available to represent the SWCC have been compared [20, 21]. These studies have generally shown that the equations proposed by Fredlund and Xing in 1994 is suitable for a large range of soil types and to a wide range of suction values [22, 23]:

$$\theta_w = C(h) \times \left[\frac{\theta_{sat}}{\left[\ln \left[\text{EXP}(1) + \left(\frac{h}{a_f} \right)^{b_f} \right] \right]^{c_f}} \right] \quad (15)$$

with:

$$C(h) = \left[1 - \frac{\ln \left(1 + \frac{h}{h_r} \right)}{\ln \left(1 + \frac{1 \times 10^6}{h_r} \right)} \right] \quad (16)$$

where,

h = matric suction (kPa)

θ_w = volumetric moisture content (%)

a_f , b_f , c_f , and h_r = SWCC fitting parameters.

At Level 1, direct measurement of suction in kPa, and volumetric water content pairs of values are required. Based on a non-linear regression fitting analysis, the user needs to compute and input the SWCC model parameters a_f , b_f , c_f , and h_r into the MEPDG. For Levels 2 and 3, the EICM will estimate the SWCC model parameters a_f , b_f , c_f , and h_r based on a model that correlates these parameters with soil index properties [10, 12].

For non-plastic soils ($wPI = 0$), the SWCC parameters are estimated using the following models:

$$a_f = 1.14a - 0.5 \quad (17)$$

where:

$$a = -2.79 - 14.1 \log(D_{20}) - 1.9 \times 10^{-6} P_{200}^{4.34} + 7 \log(D_{30}) + 0.055 D_{100} \quad (18)$$

$$D_{100} = 10^{\left[\frac{40}{m_1} + \log(D_{60}) \right]} \quad (19)$$

$$m_1 = \frac{30}{[\log(D_{90}) - \log(D_{60})]} \quad (20)$$

P_{200} = percent passing #200 US sieve (%)

D_{20} = diameter corresponding to 20% passing material (mm)

D_{30} = diameter corresponding to 30% passing material (mm)

D_{60} = diameter corresponding to 60% passing material (mm)

D_{90} = diameter corresponding to 90% passing material (mm)

D_{100} = diameter corresponding to 100% passing material (mm)

Note: There may exist some extreme cases where the computed value of a_f is negative, which will lead to erroneous results. Therefore, the value of a_f was limited to 1.0.

$$b_f = 0.936b - 3.8 \quad (21)$$

where:

$$b = \left\{ 5.39 - 0.29 \ln \left[P_{200} \left(\frac{D_{90}}{D_{10}} \right) \right] + 3D_0^{0.57} + 0.021P_{200}^{1.19} \right\} m_1^{0.1} \quad (22)$$

$$D_0 = 10^{\left[\frac{-30}{m_2} + \log(D_{30}) \right]} \quad (23)$$

$$m_2 = \frac{20}{[\log(D_{30}) - \log(D_{10})]} \quad (24)$$

$$c_f = 0.26e^{0.758c} + 1.4D_{10} \quad (25)$$

where:

$$c = \log(m_2^{1.15}) - \left(1 - \frac{1}{b_f}\right) \quad (26)$$

$$h_{rf} = 100 \quad (27)$$

D_0 = diameter corresponding to 0% passing material (mm)

D_{10} = diameter corresponding to 10% passing material (mm)

h_{rf} = matric suction for specific soil type

Further analysis of the a_f and b_f parameters performed under the NCHRP 1-40D project lead to a better estimate of the limiting a_f value and reasonable constraints to the b_f value as shown below (12):

Constraints:

If $a_f < 1$, then $a_f = 2.25 P_{200}^{0.5} + 5$

$0.3 < b_f < 4$

These constraints were incorporated in the EICM version 0.8 released in November 2005.

For plastic soils ($wPI \neq 0$), the SWCC parameters are estimated using the following models:

$$a_f = 32.835 \{\ln(wPI)\} + 32.438 \quad (28)$$

$$b_f = 1.421 (wPI)^{-0.3185} \quad (29)$$

$$c_f = -0.2154 \{\ln(wPI)\} + 0.7145 \quad (30)$$

$$h_{rf} = 500 \quad (31)$$

where:

wPI = weighted Plasticity index equal to the product of P_{200} (expressed as a decimal) and the PI .

Further analysis performed under the NCHRP 1-40D project allowed the research team to recommend the following constraint to the a_f and c_f parameters shown in the equations for plastic soils:

Constraints:

If $a_f < 5$, then $a_f = 5$

If $c_f < 0.01$, then $c_f = 0.03$

For borderline soils ($0 < wPI < 2$), it was decided to use the weighed average of the SWCC parameters computed for soils with $wPI < 2$. In this case, a_f , b_f , c_f , and h_r should be calculated by both models: the one corresponding to non-plastic soils and the one corresponding to plastic soils as described above. The weighted average of the values found should be used in the estimation of the SWCC.

As an example, if the soil has a $wPI = 0.5$:

- 1) Calculate a_f , b_f , c_f , and h_r following the models for nonplastic soils: a_{fn} , b_{fn} , c_{fn} , and h_{rn}
- 2) Calculate a_f , b_f , c_f , and h_r following the models for plastic soils using $wPI = 0.5$: a_{fp} , b_{fp} , c_{fp} , and h_{rp}
- 3) Compute a weighted average by assuming a linear variation between $wPI = 0$ and $wPI = 2$:

$$a_{favg} = a_{fn} + \frac{wPI}{2} (a_{fp} - a_{fn}) \quad (32)$$

where: $wPI = 0.5$ in this case.

- 4) Follow the same procedure to obtain b_{favg} , c_{favg} , and h_{ravg}

Determination of Moisture Conditions throughout Pavement Systems

The effect of moisture is more significant on unbound materials than on bound materials. The final equilibrium moisture content for unbound materials with $wPI \geq 2$ is estimated based on the suction of the soil predicted by the models described by equations (15) and (16). For soils with $wPI < 2$ the final equilibrium moisture content is estimated using the following model:

$$\theta_w = 4 + 1.5P_{200}^{0.6994} + 0.03TMI \quad (33)$$

where:

θ_w = Volumetric water content (%)

P_{200} = Percent passing #200 US Sieve (%)

TMI = Thornthwaite Moisture Index

Constraints:

If $P_{200} < 2\%$, use $P_{200} = 2\%$; then,

If $\theta_w > 40$, then $\theta_w = 40 + 0.11 (P_{200} - 53)$; then,

If $\theta_w > \theta_{sat}$, make $\theta_w = \theta_{sat}$

where: θ_{sat} = Saturated volumetric water content or porosity (%)

This model overrides the SWCC model for non-plastic materials when computing the equilibrium value.

Soil-atmosphere Interaction Predominance over Groundwater Table Depth

When the groundwater table is deeper than or at 4 ft. from the top of the pavement structure, the volumetric equilibrium water content will be calculated using equations (15) and (16).

The soil suction required for the mentioned equations will be obtained by using the TMI model. Details regarding the TMI model were not discussed in this document but can be found elsewhere [12]. Once the soil suction is obtained, the following procedure is followed by the EICM for moisture prediction.

- For the granular base, equilibrium suction and its corresponding volumetric water content will be calculated based on the TMI model for the upper nodal point.
- For the second and subsequent layers (subbase, compacted subgrade, etc.), the equilibrium suction and its corresponding volumetric water content will be calculated based on the TMI model for the middle point of the layer.
- For the last layer (subgrade), the equilibrium suction and its corresponding volumetric water content will be calculated based on the TMI model for the nodal point located 1 foot below the subgrade.
- Water table depth will dictate the point of zero suction or 100% saturation.

When the groundwater table depth is located within the first 4 ft. below the pavement

surface, the suction at the top nodal point in the granular base ought to be calculated based on the TMI model or the $P_{200(w/c)}$ model as shown in equation (33). The lower suction boundary will correspond to zero suction at the groundwater table depth.

Fluid Flow Model

The equilibrium water content should remain more or less constant throughout the layer unless:

- Moisture movement or fluid flow occurs from initial compaction conditions towards equilibrium condition.
- Freeze-thawing occurs.

When one or both conditions apply, the EICM proceeds as follows:

- The EICM computes volumetric water content at optimum or initial moisture condition using equation (1).
- The EICM computes soil suction at optimum or initial moisture condition through backcalculation using equation (15).
- The EICM computes unsaturated hydraulic conductivity, k_{unsat} , following a numerical approach that was proposed by Fredlund et al. in 1994 and is detailed in the NCHRP 1-40D project report [12].
- The water content at the initial condition will march towards the water content at equilibrium based on Darcy's law or as a function of the hydraulic conductivity of the layer.

Environmental Effects on Resilient Modulus of Unbound Materials

To evaluate the M_R of unbound materials used in the MEPDG, several factors influencing the modulus are considered: Stress state, moisture/density variations, and freeze/thaw effects. Although the stress sensitivity is only considered if Level 1 inputs are used in the MEPDG, the impact of temporal variations in moisture and temperature on M_R are fully considered at all levels through the composite environmental adjustment factor, F_{env} . The EICM deals with all environmental factors and provides soil moisture, suction, and temperature as a function of time, at any location in the unbound layers from which F_{env} can be determined. The resilient modulus M_R at any time or position is then expressed as follows:

$$M_R = F_{env} \times M_{Ropt} \quad (34)$$

The factor F_{env} is an adjustment factor and M_{Ropt} is the resilient modulus at optimum conditions and at any state of stress. It can be seen that the variation of the modulus with stress and the variation of the modulus with environmental factors (moisture, density, and freeze/thaw conditions) are uncoupled. Although this is not necessarily the case, several studies support the use of this assumption in predicting resilient modulus without significant loss in accuracy of prediction. The adjustment factor (F_{env}) being solely a function of the environmental factors, can then be computed by the EICM, without actually knowing M_{Ropt} .

The development of predictive equations and techniques that address the influence of changes in moisture and freeze/thaw cycles on the resilient modulus of unbound materials is described in the following two subsections.

Resilient Modulus as Function of Soil Moisture

An intensive literature review study was completed with the objective of summarizing existing models that incorporated the variation of resilient modulus with moisture [24-27]. Based on these published models, it was possible to select one that would analytically predict changes in modulus due to changes in moisture [12, 24-27]. This model read as follows.

$$\log \frac{M_R}{M_{Ropt}} = a + \frac{b-a}{1 + EXP\left(\ln \frac{-b}{a} + k_m \cdot (S - S_{opt})\right)} \quad (35)$$

where:

M_R/M_{Ropt} = resilient modulus ratio

a = minimum of $\log(M_R/M_{Ropt})$

b = maximum of $\log(M_R/M_{Ropt})$

k_m = regression parameter

$(S - S_{opt})$ = variation in degree of saturation expressed in decimal.

Based on the available literature data, maximum modulus ratios of 2.5 for fine-grained materials and 2 for coarse-grained materials were adopted. The values of a , b , and k_m for coarse-grained and fine-grained materials are given in Table 3. Fine-grained soils label refers to those with passing U.S. No. 200 sieve greater than 50%.

The graphical representation of the model is shown in Figure 4 for fine-grained and coarse-grained materials.

Table 3
Values of a, b, km for coarse-grained and fine-grained materials

Parameter	Coarse-grained materials	Fine-grained materials	Comments
<i>a</i>	-0.3123	-0.5934	Regression parameter
<i>b</i>	0.3	0.4	Corresponding to modulus ratios of 2 and 2.5, respectively
<i>k_m</i>	6.8157	6.1324	Regression parameter

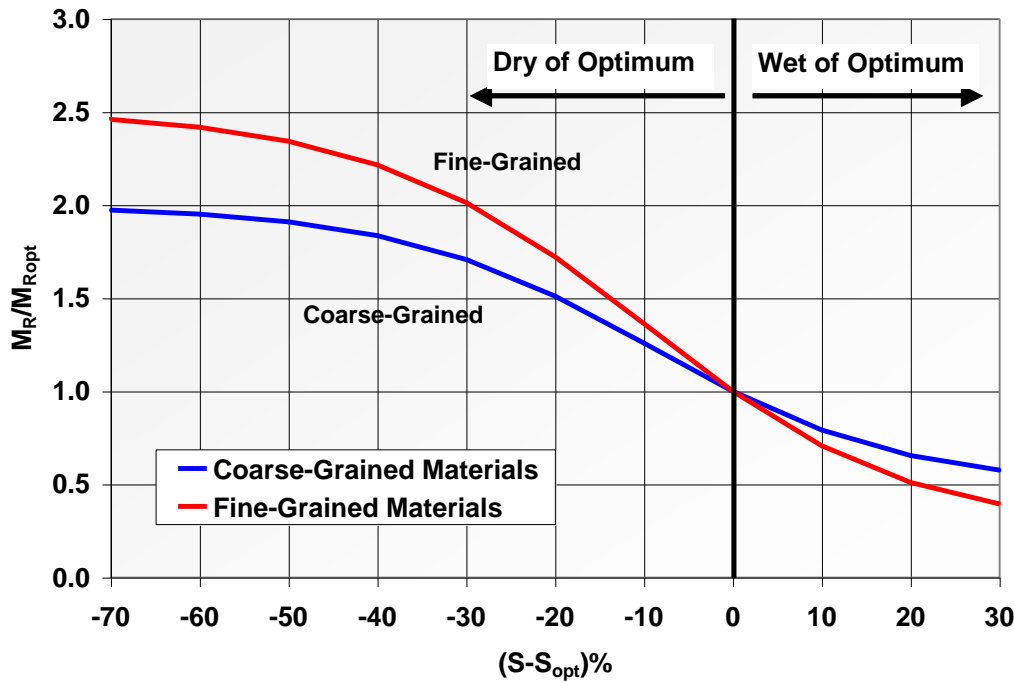


Figure 4
Effect of moisture changes on the resilient modulus

Resilient Moduli for Frozen/Thawed Unbound Materials

To study the behavior of unbound materials under freezing/thawing conditions, a significant number of sources were consulted and salient values of moduli, MR, and ratios of moduli were extracted [7-8]. The objective of the search was to obtain absolute values of moduli for frozen material (MR_{frz}) and the ratio of MR just after thawing (MR_{min}) to the MR of natural, unfrozen material (MR_{unfrz}). The ratio is used as a reduction factor (RF). Because some of the data from the literature produced RF values based on MR_{unfrz} as a reference and

some were based on M_{Ropt} as a reference, it was decided to adopt the conservative interpretation of using the smaller of M_{Runfrz} and M_{Ropt} as a reference, as shown in equation (36).

$$RF = M_{Rmin}/\text{smaller of } (M_{Runfrz}, M_{Ropt}) \quad (36)$$

The average values reported in the literature for M_{Rfrz} were found to be 20,685 MPa for coarse-grained materials; 13,790 MPa for fine-grained silt and silty sands; and 6,895 MPa for clays.

For thawed materials, the degree of M_R degradation upon thawing was found to correlate with frost-susceptibility, or the ability of the soil to sustain ice lens formation under favourable conditions. Frost-susceptibility in turn can be estimated from the percent passing the U.S. No. 200 sieve, P_{200} , and the Plasticity Index, PI . In Tables 4 and 5, the RF values recommended in the MEPDG are given for coarse-grained and fine-grained materials as a function of P_{200} and PI .

Table 4
Recommended values of RF for coarse grain materials (P200 <50%)

Distribution of Coarse Fraction*	P_{200} (%)	$PI < 12\%$	$PI = 12\% - 35\%$	$PI > 35\%$
Mostly Gravel ($P_4 < 50\%$)	< 6	0.85	-	-
	6 – 12	0.65	0.70	0.75
	> 12	0.60	0.65	0.70
Mostly Sand ($P_4 > 50\%$)	< 6	0.75	-	-
	6 – 12	0.60	0.65	0.70
	> 12	0.50	0.55	0.60

* If it is unknown whether a coarse-grained material is mostly gravel or mostly sand, assume sand.

Table 5
Recommended values of RF for materials (P200>50%)

P_{200} (%)	$PI < 12\%$	$PI = 12\% - 35\%$	$PI > 35\%$
50 - 85	0.45	0.55	0.60
> 85	0.40	0.50	0.55

Recovering materials experience a rise in modulus with time, from M_{Rmin} to M_{Runfrz} , that can be tracked using a recovery ratio (RR) that ranges from 0 to 1:

- $RR = 0$ for the "immediately after thawing" condition, when excess water makes the suction go to zero, $M_{Rrecov} = M_{Rmin}$.
- $RR = 1$ when the suction is equal to the suction dictated by the depth to the ground water table – i.e. equilibrium is achieved, $M_{Rrecov} = M_{Runfrz}$.

$$RR = \frac{\Delta t}{T_R} \quad (37)$$

where:

RR = recovery ratio

Δt = number of hours elapsed since thawing started

T_R = recovery period (number of hours required for the material to recover from the thawed condition to the normal, unfrozen condition).

The recovery period, T_R , is noted as a function of the material type/properties, as follows: $T_R = 90$ days for sands/gravels with $wPI < 0.1$; $T_R = 120$ days for silts/clays with $0.1 < wPI < 10$; and $T_R = 150$ days for clays with $wPI > 10$.

Computation of Environmental Adjustment Factor, F_{env}

To obtain the composite moduli for layers in which two or more states of the material coexist and/or the resilient modulus varies with depth and time, the environmental adjustment factor, F_{env} is calculated. The resilient modulus M_R at any time or position is determined as a product of the composite environmental adjustment factor, F_{env} , and the resilient modulus at optimum conditions M_{Ropt} .

The environmental adjustment factor, F_{env} is a composite factor, which could in general represent a weighted average of the factors appropriate for various possible conditions:

- Frozen: frozen material – F_F (factor for frozen materials)
- Recovering: thawed material that is recovering to its state before freezing occurred – F_R (factor for recovering materials)
- Unfrozen/fully recovered/normal: for materials that were never frozen or are fully recovered – F_U (factor for unfrozen material)

The F_{env} factors are calculated for all three cases, at two levels: at each nodal point and for each layer.

Adjustment Factors at Node Level

In the EICM the pavement structure is characterized by an array of nodes at which the values of moisture, suction, and temperature are calculated at any time t . The value of F_F , the adjustment factor for frozen materials, is computed at each node at which a freezing temperature occurs using the following procedure:

- M_{Ropt} is either a direct user input or can be estimated from other engineering properties such as CBR, R-value, structural layer coefficients (a_i), Penetration Index, or from gradation parameters. The estimation of M_{Ropt} is out of the scope of this paper.
- Assign values for the Frozen Resilient Modulus, M_{Rfrz} : If $wPI = 0$; use $M_{Rfrz} = 17,238$ MPa; if $wPI > 0$; use $M_{Rfrz} = 6,895$ MPa
- Compute the frozen adjustment factor, F_F (9):

$$F_F = \frac{M_{Rfrz}}{M_{Ropt_est}} \quad (38)$$

The adjustment factor for recovering materials, F_R , is computed at each node at which freezing temperatures do not occur and the recovery ratio RR is < 1 . The procedure to estimate F_R is as follows:

- Compute Recovery Ratio, RR as per equation 37.
- Compute S_{opt} as per equation 2 for Levels 1 and 2.
- Compute S_{equil} from the SWCC equation in terms of degree of saturation (22):

$$S_{equil} = C(h) \times \frac{I}{\left[\ln \left[\text{EXP}(I) + \left(\frac{h}{a_f} \right)^{b_f} \right] \right]^{c_f}} \quad (39)$$

$$C(h) = 1 - \frac{\ln \left(1 + \frac{h}{h_r} \right)}{\ln \left(1 + \frac{1 \times 10^6}{h_r} \right)} \quad (40)$$

where: h = matric suction in kPa; a_f (kPa), b_f , c_f , and h_r (kPa) are fitting parameters defined earlier.

- Compute R_{equil} as (7):

$$\log R_{equil} = \log \frac{M_{Requil}}{M_{Ropt}} = a + \frac{b-a}{1 + EXP \left[\ln \left(-\frac{b}{a} \right) + k_m (S_{equil} - S_{opt}) \right]} \quad (41)$$

where: a , b , and k_m are constants defined in Table 3.

- Compute the RF value from Tables 4 and 5.
- Compute the factor for recovering material, F_R (9):

If $(S_{equil} - S_{opt}) < 0$: $F_R = RF + R_{equil} * RR - RR * RF$

If $(S_{equil} - S_{opt}) > 0$: $F_R = R_{equil} (RF + RR - RR * RF)$

To estimate the adjustment factor for unfrozen or fully recovered materials, F_U , the following equation is used (7):

$$\log F_U = \log \frac{M_R}{M_{Ropt}} = a + \frac{b-a}{1 + EXP \left[\ln \left(-\frac{b}{a} \right) + k_m (S - S_{opt}) \right]} \quad (42)$$

where: a , b , and k_m are constants from Table 3, and S is the estimated degree of saturation at any node.

Composite Adjustment Factors, F_{env} , for Structural Layers

For a given layer (base, subbase, subgrade), frozen, thawed, and never frozen materials can coexist within a single layer, and hence a composite adjustment factor that can handle all possible cases is needed. The calculation of a composite adjustment factor is useful even when the material in a layer is all at the same state (unfrozen or recovering). This is because the adjustment factors vary from node to node (with moisture or suction) and an equivalent factor for the whole layer is needed.

To obtain an equivalent modulus, an elastic spring series analogy was considered. Using the analogy, the elements of a column (corresponding to Hour 1, for example) of a node/time matrix, are considered as elastic moduli of a series of springs (one spring per node). If the stress applied to this model is σ , then the displacement in one spring at a given node and time increment can be computed.

To get the average displacement, $\delta_{average}$, over the whole analysis period (2 weeks or 1 month), equation (43) is used:

$$\delta_{average} = \sigma \frac{1}{t_{total}} \sum_{t=1}^{t_{total}} \left[\sum_{node=1}^n \left(\frac{h_{node}}{M_{Rnode,t}} \right) \right] \quad (43)$$

where: t = time (corresponding to the column in the matrix being considered); h_{node} = length of the spring assigned to the node being considered; $M_{Rnode,t}$ = modulus for the node; and t_{total} = total number of t time increments (EICM uses 1 hour) over which the composite modulus is calculated (number of columns in the matrix).

Then the composite (equivalent) modulus can be obtained by finding a composite modulus, M_{Rcomp} , which produces the same $\delta_{average}$ over the total layer thickness for the same applied σ . Equating $\delta_{average}$ for the composite model to $\delta_{average}$ from equation (43) and cancelling σ which appears on both sides:

$$\frac{h_{total}}{M_{Rcomp}} = \frac{1}{t_{total}} \sum_{t=1}^{t_{total}} \left[\sum_{node=1}^n \left(\frac{h_{node}}{M_{Rnode,t}} \right) \right] \quad (44)$$

where: h_{total} = total height of the considered layer/sublayer.

Because the resilient modulus at any node/time can be expressed as the product of an adjustment factor times the resilient modulus at optimum, equation (44) can be replaced with equation (45). A composite adjustment factor, F_{env} , for the considered sub-layer (sub-matrix) can be obtained from equation (46):

$$\frac{h_{total}}{F_{env} M_{Ropt}} = \frac{1}{t_{total}} \sum_{t=1}^{t_{total}} \left[\sum_{node=1}^n \left(\frac{h_{node}}{F_{node,t} M_{Ropt}} \right) \right] \quad (45)$$

$$F_{env} = \frac{h_{total} t_{total}}{\sum_{t=1}^{t_{total}} \left[\sum_{node=1}^n \left(\frac{h_{node}}{F_{node,t}} \right) \right]} \quad (46)$$

where: F_{env} = composite adjustment factor for the considered sublayer, and $F_{node,t}$ = adjustment factor at a given node and time increment (which could be F_F , F_R , or F_U , depending on the state of the material).

The procedure should be applied for the entire design period (e.g., 20 years divided into months or 2-week periods) since the adjustment factors vary from node to node, even within

a layer (or sublayer) in which all material is at the same state (frozen, unfrozen, or recovering).

Determination of the Temperature throughout Pavement Systems

The effect of moisture is more significant on unbound materials than on bound materials. On the other hand, temperature affects both the bound (asphalt and cement) and unbound layers significantly. At very cold temperatures, the asphalt stiffness is close to that of PCC, whereas at very warm temperatures, its stiffness is closer to an unbound material.

The durability of PCC materials is affected greatly by the freeze-thaw environment it operates under. Temperature and moisture related curling and warping phenomena play a significant role in defining the PCC pavement fatigue behaviour. Temperature and moisture also play a role in the opening and closing of joints in JPCP and cracks in CRCP, which affect performance.

In unbound materials, cooler temperatures result in frost formation and a subsequent increase in modulus. On the other hand, warmer temperatures cause thawing which results in increased moisture contents and a subsequent decrease in modulus values. During the thawing process, the resilient modulus of unbound materials may go well below the optimum value (0.5 to 0.85 times M_{Ropt}).

The CMS and CRREL models in the EICM are primarily responsible for most the temperature calculations. The CMS model was originally developed at the University of Illinois [2]. It is a one-dimensional, forward finite difference heat transfer model to determine frost penetration and temperature distribution in the pavement system. The model considers radiation, convection, conduction, and the effect of latent heat. It does not consider transpiration, condensation, evaporation, or sublimation. These latter effects are neglected because of the uncertainty in their calculations and because their omission does not create significant errors in the heat balance at the surface of the pavement. Heat fluxes caused by precipitation and moisture infiltration are also neglected.

For pavement layers (AC or PCC), the EICM assumes that the user input heat capacity and thermal conductivity do not vary over time. However, for unbound layers (base courses and soils), as the moisture and frost contents change with time, so do the heat capacity and thermal conductivity. The user input dry heat capacity and dry thermal conductivity, which along with the water and ice content predicted by the EICM, are used to calculate the wet

heat capacity and wet thermal conductivity. In this manner the heat/temperature calculations of the EICM are coupled with the EICM's moisture predictions.

Once the thermal properties that define the heat flow through the pavement and unbound layers have been established and the boundary conditions have been identified, it is necessary to determine the amount of heat inflow/outflow at the pavement surface. The two processes by which heat is added or subtracted from the pavement surface are convection and radiation.

The second model used in the MEPDG is the CRREL model (4). It is a one-dimensional coupled heat and moisture flow in the subgrade soil at temperatures that are above, below and at the freezing temperature of water. The model predicts the depth of frost and thaw penetration. It also estimates the vertical heave due to frost formation and vertical settlement when the soil thaws. The CRREL model uses the temperature profiles through the asphalt layers established by the CMS model to compute changes in the soil temperature profile, and thus frost penetration and thaw settlement.

Heat Flux Boundary Conditions for CMS Model

Temperatures throughout the pavement structure are dominated by atmospheric conditions at the surface. While it is easy to measure the air temperatures, there is not a direct correspondence between the air temperatures and pavement surface temperatures. To estimate the pavement temperature, the energy balance at the surface used in the CMS model is described by equation (47) [28, 29]:

$$Q_i - Q_r + Q_a - Q_e \pm Q_c \pm Q_h \pm Q_g = 0 \quad (47)$$

where: Q_i = incoming short wave radiation; Q_r = reflected short wave radiation; Q_a = incoming long wave radiation; Q_e = outgoing long wave radiation; Q_c = convective heat transfer; Q_h = effects of transpiration, condensation, evaporation, and sublimation; and Q_g = energy absorbed by the ground.

The net all-wave length radiation at the surface is Q_n is presented in equation (48).

$$Q_n = Q_s - Q_l \quad (48)$$

where: Q_s = net short wave radiation; and Q_l = net long wave radiation.

$$Q_s = Q_i - Q_r \quad (49)$$

$$Q_l = Q_a - Q_e \quad (50)$$

Q_s has been given by Baker and Haines [30] as presented in equation (51):

$$Q_s = a_s R^* \left[A + B \frac{S_c}{100} \right] \quad (51)$$

where: a_s = surface short wave absorptivity of pavement surface; R^* = extraterrestrial radiation incident on a horizontal surface at the outer atmosphere, which is a function of the latitude of the site; A , B = constants that account for diffuse scattering and adsorption by the atmosphere; S_c = percentage of sunshine which accounts for the influence of cloud cover.

In equation (50), Q_a , the long wave incoming radiation, and Q_e , the outgoing long wave radiation, are given by equations (52) and (53):

$$Q_a = Q_z \left(1 - \frac{NW}{100} \right) \quad (52)$$

$$Q_e = Q_x \left(1 - \frac{NW}{100} \right) \quad (53)$$

Thus Q_l in equation (54) is:

$$Q_l = (Q_z - Q_x) \left(1 - \frac{NW}{100} \right) \quad (54)$$

where: Q_z is the incoming long wave radiation given by equation (54); and $\left(1 - \frac{NW}{100} \right)$ represents the cloud cover correction as presented in equation (55):

$$Q_z = \sigma_{sb} T_{air} \left(G - \frac{J}{10^{\rho p}} \right) \quad (55)$$

where: N = cloud base factor (0.9 to 0.80 for cloud heights of 305 m to 1,830 m (Geiger 1959); W = $100 - S_c$ (average cloud cover during day or night); T_{air} = air temperature in °R; σ_{sb} = Stefan-Boltzmann constant, $5.67 \times 10^{-8} \text{ W}/(\text{m}^2 \text{ K}^4)$; G = 0.77; J = 0.28; ρ = 0.074; p = vapor pressure of the air (1 to 10mm Hg); and Q_x = outgoing long wave radiation without a correction for cloud cover as presented in equation (56).

$$Q_x = \sigma_{sb} \varepsilon T_s^4 \quad (56)$$

where: ε = emissivity of the pavement (1 – albedo) which depends on pavement color, texture and temperature (A typical value is 0.93); and T_s = surface temperature in °R.

The rate of heat transfer by convection, Q_c , is presented in equation (57):

$$Q_c = H(T_{air} - T_s) \quad (57)$$

with T_{air} and T_s expressed in °F; and H = convection heat transfer coefficient.

The convection heat transfer coefficient, H , can be expressed as presented in equation (58) [2, 31]:

$$H = 122.93 [0.00144T_m^{0.3}U^{0.7} + 0.00097(T_s - T_{air})^{0.3}] \quad (58)$$

where: T_s = surface temperature, in °C; T_{air} = air temperature, in °C; T_m = average of surface and air temperature, in °K; and U = average daily wind speed in m/s.

The maximum value of the heat transfer coefficient is partly controlled by the stability criteria established for the finite difference approach in computations within the EICM. The suggested maximum value is 17 W/(m²K). The effects of transportation, condensation, evaporation and sublimation (Q_h) have been neglected in the formation because they are either too small to be significant or the effects cancel each other out in the energy balance.

The above calculations determine the surface temperature and thus control the temperature throughout the underlying materials. The depth of frost is established by comparing the computed temperatures with the freezing temperatures of the soil. The depth of frost penetration has been identified as the position of the 30°F isotherm. Finally, the finite difference approach is used to determine the nodal temperatures. Details of the finite difference grid and the formulation of the heat conduction equations can be found elsewhere [2].

After the amount of heat inflow/outflow due to convection and radiation at the pavement surface is determined, this amount of heat is added/subtracted from the quantity of heat at the

upper boundary. The EICM iterates a single time step, calculating a new temperature profile for the pavement system. This updated temperature profile is used for convection and radiation calculations at the next time step.

Recent Efforts Aimed at Enhancing the EICM

Under the NCHRP 9-23 Project entitled *Environmental Effects in Pavement Mix and Structural Design Systems*, the EICM was subjected to evaluation and calibration [10]. As part of the research Project NCHRP 1-40D entitled *Models Incorporated into the Current Enhanced Integrated Climatic Model: NCHRP 9-23 Project Findings and Additional Changes after Version 0.7*, the new models recommended by the NCHRP 9-23 project research team were integrated with the revisions recommended by the NCHRP 1-40D project research team after the EICM version 0.7 was implemented [12].

Since the last revisions made to the EICM models, several efforts have been exerted by the pavement research community for refinement and enhancement of the predictive methodology developed for the EICM. Even when the results of such recent research efforts have not been yet implemented within the EICM, they are expected to be considered in future revisions of the methodology in the near future. Some of the most important improvements found in the literature are presented in this section.

National Database of SWCC Parameters and Selected Soil Index Properties

Several types of input parameters are required by the EICM in order to accurately predict the environmental factors. These include two main categories: the climatic information and the material properties for unbound (granular base, subbase, and subgrade) materials. The climatic information is readily available to the guide user by a set of more than 800 weather stations with hourly information that includes precipitation, temperature, wind speed, cloud cover and relative humidity. The unbound material information, on the other hand, ranges from routine index properties, that are well-known by the pavement engineering practitioners and researchers, to a specialized set of moisture retention parameters (soil-water characteristic curve) that are fundamental for environmental considerations of the moisture prediction and soil stiffness of all unbound layers. These material properties of the soil-water characteristic curve have been used quite frequently by the agricultural sciences and unsaturated soil mechanics communities; but are relatively unfamiliar to the pavement community.

The effort to create a national database, that comprehends important unbound material information required as input for the EICM, was taken over by NCHRP 9-23A project entitled *A National Catalog of Subgrade Soil-Water Characteristic Curve (SWCC) Default Inputs and Selected Soil Properties for Use with the MEPDG* (32). This database contains information for use at the three optional hierarchical levels of the analysis implemented in the MEPDG. It comprehends a full set of Level 3 data and most Level 1 and 2 information, including SWCC parameters and saturated hydraulic conductivity. In addition, the information collected allowed for predictions of typical resilient modulus and CBR values based on soil index properties.

This database is based and has been developed on soil properties directly measured in the field for agricultural and geotechnical (pavement) engineering purposes to depths up to 100 inches (8 – 9 ft.). The database comprises 31,100 soil units distributed in more than 9,800 soil profiles covering the continental United States, Hawaii and Alaska, and Puerto Rico. Data from the U.S. Department of Agriculture’s (USDA) Natural Resources Conservation Service (NRCS) was downloaded and summarized in both tabular and spatial files. The tabulated data was organized by soil profiles, each of them comprising one or more soil units. The spatial data allowed for the creation of 814 Soil Unit Maps via GIS within the entire United State and Puerto Rico. Finally, a user-interface was created in Excel© to allow searching for specific locations within a state, by using the maps created in the project.

Figures 5 and 6 are presented as example of the NCHRP 9-23A product for the State of Louisiana. As shown in Figure 5, state maps are divided with a numbered grid, which allows the user to narrow the search to a smaller region within the state. Also, maps were created for each region within each state. The map of region 14 is presented as an example in Figure 6. By inputting the Mapchart number, corresponding to the soil unit of interest from the small region, in the Excel® file interface, a summary report comprising all available information is available, as shown in Figure 7.

The database developed is considered a tremendous asset to the implementation of the MEPDG. The SWCC parameters, which are contained in this database, represent the largest database available in the world. This database should also allow further analysis to be conducted in order to better estimate default parameters for the level 3 analyses. Furthermore, and most important, this database is useful to eventually revise and update the SWCC models currently available in the MEPDG.

State of Louisiana

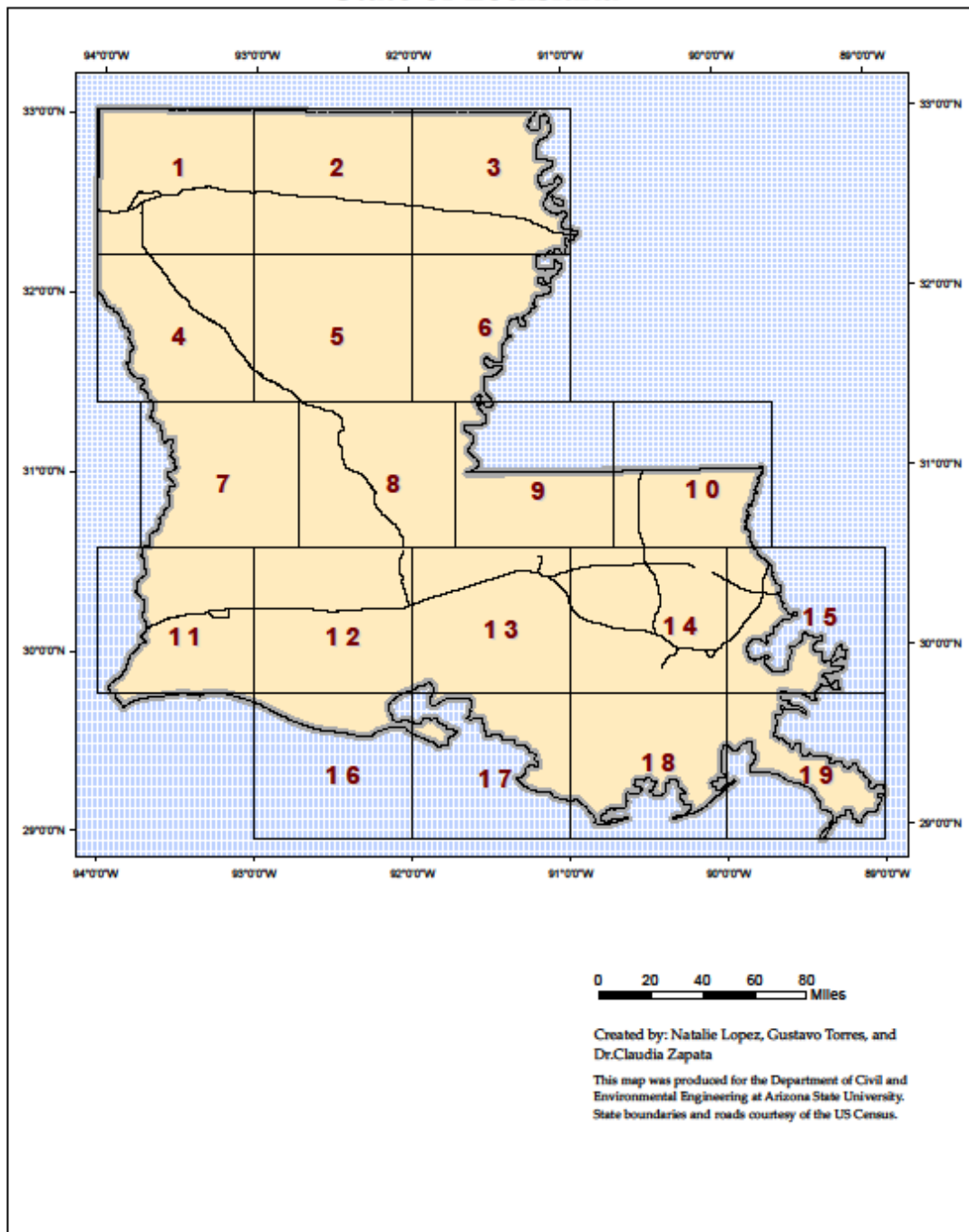


Figure 5
State of Louisiana map with region grid [32]

Louisiana - Soil Unit Map 14

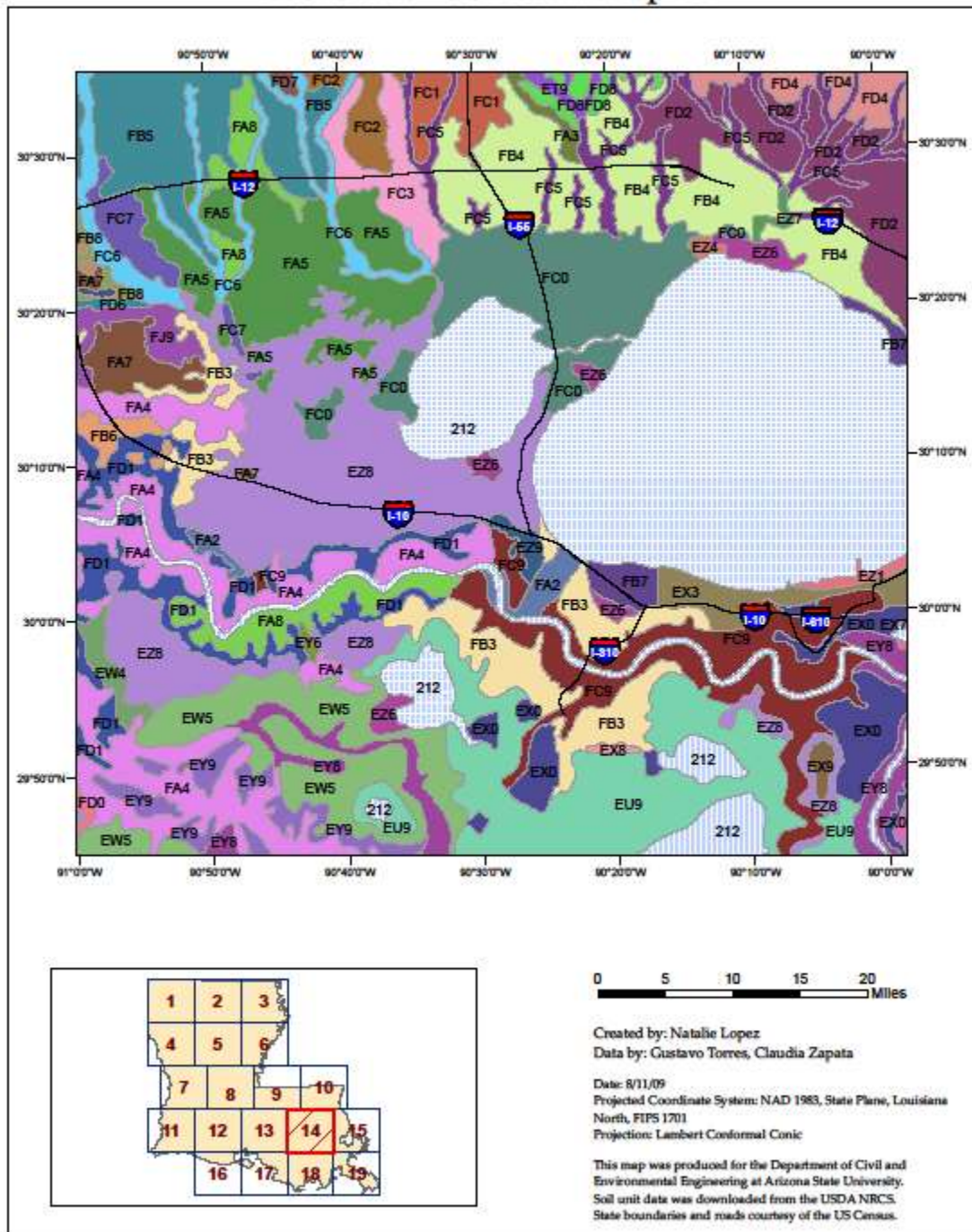


Figure 6
 Region 14 for Louisiana [32]


 National Catalogue of Natural Subgrade Properties Needed for the ME-PDG Input									
Map Char	FA5								
Mapunit Key	667683								
Mapunit Name	Springfield-Natalbany-Encrow-Colyell (s2864)								
Component Name	Colyell								
	Top Layer	Layer 2	Layer 3	Layer 4	Layer 5	Layer 6	Layer 7	Layer 8	Layer 9
AASHTO Classification	A-4	A-4	A-7-6	A-7-6					
AASHTO Group Index	6	5	32	19					
Top Depth (in)	0.0	3.1	11.8	39.0					
Bottom Depth (in)	3.1	11.8	39.0	59.8					
Thickness (in)	3.1	8.7	27.2	20.9					
% Component	25	25	25	25					
Water Table Depth - Annual Min (ft)	0.8	0.8	0.8	0.8					
Depth to Bedrock (ft)	N/A								
STRENGTH PROPERTIES									
CBR from Index Properties	11	13	4	5					
Resilient Modulus from Index Properties (psi)	11,621	12,908	5,730	7,558					
INDEX PROPERTIES									
Passing #4 (%)	100.0	100.0	100.0	100.0					
Passing #10 (%)	100.0	100.0	100.0	100.0					
Passing #40 (%)	100.0	100.0	100.0	100.0					
Passing #200 (%)	97.5	97.5	97.5	97.5					
Passing 0.002 mm (%)	7.0	12.5	47.0	29.0					
Liquid Limit (%)	22.0	23.5	55.0	41.0					
Plasticity Index (%)	8.5	7.0	28.5	18.0					
Saturated Volumetric Water Content (%)	43.0	44.0	44.0	40.0					
Saturated Hydraulic Conductivity Ksat (ft/hr)	0.11	0.11	0.01	0.03					
SOIL-WATER CHARACTERISTIC CURVE PARAMETERS									
Parameter af (psi)	9.5142	8.8036	0.5313	10.7499					
Parameter bf	0.9430	0.9069	1.0255	1.0082					
Parameter cf	1.0789	1.0745	0.2021	0.4163					
Parameter hr (psi)	3000.00	3000.00	3000.20	2999.99					

Figure 7
Example of a printable report displayed in the excel interface [32]

Integrating the National Database of Subgrade Properties with the MEPDG

In order to ease the use of the database and the maps developed during the NCHRP 9-23A project, a Google-based interactive tool capable of displaying soil unit maps and generate

reports summarizing available subgrade data was envisioned and produced as part of NCHRP 9-23B project entitled *Integrating the National Database of Subgrade Soil Water Characteristic-Curves and Soil Index Properties with the MEPDG* [33]. The importance of this tool is that it can be easily linked to the MEPDG software and/or can be used by any practitioner interested in preliminary information of the site conditions needed in the design and analysis of new and rehabilitated pavement structure.

Once linked to the MEPDG, the developed searching tool will provide direct access to the maps and soil properties during operation of the MEPDG software through interactive use of the user-input coordinate points (defined by latitude and longitude). It makes use of the input coordinates of latitude and longitude to access both the appropriate Soil Unit Map and a complete tabular summary of soil property data required by the EICM at that particular location.

The tool is also capable of identifying each road segment by its official state mileposts and link them to their respective latitude and longitude and the soil unit areas, making it possible for the user to input a specific highway or route milepost and immediately access the major Soil Unit Map located at that route milepost and a tabular summary of all relevant soil property data. It should be mentioned that since the Milepost Marker Data available was limited, the milepost searching feature does not work for the totality of the US Road Network. However, the Milepost Marker Database can be continuously updated as more data becomes available.

Currently, the interactive searching tool can be accessed by visiting the following link: <http://nchrp923b.lab.asu.edu/index.html>. Figure 8 presents a screenshot of the main web portal for the searching tool developed under NCHRP 9-23B project.

Development of New Models to Estimate the SWCC Parameters for Non-Plastic Materials

As previously mentioned, the equations proposed by Fredlund & Xing in 1994 (22, 23) was found to be the most suitable expression to correlate the matric soil suction with the soil moisture content for a large range of soil types and to a wide range of suction values. Equations (17) to (27) present a set of correlations, derived for non-plastic soils under the NCHRP 9-23 project, to estimate the a_f , b_f , c_f , and h_r fitting parameters for the Fredlund & Xing equations [10]. Further analysis of the research team under the NCHRP 1-40D project led to the refinement of the models by including reasonable constraints for the set of correlations [12]. Such correlations were developed using a total of 154 different non-plastic

materials and are basically function of the grain size distribution through the use of the diameters corresponding to 10, 20, 30, 60, and 90% passing material as well as the percent passing the No 200 sieve, P_{200} .

In 2011, Torres proposed a new set of correlations for non-plastic materials [34]. These new expressions were developed using the database created under NCHRP 9-23A project [32]. About 4,500 different non-plastic materials were included in the analysis performed by Torres, which is supposed to yield more robust correlations than those from NCHRP 9-23 project.

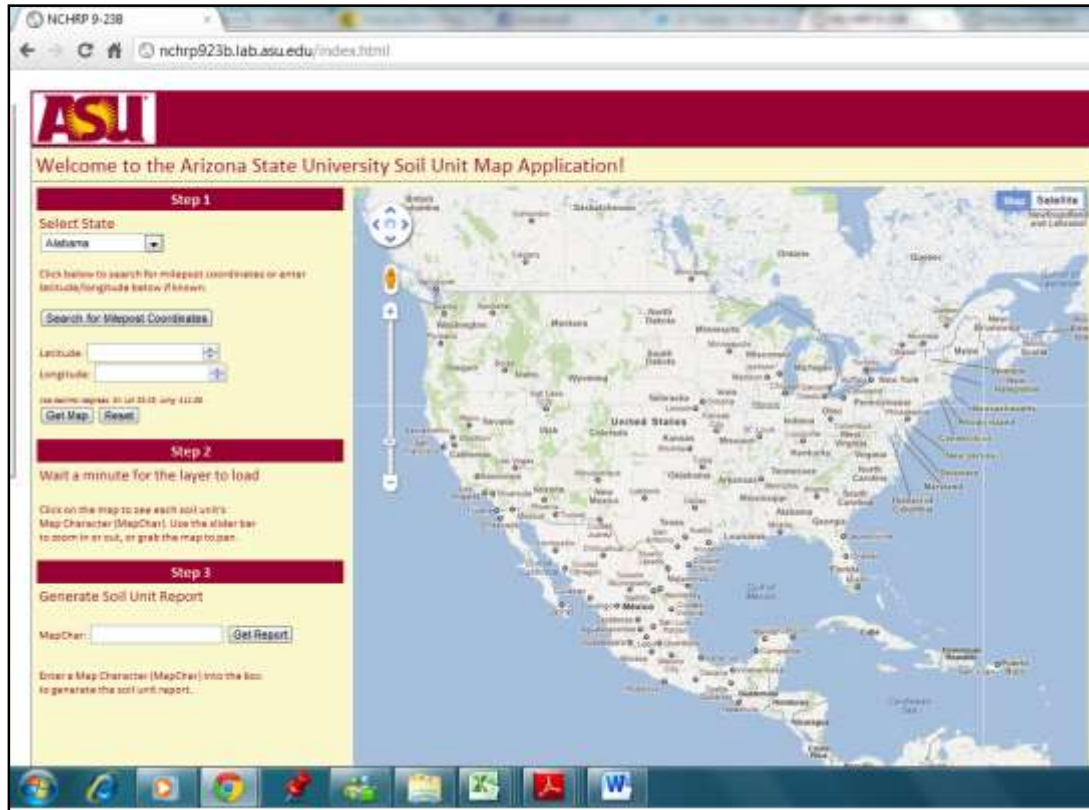


Figure 8
Searching tool main web portal [33]

Equations (59) to (62) show the correlations developed by Torres:

$$a_f = -967.21D_{10}^2 + 218.37D_{10} - 2.7 \quad (59)$$

where: D_{10} is the diameter corresponding to 10% passing material (mm)

Constraint: if $D_{10} < 0.020$, then $a_f = 1.28$

$$\log b_f = -0.0075 a_f^3 + 0.1133 a_f^2 - 0.3577 a_f + 0.3061 \quad (60)$$

$$c_f = 0.0058 a_f^3 - 0.0933 a_f^2 - 0.4069 a_f + 0.3481 \quad (61)$$

$$h_r = 100 \quad (62)$$

The expression to estimate a_f is function of the diameter D_{10} . The effective particle size D_{10} has been related in the past to the coefficient of permeability by Hazen and therefore, it seems logical that it correlates well with moisture retention characteristic [35]. Both SWCC parameters b_f and c_f were found to correlate with a_f . According to Torres, the dependency of b_f and c_f with a_f was found to be convenient since it eliminates the possibility of discontinuities in the SWCC function. Finally, the h_r parameter yielded a constant value of 100.

Figure 9 shows measured versus predicted moisture content in terms of degree of saturation. The measured degrees of saturation were found by fitting the Fredlund & Xing model to measured data [22]. The predicted values were obtained by using equations 59 to 62 to estimate the SWCC fitting parameters. A coefficient of determination R^2 of 0.89 and standard error ratio S_e/S_y of 0.33 are indicators of good predictions. Therefore, if considered in future revisions of the EICM methodology, the new set of correlations for non-plastic materials proposed by Torres is expected to enhance the predictions of moisture conditions for pavement structures.

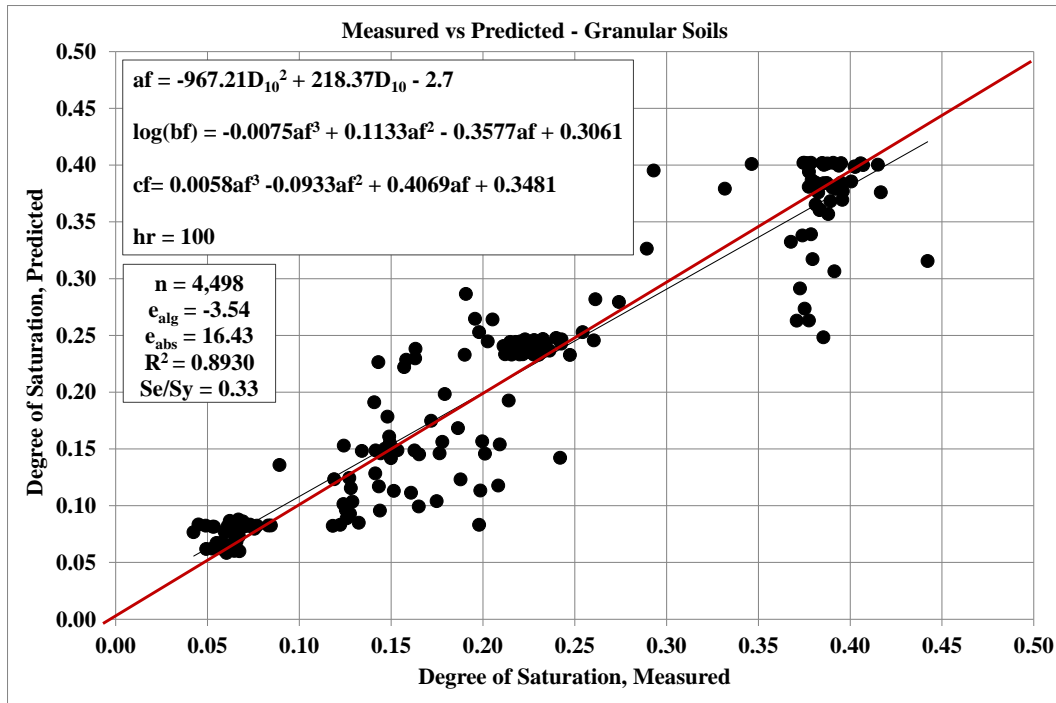


Figure 9
Measured versus predicted degree of saturation for granular soils [34]

Enhancement of Resilient Modulus Prediction as Function of Soil Moisture

The MEPDG considers the changes in moisture content in the subgrade over the design life of a pavement through the EICM. The EICM incorporates variations in moisture content directly upon the prediction of the resilient modulus, M_R , by using an environmental factor for unfrozen unbound materials (F_U). The model previously shown in equation (42) was developed at Arizona State University by Witczak et al. and is currently used to calculate the F_U value in the EICM [7].

In the current EICM version, the values for a and k_m fitting parameters in equation (42) were selected as the best estimates for the database available at the time the model was developed. The values for b were conservatively assumed and correspond to maximum modulus ratios of 2 and 2.5 for coarse-grained and fine-grained materials respectively. It is important to note that only one unique relationship was developed for all fine-grained materials.

In 2010, Cary and Zapata created a database of modulus ratios in an attempt to enhance the moisture dependent resilient modulus model [36]. The database revealed that the suggested model fitting parameters may not appropriately reflect the actual response of F_U as function of moisture fluctuations.

Figure 10 shows the data employed for the study conducted by Cary and Zapata. Although

the current coarse-grained material model fits the data relatively well, the fine-grained material data presents a significantly different trend and therefore, the use of the current model may lead to under-prediction of the modular ratio/ environmental factor F_U . The need for a refinement of the model to pursue more accurate results in the use of the EICM was obvious base on such observations.

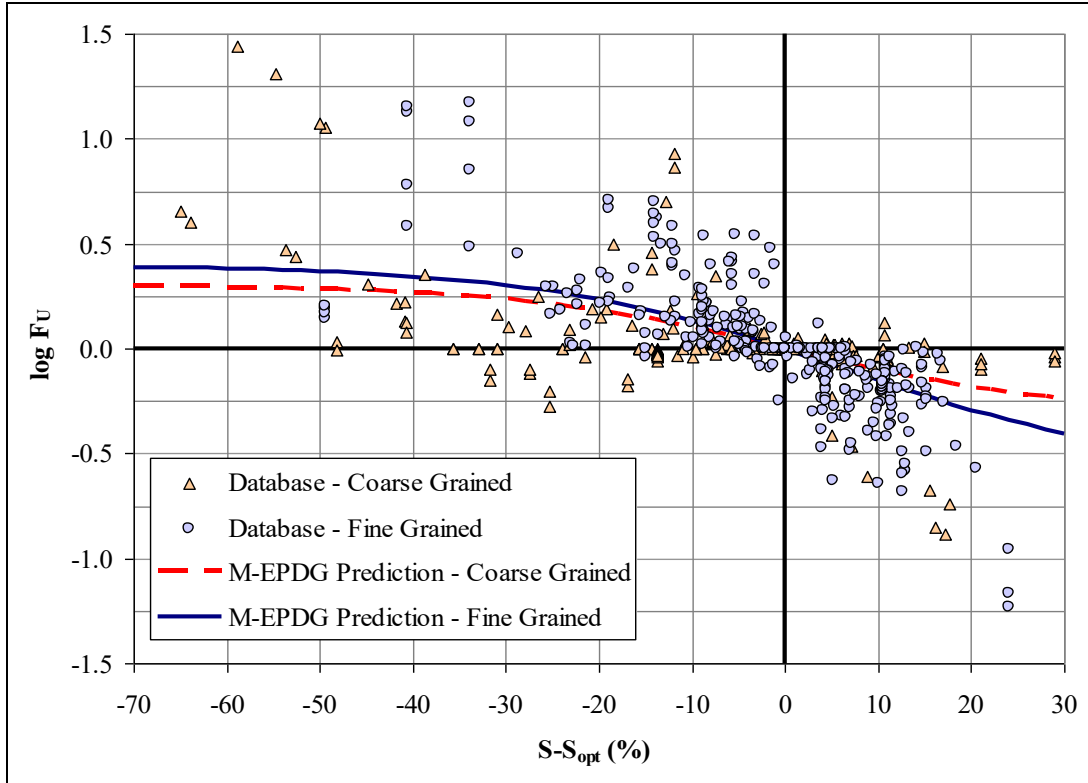


Figure 10
Data collected in the study conducted by Cary and Zapata (36)

Cary and Zapata proposed a set of expressions to estimate the F_U not only as function of moisture fluctuations but also as function of the soil type. Equations (63) and (64) estimate the F_U for materials having little to no plasticity and for plastic materials respectively:

$$F_{U-PC} = 10^{\left(-0.40535 + \frac{1.20693}{1 + e^{\left(0.68184 + 1.33194 \cdot \left(\frac{S - S_{opt}}{100} \right) \right)}} \right)} \times 10^{C_2(PC - 100)} \quad (63)$$

where,

F_{U-PC} = environmental factor for unfrozen unbound materials adjusted for percent compaction

$(S - S_{opt})$ = variation in degree of saturation S expressed in decimal with respect to the degree

of saturation at optimum conditions S_{opt}

$C_2 = 0.03223$, corresponding to 100% standard compaction energy as the reference baseline, details about the determination of this constant can be found elsewhere (36)

PC = percent compaction defined as the percentage of standard dry density

$$F_{U-STD} = 10 \left[m \times \left(\alpha + \beta \cdot e^{-wPI} \right)^{-1} + \frac{(\delta + \gamma \cdot wPI^{0.5}) - (\alpha + \beta \cdot e^{-wPI})^{-1}}{1 + e^{\left(\ln \left(\frac{-(\delta + \gamma \cdot wPI^{0.5})}{(\alpha + \beta \cdot e^{-wPI})^{-1}} \right) + (\rho + \omega \cdot e^{-wPI})^{0.5} \cdot \left(\frac{S - S_{opt}}{100} \right) \right)} \right] \quad (64)$$

where,

F_{U-STD} = environmental factor for unfrozen unbound subgrade materials,

wPI = weighted PI , the product of P_{200} (expressed as a decimal) and the PI of the soil,

$\alpha = -0.600$,

$\beta = -1.87194$,

$\delta = 0.800$,

$\gamma = 0.080$,

$\rho = 11.96518$,

$\omega = -10.19111$, and

$m = 1.002$

Figure 11 illustrates how the enhanced model describes the variation of the F_U for all soil types investigated (granular non-plastic materials and subgrade soils), as a function of degree of saturation and soil type. One of the most important findings of this study clearly supports the extreme conservative value of the F_U model used in the current version of the EICM, particularly in the dry zones of equilibrium. The current EICM model shows an upper maximum F_U value of 2.5 for fine grained subgrades. However, the results of the study performed by Cary and Zapata have shown that F_U values of 10-12 may be achieved (in drier conditions) for subgrades, depending upon the wPI value of the material. This was a significant conclusion that illustrates the excessive degree of conservatism in the current version of the EICM.

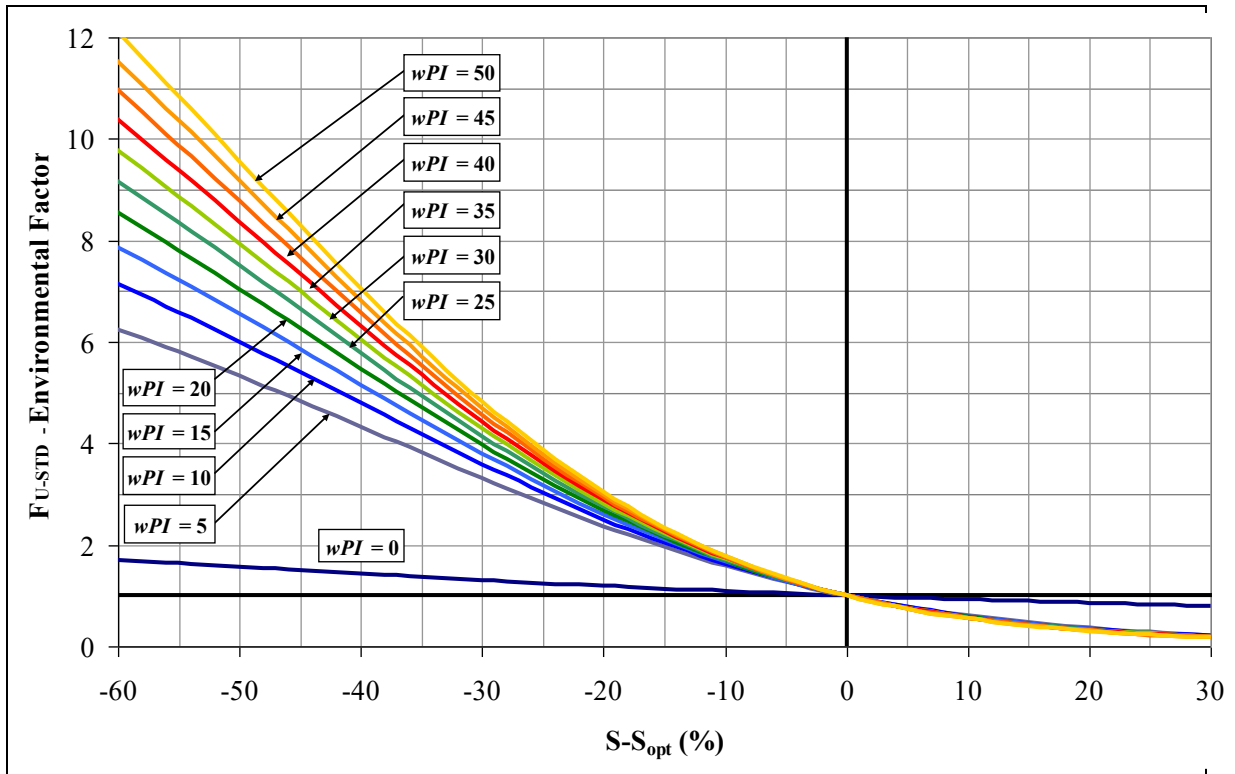


Figure 11
Variation of F_u as a function of $(S-S_{opt})$ and wPI [36]

The two sub-models developed by Cary and Zapata, one for non-plastic granular base/sub-base materials and the other for fine grained subgrade, yield an R^2_{adj} near 0.60 (considered good for data collected from a multiple of research sources in a literature review) and predict F_U values consistent with those found in the database of actual test measurements. Given the goodness of fit and the completeness of the prediction model, its adoption in future revisions of the EICM was highly recommended by Cary and Zapata [36].

Matric Suction as Fundamental Variable for the Prediction of Resilient Modulus Changes

It has been recognized that seasonal changes in the stress state should be related to changes in matric suction, as a fundamental variable within the stress state of unsaturated soils, and not simply to the moisture content of the material [37]. The moisture flow, in the absence of gravitational gradient, is dictated by matric suction or pore water pressure gradients within unsaturated and saturated soils, respectively.

The approach adopted by the current version of the EICM to take into account the seasonal environmental changes for M_R predictions, employs the modular ratio/adjustment factor F_U [7]. This environmental factor takes into account the contribution of matric suction, via the use of degree of saturation, independently from the contribution of the externally applied stress.

In 2008, Cary developed a model that considers the matric soil suction as a fundamental predictive stress state variable [37]. Details about the development of the model can be found in the literature published by Cary and Zapata in 2010 and 2011 [38-39]. A major goal of the study conducted by Cary and Zapata was to consider the effect of seasonal variations in matric suction in a more fundamental way upon the resilient modulus of materials. It has been recognized that any seasonal change in the stress state can be better related to changes in matric suction, as a fundamental variable within the stress state of unsaturated soils, instead of simply using the moisture content change or the degree of saturation. The model considers a smooth transition from unsaturated to saturated conditions in the soils. The expression proposed by Cary and Zapata is a variation to the widely known Universal Model [40], and is expressed in equation 65 as follows:

$$M_R = k'_1 \cdot p_a \cdot \left(\frac{\theta_{net} - 3 \cdot \Delta u_{w-sat}}{p_a} \right)^{k'_2} \cdot \left(\frac{\tau_{oct}}{p_a} + 1 \right)^{k'_3} \cdot \left(\frac{(\psi_{m_0} - \Delta \psi_m)}{p_a} + 1 \right)^{k'_4} \quad (65)$$

where,

p_a = atmospheric pressure

$k'_1 \geq 0$, $k'_2 \geq 0$, $k'_3 \leq 0$ and $k'_4 \geq 0$ are regression constants

$\theta_{net} = \theta - 3u_a$, net bulk stress and u_a is pore air pressure

Δu_{w-sat} = build-up of pore water pressure under saturated conditions. In this case, $\Delta \psi_m = 0$

τ_{oct} = octahedral shear stress

ψ_{m_0} = initial matric soil suction

$\Delta \psi_m$ = relative change of matric soil suction with respect to ψ_{m_0} due to build-up of pore water pressure under unsaturated conditions, in this case $\Delta u_{w-sat} = 0$

Even though the EICM approach to address the seasonal environmental changes and an enhanced version of the same model suggested by Cary and Zapata in 2010 are adequate for practical purposes; by using suction directly, the margin of uncertainty in resilient modulus predictions can be reduced as shown in Figures 12 and 13 [7, 36, 39]. The examples in

Figures 12 and 13 show the goodness of fit obtained by using the current EICM model (Figure 12) and the model proposed by Cary and Zapata (Figure 13) respectively, to fit test results from a granular base material. The statistics in the figures indicate that the predictions are clearly improved by introducing suction directly as a predictive variable. It should be noted that the model proposed by Cary and Zapata not only considers the seasonal environmental changes in suction but also introduces the effect of the pore water pressure build-up due to dynamic loading.

Given that measuring suction and its variation under applied dynamic load is still a challenging task, the capability of measuring a full stress state resilient modulus is currently viable just to research institutions. However, Cary and Zapata believe that as such testing capabilities are implemented into the state of the practice and a larger database is developed, the full stress state model is by far the best model available to predict a resilient modulus response that captures the seasonal environmental changes [39]. Thus, this model can potentially override the adjustment factor approach currently implemented in the EICM, reducing the margin of uncertainty in the predictions.

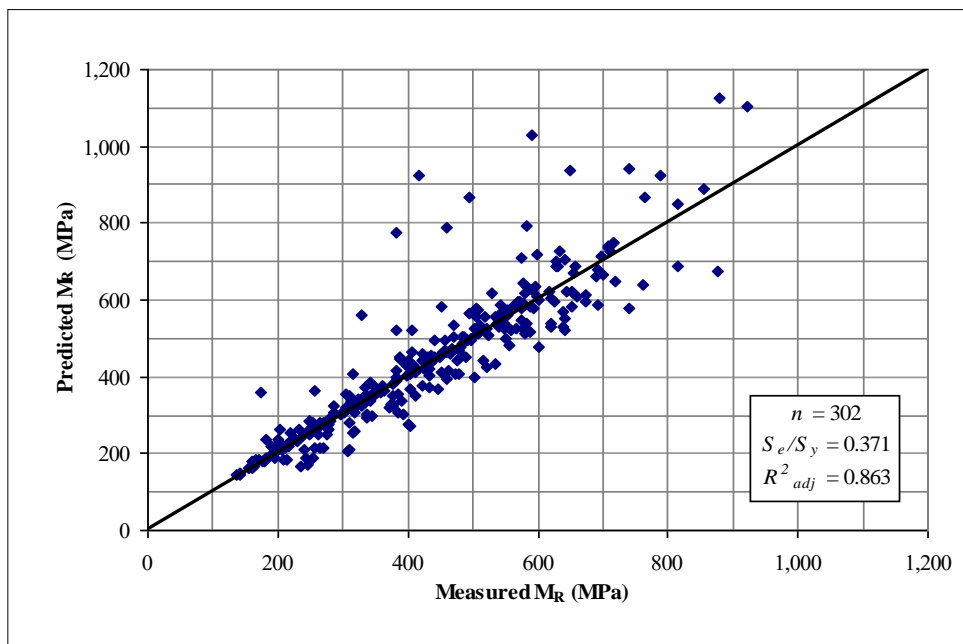


Figure 12
Using the EICM model to estimate the adjustment factor F_u (equation (42))

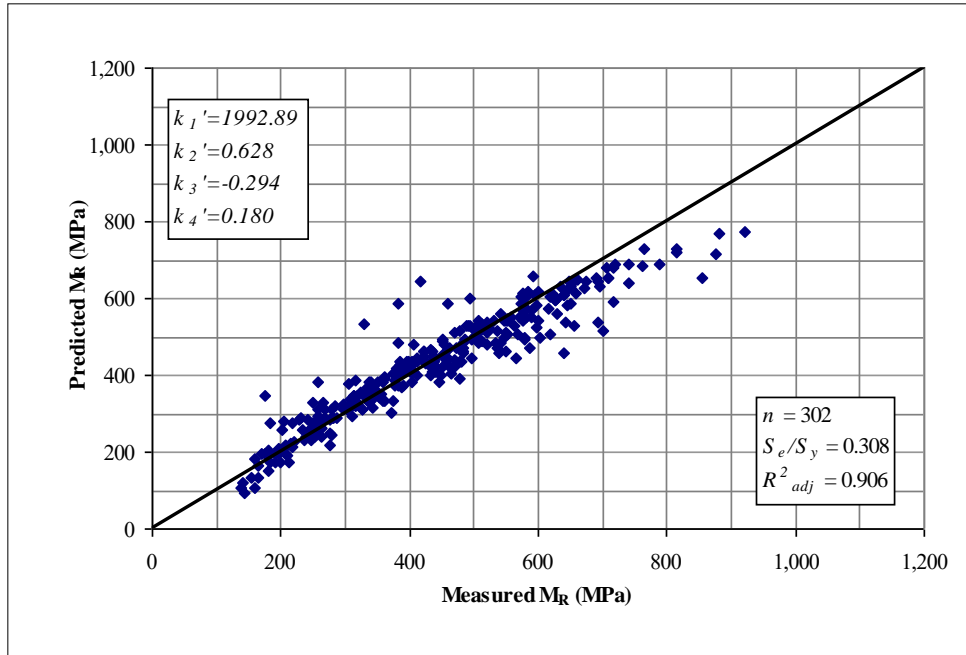


Figure 13
Using the matric suction dependent model (equation (65))

Additional Considerations for Future Revisions of the EICM

Different concerns regarding the methodology employed by the EICM for taking into account the effects of seasonal environmental changes have been reported since the very first MEPDG version was released. Some of the issues reported by the pavement engineering community have been addressed in subsequent versions of the EICM but solutions for some others are still needed. In the following sections, some of the issues reported in the literature are commented.

Climatic Data

Several states in the US have conducted independent studies to validate the EICM, and assess the effects of water content changes on the pavement performance. Some of these states, like New Jersey, have encountered difficulties in matching the predictions made by the EICM for moisture content with field observations [41]. Some studies demonstrated the importance of using accurate climatic data for obtaining realistic pavement performance predictions when using the MEPDG [42-43]. It has been determined that reliable climatic data sets can be obtained by using as many applicable nearby weather stations as possible when generating virtual stations with the MEPDG [42]. However, for some regions it was found that the EICM model in the MEPDG does not contain sufficient and site-specific climatic data for

realistic predictions of moisture and temperature changes in pavement layers. That may explain the discrepancy found between field measured and predicted moisture and temperature for New Jersey and some other states [41].

Therefore, there is a need to examine current and emerging needs for climatic data that can be incorporated in the EICM model. Current efforts are devoted by the Federal Highway Administration to evaluate the quality and suitability of LTPP climatic data for use in MEPDG calibration and pavement analysis. Also, state transportation agencies are focusing on improving local climate characterization methodologies. As a larger and more accurate climatic database is developed for the different regions in the continental US, the uncertainty in the EICM predictions is expected to be reduced.

Limitations in Temperature Profile Predictions for Bound Materials

Discrepancies between field measurements and EICM predicted frost depths for cement treated bases were reported by Rabab'ah and Liang in 2007 [44]. Field monitoring results of moisture and frost depth at an instrumentation site in Ohio were used to evaluate the EICM predictions. Rabab'ah and Liang obtained moisture profiles reasonably consistent with those observed in the measured data. However, they reported that apparently the EICM gives poor predictions of frost depths for bound materials. Rabab'ah and Liang stated that properties, such as thermal conductivity and heat capacity, need to be better quantified for bound base materials. In their study, Rabab'ah and Liang recommended further development of the EICM model capability to account for different types of treated (bound) granular base materials.

Effect of Soil Density on EICM Predictions

One of the general assumptions considered by the EICM model is that all compacted layers are compacted at optimum moisture content and maximum dry density. Also, it is assumed that the density will remain constant along the pavement design life while the moisture content changes towards equilibrium values. These assumptions are based on the fact that most of the soils will be compacted at optimum conditions in the field, and most of the resilient modulus tests results available in the literature were obtained from specimens compacted at optimum conditions. However, it is well known that "as compacted" densities in the field will hardly achieve optimum conditions. It is also known that soil density will not be constant along the pavement design life.

The estimation of the saturated volumetric moisture content depends on the dry density of the soil as explained by equations (1) to (3) in previous sections. As a consequence, soil density

constitutes a fundamental parameter for the EICM in the prediction of moisture content changes. Therefore, by assuming that all compacted layers in a pavement structure achieve optimum conditions during construction, some uncertainty in the EICM moisture predictions may be introduced. A sensitivity analysis in the EICM predictions due to variation of “as compacted” soil density is recommended to determine whether the assumption adopted by the model is convenient.

The assumption that all compacted layers are compacted at optimum conditions may result in an unconservative unbound material characterization as compacted specifications could be met even at dry densities lower than maximum [45]. As a consequence field resilient moduli might be in some cases significantly different than those assumed by the EICM corresponding to optimum conditions. When comparing the predicted performance obtained by using both a modulus at optimum conditions and an average modulus value, Kim et al. observed differences of up to 20% in the permanent strain [45]. Obviously, by considering modulus at maximum dry density, the pavement performance is being over-estimated. Therefore, there is a need for implementing the field compaction scenario in the EICM models for resilient modulus prediction.

OBJECTIVES

There were six major objectives in this study:

1. Conduct FWD testing seasonally for a period of 3 years. Develop formulas to represent the subgrade M_R throughout the year.
2. Develop a web-based software package to interface databases from DOTD and NCHRP soil units so that soil types with associated parameters could be located and downloaded for DOTD roadways as well as other locations in Louisiana.
3. Conduct Shelby tube sampling to a depth of at least 20 ft. on 50% of the research test sites and perform soil classifications on the samples.
4. Compare soil types and strata between the NCHRP soil unit data and Shelby tube data.
5. Assess each site with PavementME to determine subgrade soil M_R using soil data from both the NCHRP soil units and Shelby tube samples over a three-year period.
6. Compare PavementME results with FWD test results for the seasonal changes in the subgrade M_R .

SCOPE

Researchers detected 14 sites from the four major geologic regions in Louisiana. Field testing was conducted on the roadway shoulders at a distance of approximately 4 ft. from the edge of the travel lane. All 14 sites were assessed with the FWD seasonally for a period of at least 3 years. Shelby tube samples were taken from 7 of the 14 research sites. Material from those samples was used to determine the soil type with its associated strata as well as determine the in place subgrade M_R . Samples were then remolded to determine its M_R when compacted at optimum moisture content. A computer software package was developed in order to obtain the soil types with associated data from the NCHRP soil unit database for Louisiana. PavementME was used to assess the 14 research sites for a period of 3 years.

METHODOLOGY

Research Test Site Selection

There are 64 parishes and nine DOTD Districts in Louisiana. Though the premier process would have been to select several test sites in each parish, the feasibility of doing so was prohibitive. Instead, the research team decided to monitor test sites in the four major geologic regions that cover most of the state: Wilcox group, Claiborne group, Holocene Alluvium, and Pleistocene Terraces, as presented in Figure 14. In the Wilcox and Claiborne regions, three test sites were selected so as to better capture variations in those regions. In contrast, four sites were selected in the Holocene and Pleistocene regions due to the fact that those sites spanned larger regions of the state. For instance, the Holocene region basically runs from the top (North) to the bottom (South) of the state and the Pleistocene region runs from Texas (West) to Mississippi (East) of the state, as presented in Figure 14. The specific locations of the 14 test sites are presented in Table 6.

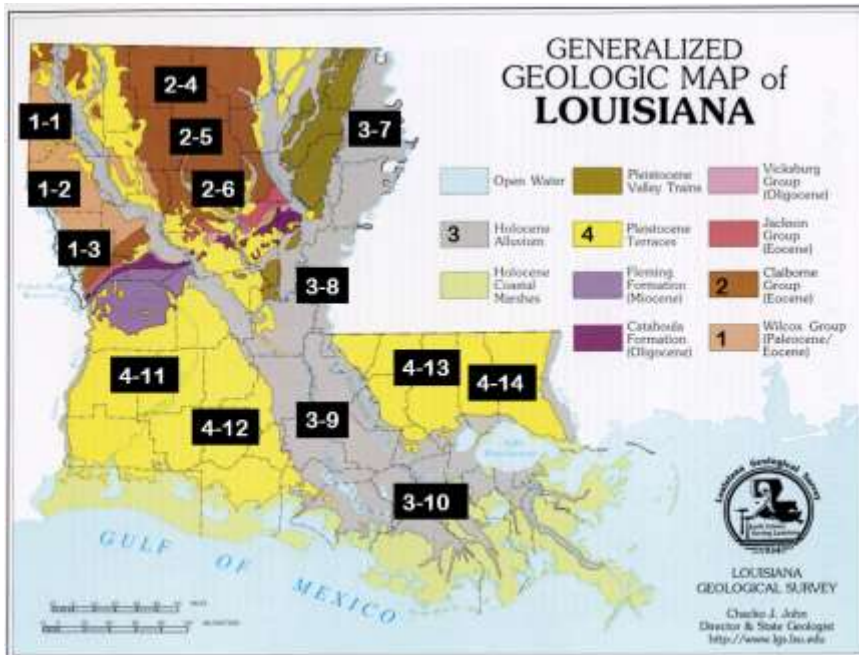


Figure 14
Geologic map of Louisiana with regional locations of 14 sites

Table 6
Locations of the 14 research test sites

Site	Highway	District	Parish	Project Number	CSLM	Latitude	Longitude
1-1	LA 1	4	Caddo	450-02-0020	9.340	32.84678	-93.983156
1-2	US 171	4	Desoto	025-07-0019	1.300	32.212279	-93.836433
1-3	US 171	8	Sabine	025-03-0030	2.600	31.588387	-93.523306
2-4	LA 2	4	Claiborne	085-07-0016	10.300	32.81035	-93.076825
2-5	US 165	5	Jackson	023-06-0066	21.300	32.431747	-92.678199
2-6	LA 34	5	Ouachita	067-08-0010	3.300	32.416962	-92.359725
3-7	US 65	5	Madison	020-07-0020	9.700	32.53441	-91.169194
3-8	US 84	58	Concordia	022-07-0071	8.900	31.605306	-91.670529
3-9	US 71	3	St. Landry	008-05-0035	8.400	30.641305	-91.89723
3-10	LA 1	61	West Baton Rouge	050-07-0067	0.600	30.331319	-91.256442
4-11	US 171	7	Beauregard	024-03-0015	8.800	30.530792	-93.232388
4-12	LA 13	3	Acadia	057-03-0047	17.900	30.461712	-92.411537
4-13	US 61	61	West Feliciana	019-05-0035	9.000	30.903651	-91.342243
4-14	LA 21	62	St. Tammany	030-02-0028	3.000	30.647579	-89.893062

Soil Type Identification

Two methods were used to determine the soil types and their depths: Shelby tube sampling and NCHRP soil unit data. Appendix A presents the soil classification data from Shelby tube sampling conducted at seven test sites. Shelby tube sampling and FWD testing, discussed in detail later, were conducted at approximately 4 ft. from the edge of the travel lane on the shoulder. The shoulder was selected for testing so that traffic control would not be needed. The strata for the soil types were plotted as presented in Figure 15 and will be discussed in more detail later.

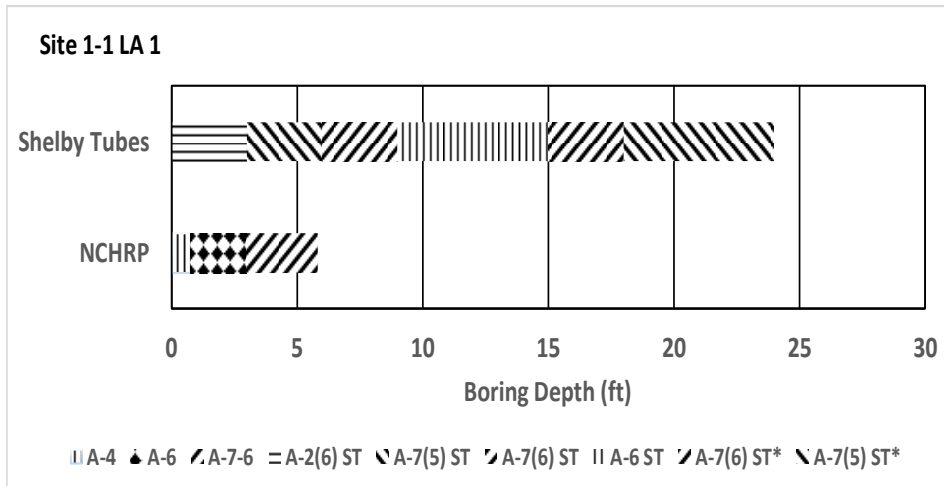


Figure 15
Soil type and strata for LA 1 – Site 1-1

NCHRP soil unit data was acquired in part from the NCHRP 9-23b database [33]. LTRC further developed this application for the purpose of visualizing soil areas beneath DOTD roadways and/or roadway project segments [46].

The application allows for searching by Control Section (format ###-##), Linear Referencing System (LRS ID format ###-##-#-###), Project number (format H.#####.#), or Legacy project number (format ###-##-#####; projects prior to 2010) [46].

After search criteria are entered, the soil areas that intersect with the search location are listed with web page links to the specific natural subgrade soil properties. The user can view onscreen or export a list of soil types to pdf file. The output data for the 14 sites can be found in Appendix B.

Data contained in this GIS web application are:

1. The DOTD LRS ID and Control Section GIS route features developed and maintained by the DOTD, Office of Multimodal Planning, GIS & Mapping Group. The data is available via ArcServer published web services hosted at DOTD.
2. The DOTD Projects information housed in the state LaGov DB2 database. The data is available via ArcServer published web services hosted at DOTD.
3. Links to soil index properties and soil-water characteristic curves for each soil type. The soil properties are sourced from the NCHRP 9-23a project.

Resilient Modulus Testing in the Laboratory

One of the objectives of this research was to determine if the MEPDG algorithms for the relationship between changes in subgrade M_R versus changes in moisture content were similar to those found in Louisiana. This was accomplished by conducting M_R tests on soils obtained from Shelby testing using the AASHTO T-307 M_R method as well as the NCHRP 1-28A M_R method [47-48]. One hundred and ten tests which equates to 55 plotted points, were produced using the AASHTO T-307 M_R method. Eight tests, which equates to 4 plotted points were conducted using the NCHRP 1-28A M_R method. The researchers wanted to determine if any significant differences existed between the two methods when plotted, as presented in Figure 16.

Resilient modulus specimens were tested in their field condition and at their optimum moisture content. Field condition specimens were obtained directly from the Shelby tubes. Remolded specimens were constructed using the standard proctor method and at optimum moisture content [47-48].

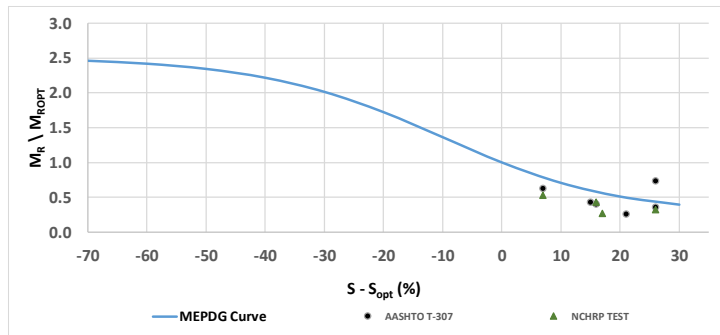


Figure 16
 M_R/M_{Ropt} versus $S-S_{opt}$ example

FWD Tests

Ten points were measured with the FWD for each of the 14 sites. The points were 10 ft. apart. Dynatest's ELMOD 6 backcalculation software was used to obtain the subgrade M_R [49]. The laboratory equivalent M_R was obtained from formulas developed by LTRC [50]. The values from the 10 points were averaged and were considered to represent the M_R for the site from which they were taken from.

Tests were conducted seasonally (4 times per year) for a period of 3 years. The M_R values for all 14 sites were plotted separately. Regression modeling was used to obtain equations so that a M_R value could be calculated for each month of the year. Figure 17 presents the results from FWD and PavementME simulations for Sites 2-5 while the remaining sites will be

discussed in detail later. The values on the x-axis range from 1 to 12 with January corresponding to the number 1 and the rest of the months of the year corresponding respectively with their numerical value. In addition, the sites were also grouped based upon the dominate soil type and regression modeling was used to obtain equations for their relationship, discussed in detail later. The dominate soil types discovered on the research sites were A-4, A-6, and A-7.

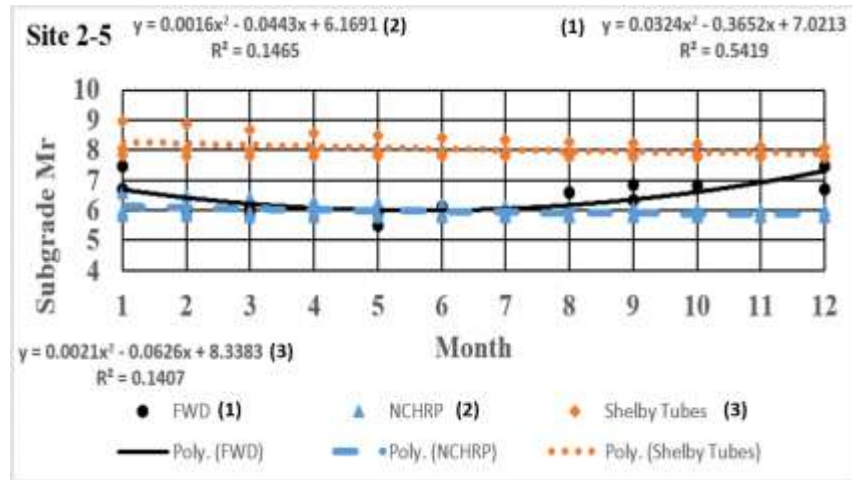


Figure 17
Subgrade M_R seasonal variation results

PavementME Site Assessment

Part of this study was to compare the seasonal changes in the moisture content of the subgrade from PavementME to those obtained from the FWD for a similar three-year time period as presented in Figure 17 [6-8]. The available data points for each month were plotted on the graph. From there, a curve was fit, and the corresponding equation and its R^2 value are shown in Figure 17.

The soil type and its corresponding strata inputs used in PavementME were obtained from the Shelby tube samples and NCHRP soil units while the traffic data and AC inputs were based upon defaults within PavementME itself. The climatic data used in the analysis corresponded with the locations of the research test sites. The output results were plotted on a graph which also contained the FWD results as presented in Figure 17.

DISCUSSION OF RESULTS

Soil Type Identification

Figures 18 to 23 present the soil types and corresponding depths based on data from Shelby tube sampling and NCHRP soil units for Sites 1-2, 2-4, 2-5, 3-8, 4-12, and 4-13, respectively, while Figure 15, previously shown, presented the results for Site 1-1. Appendix B contains the soil types and depths corresponding to NCHRP soil units for the remainder of the sites. One of the objectives for this research study was to determine if Shelby tube samples and NCHRP soil units had similar soil types and depths.

As presented in Figure 15, the first and second soil strata from the Shelby tubes and NCHRP soil units were of different soil types and depths. The soils from the third soil strata from the NCHRP soil units matches with the Shelby tube sample soil type but not depth.

The soil type in the stratas 1 to 3 are similar between the Shelby tube samples and the NCHRP soil unit samples but the depths differ for Site 1-2 as presented in Figure 18.

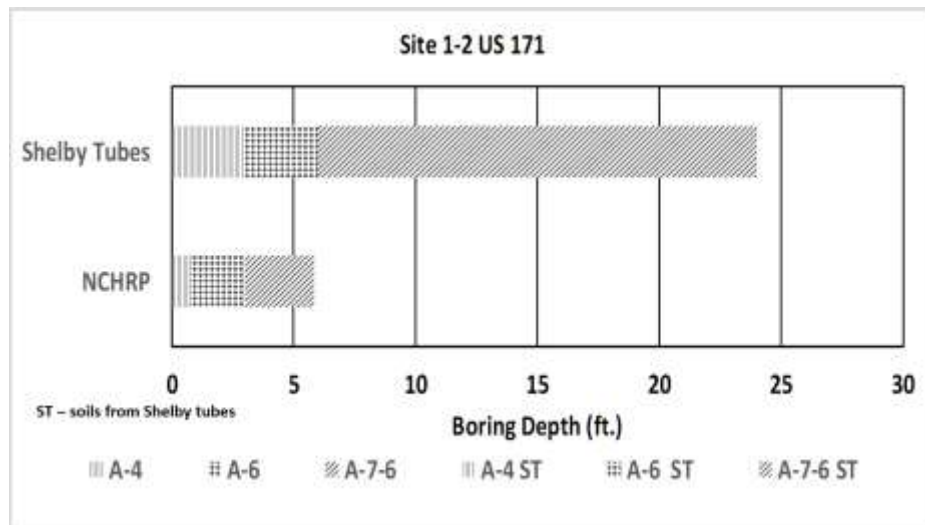


Figure 18
Soil type and strata for US 171 – Site 1-2

Comparison of soil strata for Site 2-4 as presented in Figure 19 indicated that the soil types in the first and second strata were similar between the samples from the Shelby tubes and NCHRP soil units but the depths differed. The soil types and depths from the third strata in the NCHRP soil unit sample differed from the Shelby tube sample.

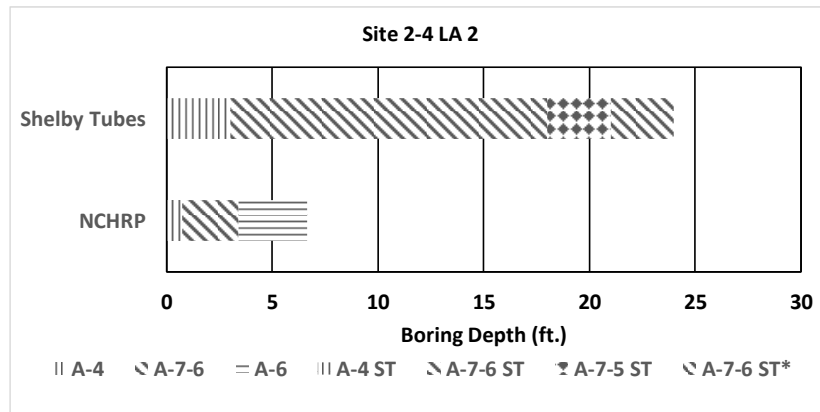


Figure 19
Soil type and strata for Site 2-4; LA 2

The soil types and depths in the first to third strata were different between the Shelby tube samples and the NCHRP soil unit sample, as presented in Figure 20.

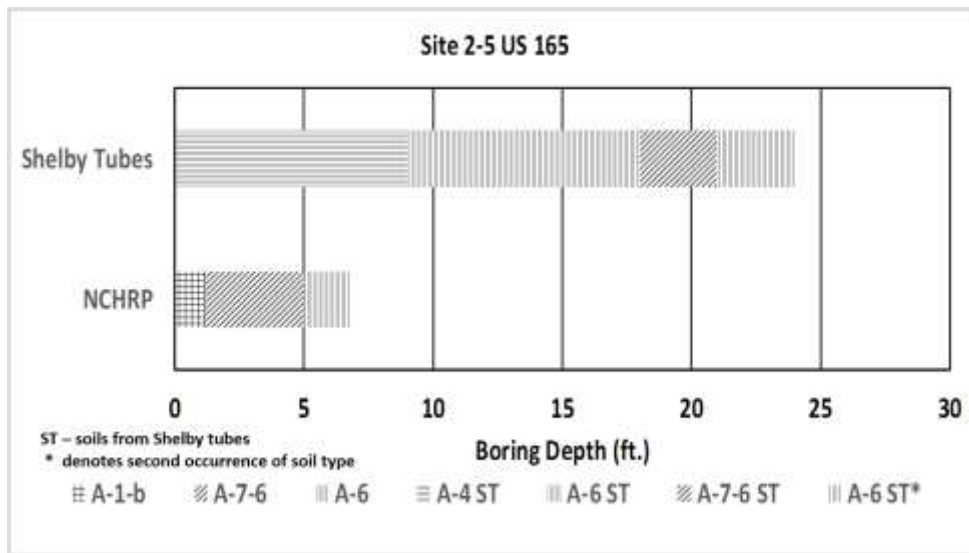


Figure 20
Soil type and strata for Site 2-5; US 165

As presented in Figure 21, the soil types for the first and second strata differ between the Shelby tube sample and NCHRP soil unit sample but the depths differ.

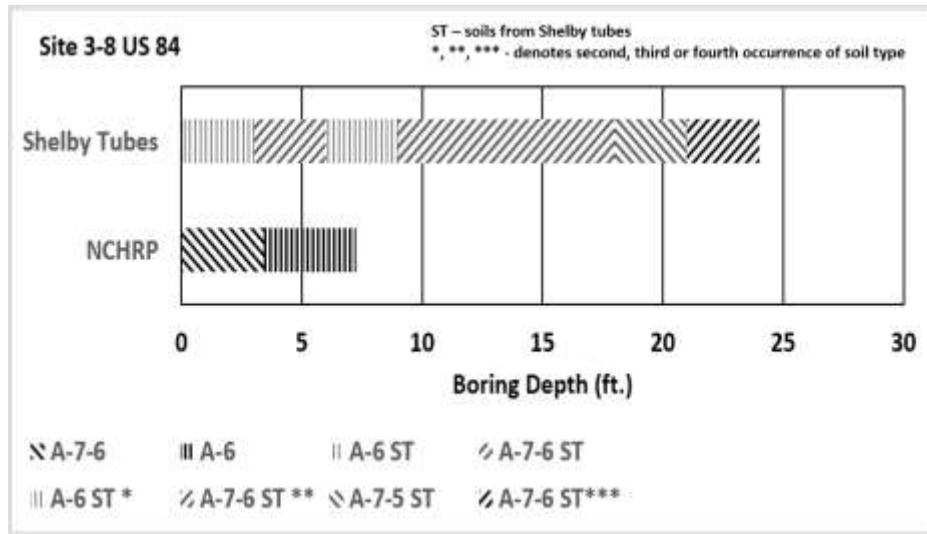


Figure 21
Soil type and strata for Site 3-8; US 84

Regarding Site 4-12, the soil types in the first to third strata from the NCHRP soil unit samples correspond in soil type but not depth to the Shelby tube samples, as presented in Figure 22.

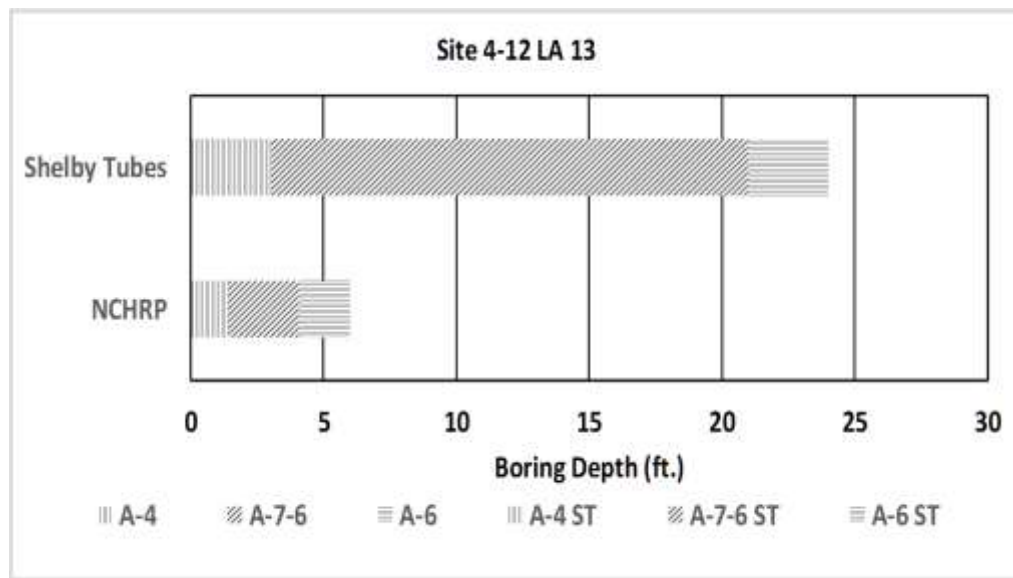


Figure 22
Soil type and strata for Site 4-12; LA 13

The soil types in the first and second strata in the NCHRP soil unit samples and Shelby tube samples differ for Site 4-13 as presented in Figure 23. There is some overlap in soil type between the NCHRP soil unit sample and Shelby tube sample in the third strata of both.

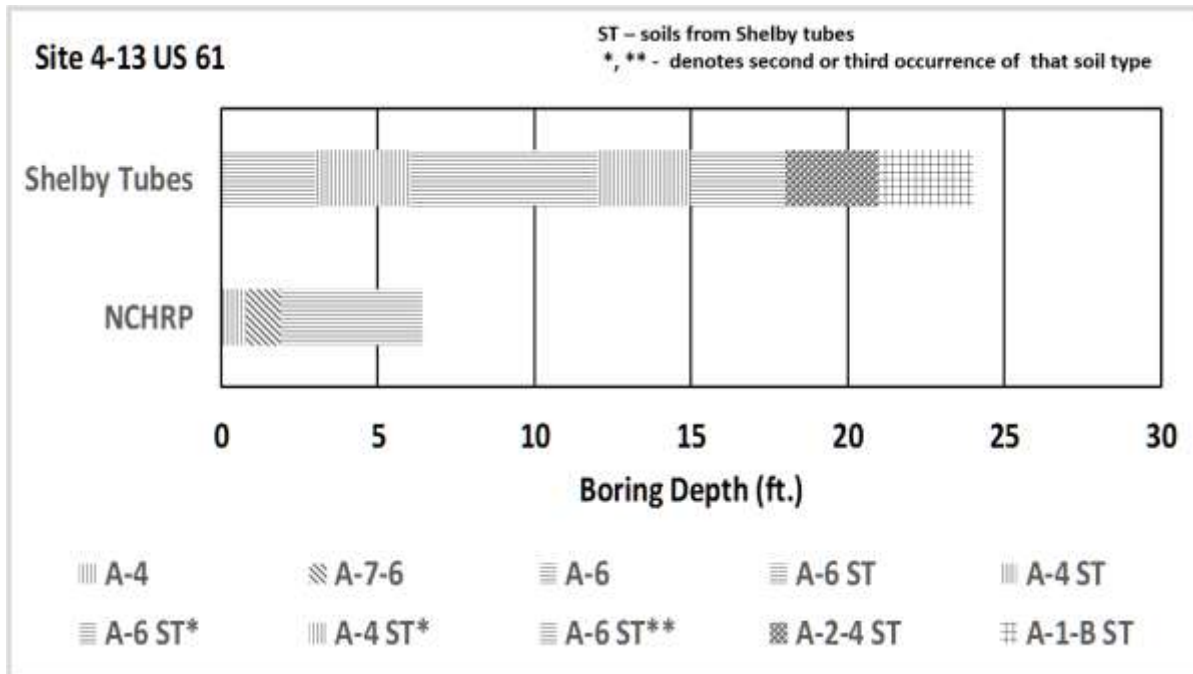


Figure 23
Soil type and strata for site 4-13; US 61

Table 7 presents a summary of the analyses of the soil types in each strata for the NCHRP soil unit samples and Shelby tube samples. Because the depths of each soil type in the strata all differed they will not be presented in Table 7 or discussed any further. The table is arranged such that the soil type in each strata will be referred to as either “soil similar” or “soil different.” Soil similar means that the soil types from the NCHRP soil unit samples were similar to those of the Shelby tube samples whereas soil different means the opposite. Only three strata are shown since that was the maximum amount of strata present in the NCHRP soil unit samples. In the first strata, 43 percent of sites had similar soil types while the second and third strata had 43 percent and 67 percent similar soil types, respectively. The overall average of the similar soil types in the strata was 50 percent. Considering the high variability in soil types that can be found in anyone location, the soil types from the NCHRP soil unit samples may be considered to provide a reasonable estimate of the soils present for the purpose of pavement design [46].

Table 7
Summary of soil type and soil strata comparisons

Site	Strata 1	Strata 2	Strata 3
1-1	Soil different	Soil different	Soil similar
1-2	Soil similar	Soil similar	Soil similar
2-4	Soil similar	Soil similar	Soil different
2-5	Soil different	Soil different	Soil different
3-8	Soil different	Soil different	N/A
4-12	Soil similar	Soil similar	Soil similar
4-13	Soil different	Soil different	Soil similar

Resilient Modulus Laboratory Testing

Figure 24 presents the results of M_R testing from points taken from the seven Shelby tube sites and plotted on the MEPDG EICM curve for fine grain soils [24-27, 51]. The fine grain soils curve was used since the soils obtained from the Shelby tubes samples in this project were primarily fine grained. As shown in that curve there was a large scatter $r^2 = -0.266$ of the data around the MEPDG EICM curve.

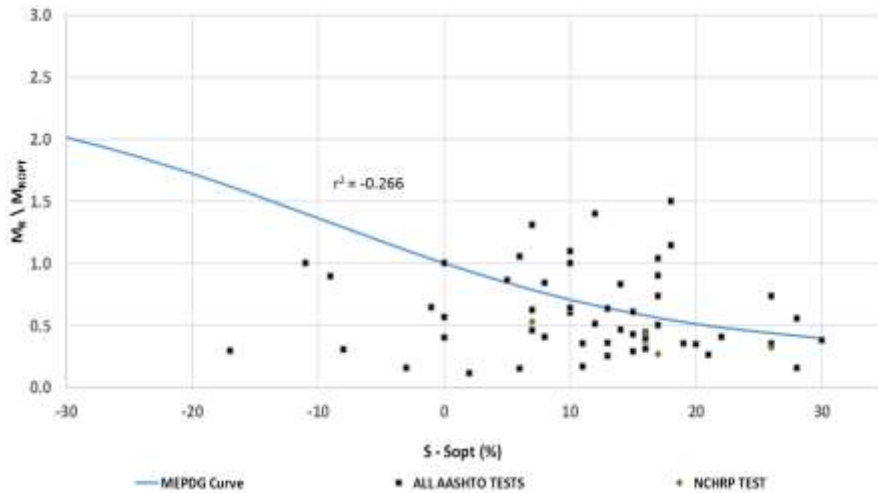


Figure 24
MEPDG EICM model with test points

The authors' theorized that the large scatter of the data around the MEPDG EICM curve occurred due to significant differences between the dry densities of the in place M_R samples and the maximum dry densities of the laboratory remolded M_R samples. Details and validation of that theory were published elsewhere, hence only portions of it will be discussed in this report [51]. The first step in testing this theory was to plot the (in place dry density – maximum (max) dry density) versus (in place moisture content – optimum moisture

content) for each of the soils from the seven Shelby tube sites. Figure 25 presents the results from one of those sites.

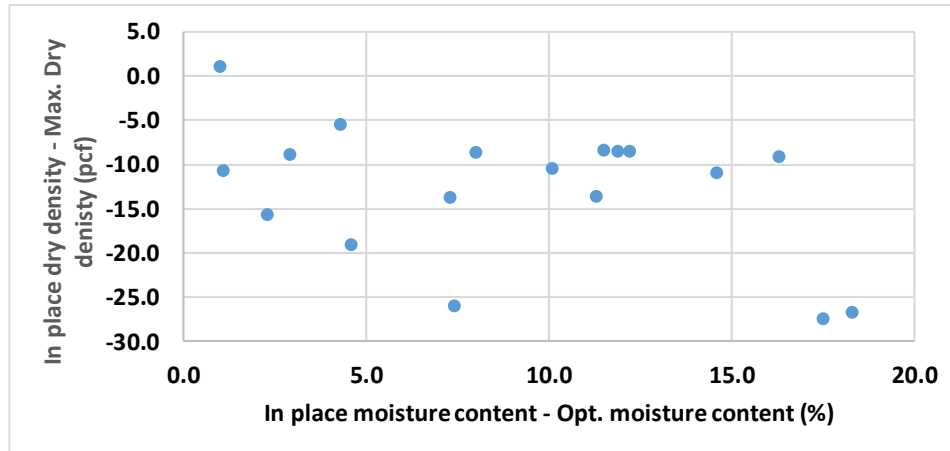


Figure 25

In place moisture content – Opt. moisture content versus in place dry density – maximum dry density relationship

The next step was to select only the data points that were within (\pm) 5 pcf from each site as the authors’ postulated that those data points would better fit the MEPDG EICM curve. Data meeting that criteria were plotted on Figure 26 and will hereafter be referred to as the modified data set. On a previous study, LTRC conducted M_R tests on 4 soils from Louisiana roadways who soils were molded using standard proctor energy with plasticity indices of 53, 26, 17, and 7 [52]. Those points were shown on Figure 26 as well.

As theorized by the authors, the scatter of the data from the modified data set as presented in Figure 26 had an $r^2 = -0.787$ as opposed to an r^2 of -0.266 of the original data set as presented in Figure 25. This implies the following:

1. When the in-place density of the field specimens are within \pm 5 pcf of the remolded sample using standard proctor compactive energy, one can expect the (M_R/M_{ROPT}) plotted in Figure 26 to be reasonably similar.
2. The MEPDG EICM curve may not represent M_R changes in the field since in place field densities of natural subgrade are generally different from remolded samples in the laboratory using standard proctor compactive energy.
3. Remolded samples using standard proctor compactive energy follow a trend similar to the MEPDG EICM curve for the soils tested in this study.

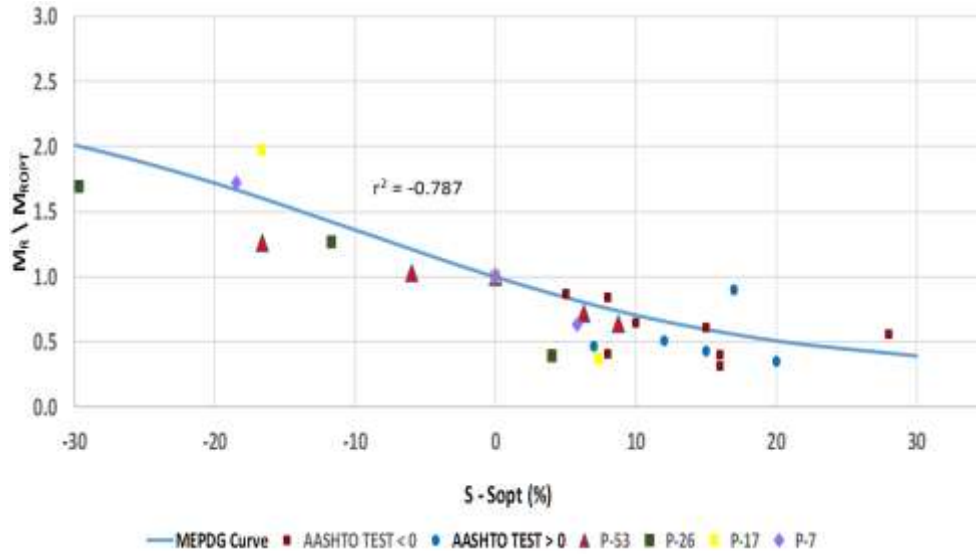


Figure 26
MEPDG EICM curve with refined data set

Seasonal Subgrade M_R Results from FWD Testing and PavementME

Figure 27 presents the seasonal changes in subgrade M_R from FWD testing and PavementME for Site 1-1. Regarding the FWD testing, it is evident that there was little variation in the seasonal variation in the subgrade M_R based upon the shape of the curve. The overall yearly average was 7.0 ksi. For this site, soil data from the NCHRP soil unit data and Shelby tube samples were available. As with the FWD tests, there was little seasonal variation in the subgrade M_R . There was, however, a difference in the magnitude of the data between the FWD and the PavementME data sets with the PavementME data sets having the higher magnitude. The yearly average for the subgrade M_R for the Shelby tubes and NCHRP soil unit data sets were 7.63 and 8.0, respectively. For this site, PavementME consistently produced M_R values greater than the FWD yet it is the authors' opinions that the difference in magnitude between the FWD and the Shelby tubes and NCHRP subgrade M_R values (0.63 and 1.0 ksi) are not significant. Note: For the purposes of determining whether the averages between data sets are similar or different, data sets whose difference in yearly average were less than or equal to 1.5 ksi were used with averages less than 1.5 ksi being similar and vice versa.

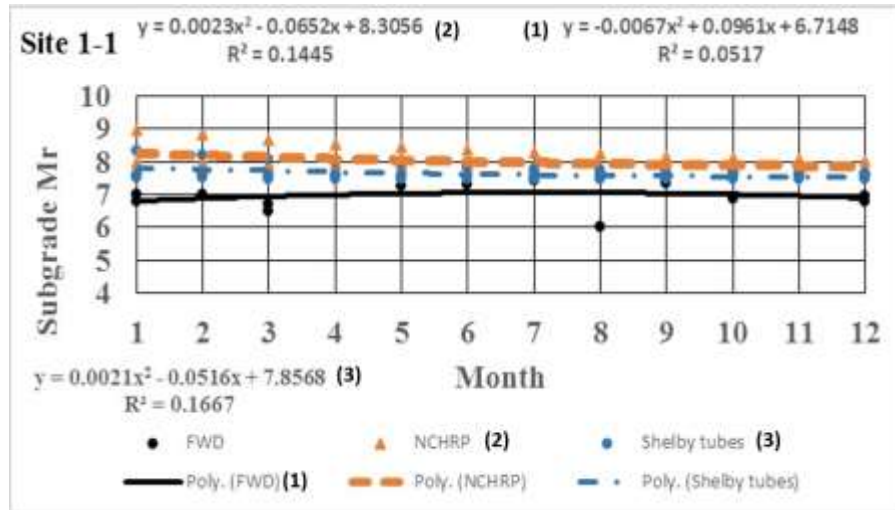


Figure 27
Seasonal variation in subgrade M_R from FWD and PavementME for Site 1-1

Figure 28 presents the results for Site 1-2. The FWD test results indicated that there were only minor changes in the subgrade M_R throughout the seasons for the years tested in this study. The overall average of the subgrade M_R was 6.1 ksi. For this site data was available for Shelby tube samples as well as the NCHRP soil unit data set. As presented in Figure 28, the results from the PavementME analyses indicated that the results from the Shelby tube and NCHRP data set were nearly identical and both had values higher than the FWD data set. The overall average of the subgrade M_R was 7.4 and 7.5 ksi for the NCHRP and Shelby tube data set, respectively. The difference between the overall subgrade M_R between the FWD and PavementME (NCHRP-Shelby tube) data sets was approximately 1.35 ksi. As with Site 1-1, the authors feel that this was not significantly different from an engineering standpoint.

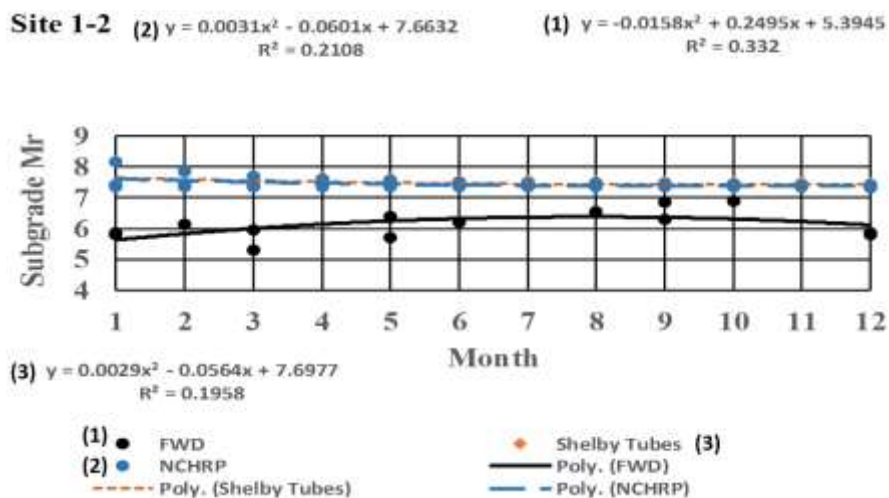


Figure 28
Seasonal variation in subgrade M_R from FWD and PavementME for Site 1-2

Figure 29 presents the results for Site 1-3. As with the previously discussed sites, there were minimal seasonal variation in the subgrade M_R from the FWD tests. The yearly overall subgrade M_R average was 7.4 ksi. On this site, soil data was only available from the NCHRP soil unit data. Similar to the previously discussed sites, there was only minimal differences between the FWD data set and PavementNE data set and the PavementME data set had values higher than the FWD data set. The overall subgrade M_R average for the PavementME data set was 7.9 ksi. The difference between the overall average between the FWD and PavementME data set was approximately 0.5 ksi, which, in the authors' opinions, is insignificant.

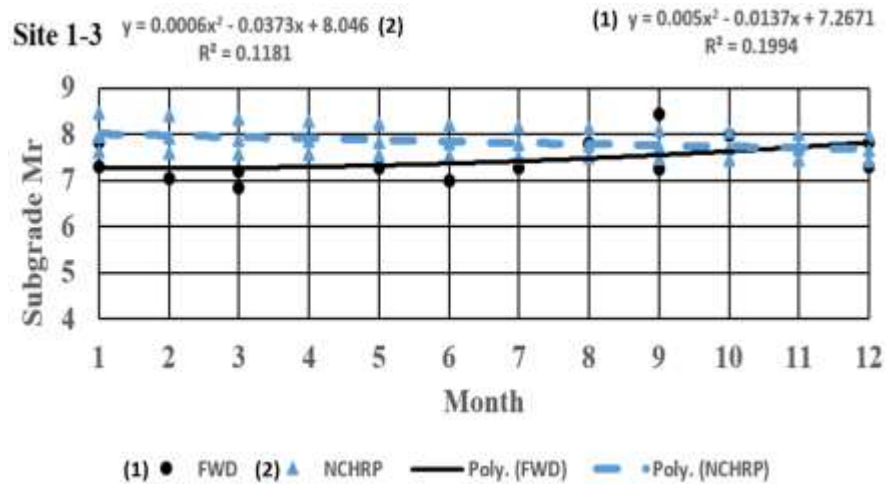


Figure 29
Seasonal variation in subgrade M_R from FWD and PavementME for Site 1-3

Figure 30 presents the seasonal changes in the subgrade M_R from FWD testing and PavementME analysis for Site 2-4. As with the previous sites, there was minimal seasonal variation in the subgrade M_R based upon FWD tests and the overall yearly average was 9.6 ksi. For this site, soils data was available from both the NCHRP soil unit data and Shelby tube samples. The seasonal variation in the subgrade M_R from PavementME for the NCHRP soil unit and Shelby tube data set was similar and the overall yearly averages were 7.9 and 7.5 ksi, respectively. For this site the trend difference between the FWD and PavementME subgrade M_R data sets differed in two ways. First the data sets from the PavementME analyses produced subgrade M_R values less than the FWD in contrast to the previous sites. Second, the magnitude of the overall yearly averages between the FWD data set and PavementME data were 1.7 and 2.1 ksi for the NCHRP soil unit data and Shelby tube data.

In this case, it is the authors' opinions that the differences in subgrade M_R is somewhat significant.

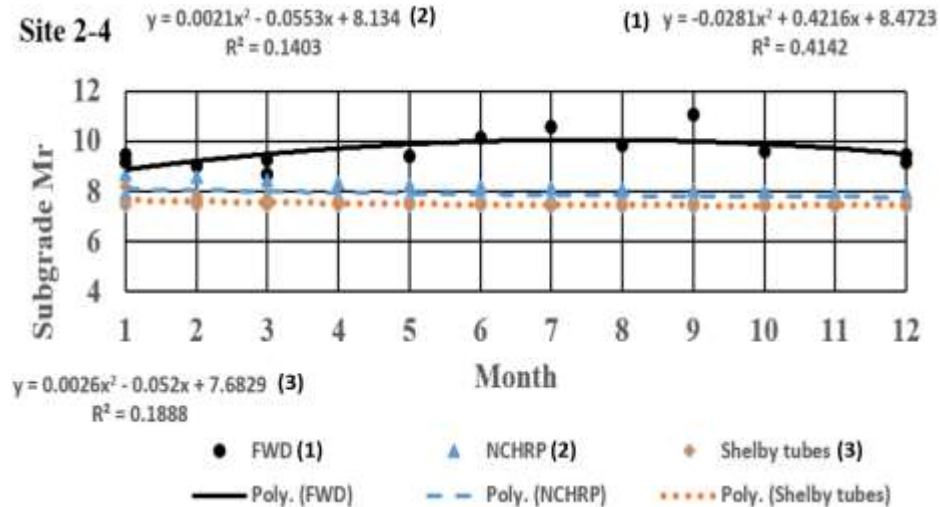


Figure 30
Seasonal variation in subgrade M_R from FWD and PavementME for Site 2-4

Figure 17 presents the seasonal changes in the subgrade M_R from FWD testing and PavementME analysis for Site 2-5. Based on the results from the FWD tests, there was little variation in the subgrade M_R and the overall yearly average was 6.5 ksi. For this site, soil data was available from the NCHRP soil units and Shelby tube samples. The PavementME results for the NCHRP soil unit data analysis produced a curve which was generally below the curve for the FWD tests and the subgrade M_R overall average was 6.0 ksi. This implies that there was no significant difference between these two groups. In contrast, the results from the PavementME analysis for the Shelby tube soil samples produced a curve that was greater than the FWD data set and its average was 8.0. In this case, the results from the PavementME analysis for the Shelby tube data was different than both the FWD data set and the PavementME analysis from the NCHRP soil units.

Figure 31 presents the seasonal changes in the subgrade M_R from FWD testing and PavementME analysis for Site 2-6. As with the previous sites, there was minimal variation in the subgrade M_R for the FWD data set and the overall yearly average was 10.5 ksi. In contrast to most of the previous sites with the exception of Site 2-5, the PavementME analysis with the NCHRP soil unit data set produced a curve with subgrade M_R values less than the FWD data set. The overall average for the subgrade M_R from the PavementME data set was 8.2 ksi which was 2.3 ksi less than the overall average for the FWD data set. The authors consider this difference to be significant.

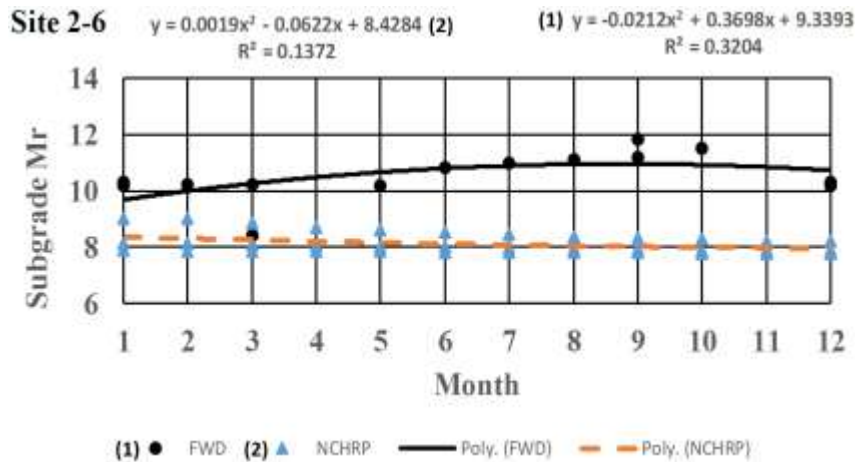


Figure 31
Seasonal variation in subgrade M_R from FWD and PavementME for Site 2-6

Figure 32 presents the seasonal changes in the subgrade M_R from FWD testing and PavementME analysis for Site 3-7. Similar to the previous sites, there was minimal variation in the subgrade M_R for the FWD data set and the overall yearly average was 5.9 ksi. The results from the PavementME analysis using soil data from the NCHRP soil unit data set indicated that minimal variation in the subgrade M_R occurred. The overall average was 7.2 ksi which was 1.3 ksi greater than the subgrade M_R from the FWD data set. The authors considered the differences between the overall averages to be insignificant.

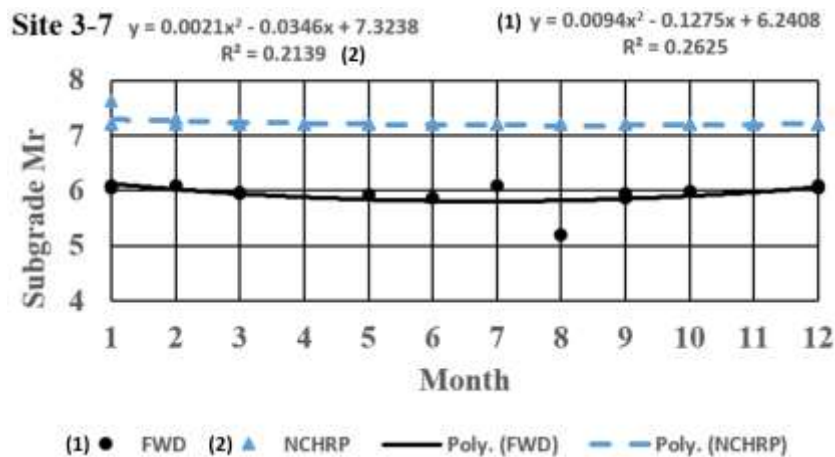


Figure 32
Seasonal variation in subgrade M_R from FWD and PavementMR for Site 3-7

Figure 33 presents the seasonal changes in the subgrade M_R from FWD testing and PavementME analysis for Site 3-8. The FWD test results indicated that there were only minor changes in the subgrade M_R throughout the seasons for the years tested in this study.

The overall average of the subgrade M_R was 5.2 ksi. The results from the PavementME analyses indicated that the results from the NCHRP data set had values higher than the FWD data set. The overall average of the subgrade M_R were 8.0 ksi for the NCHRP soil unit and Shelby tube data. The difference between the overall subgrade M_R between the FWD and PavementME NCHRP soil unit and Shelby tube data sets were approximately 2.8 ksi. It is the authors' opinions that this was significantly different from an engineering standpoint.

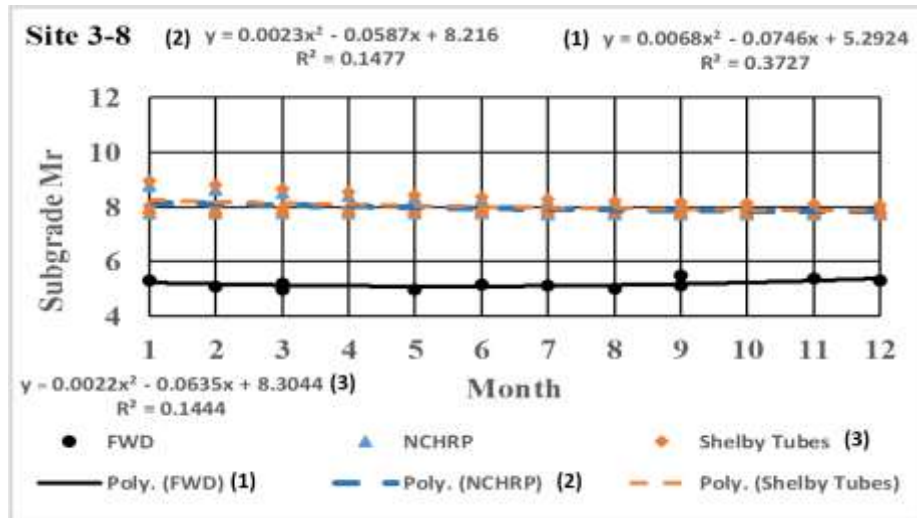


Figure 33
Seasonal variation in subgrade M_R from FWD and PavementME for Site 3-8

Figure 34 presents the results for Site 3-9. As with the previously discussed sites, there was minimal seasonal variation in the subgrade M_R from the FWD tests. The yearly overall subgrade M_R average was 5.1 ksi. On this site, soil data was only available from the NCHRP soil unit data. The PavementME data set had values higher than the FWD data set. The overall subgrade M_R average for the PavementME data set was 7.1 ksi. The difference between the overall average between the FWD and PavementME data set was approximately 2.0 ksi, which is, in the authors' opinions, significant.

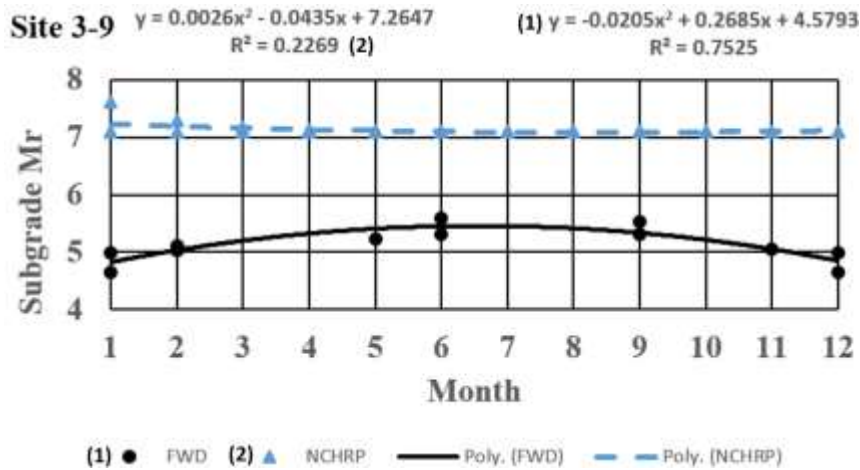


Figure 34
Seasonal variation in subgrade M_R from FWD and PavementME for Site 3-9

Figure 35 presents the seasonal changes in the subgrade M_R from FWD testing and PavementME analysis for Site 3-10. The FWD test results indicated that there were only minor changes in the subgrade M_R throughout the seasons for the years tested in this study. The overall average of the subgrade M_R was 5.6 ksi. For this site, data were available from the NCHRP data set only. As presented in Figure 35, the results from the PavementME analyses indicated that the results from NCHRP data set were larger than the FWD data set. The overall average of the subgrade M_R was 7.9 for the NCHRP data set. The difference between the overall subgrade M_R between the FWD and PavementME NCHRP data sets was 2.3 ksi. It is the authors' opinions that this was significantly different from an engineering standpoint.

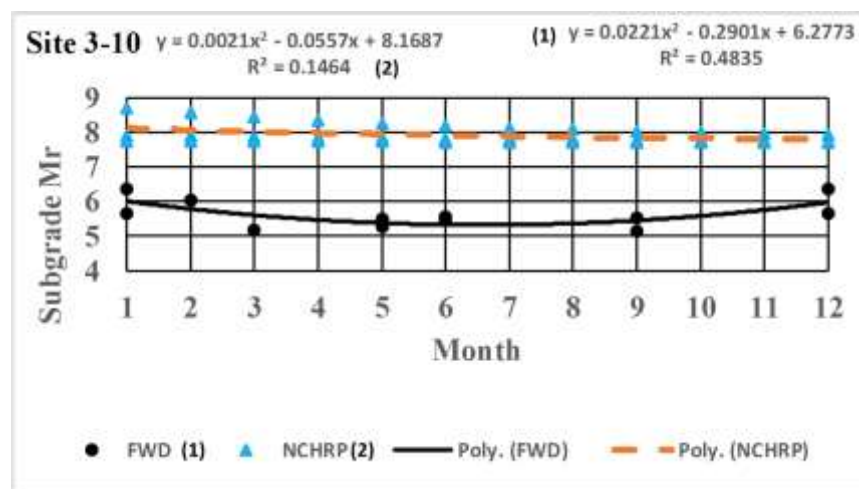


Figure 35
Seasonal variation in subgrade M_R from FWD and PavementME for Site 3-10

Figure 36 presents the results for Site 4-11. As with the previously discussed sites, there was minimal seasonal variation in the subgrade M_R from the FWD tests. The yearly overall subgrade M_R average was 5.2 ksi. On this site, soil data was only available from the NCHRP soil unit data. The PavementME data set had M_R values higher than the FWD data set. The overall subgrade M_R average for the PavementME data set was 8.0 ksi. The difference between the overall average between the FWD and PavementME data set was approximately 2.7 ksi, which in the authors' opinions is significant.

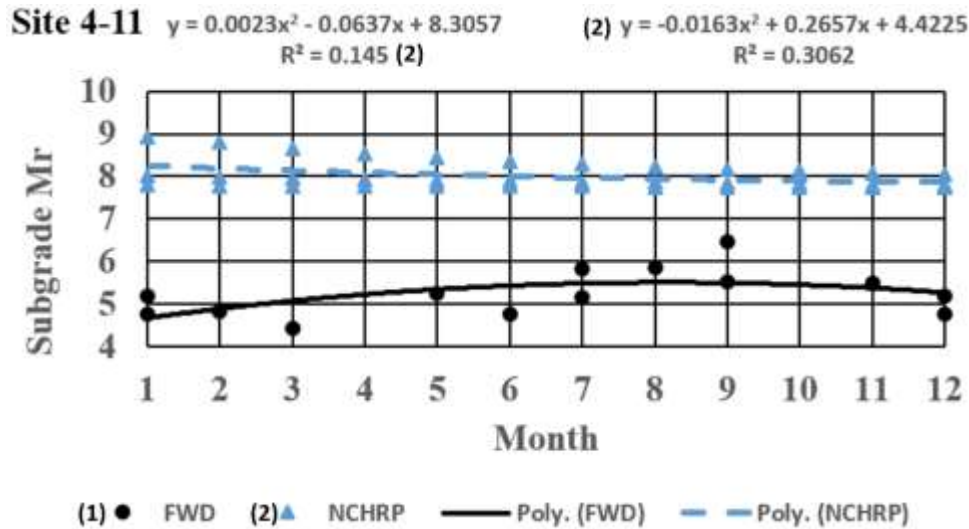


Figure 36
Seasonal variation in subgrade M_R from FWD and PavementME for Site 4-11

Figure 37 presents the results for Site 4-12. The FWD test results indicated that there were only minor changes in the subgrade M_R throughout the seasons for the years tested in this study. The overall average of the subgrade M_R was 7.0 ksi. For this site, data were available for Shelby tube samples as well as the NCHRP data set. As presented in Figure 37, the results from the PavementME analyses indicated that the results from the Shelby tube and NCHRP data set were nearly identical and both had values higher than the FWD data set. The overall average of the subgrade M_R was 7.9 and 7.5 ksi for the NCHRP and Shelby tube data set, respectively. The difference between the overall subgrade M_R between the FWD and PavementME (NCHRP-Shelby tube) data sets was approximately 0.7 ksi. It is the authors' opinions that this was not significantly different from an engineering standpoint.

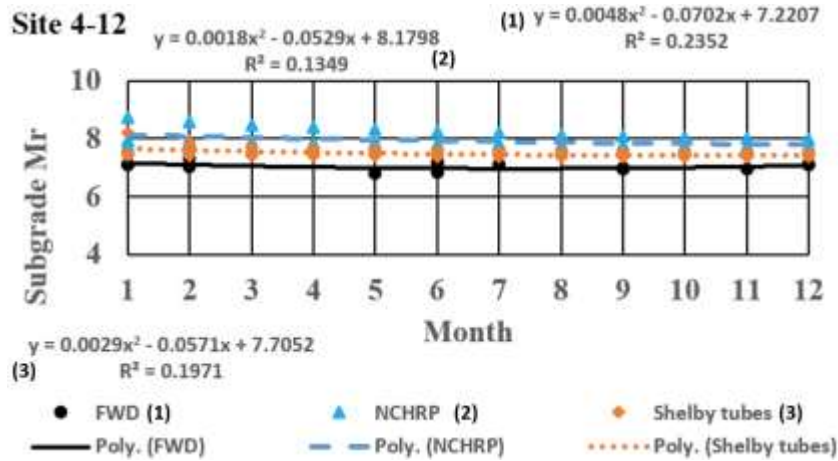


Figure 37
Seasonal variation in subgrade M_R from FWD and PavementME for Site 4-12

Figure 38 presents the seasonal changes in the subgrade M_R from FWD testing and PavementME analysis for Site 4-13. The FWD test results indicated that there were only minor changes in the subgrade M_R throughout the seasons for the years tested in this study. The overall average of the subgrade M_R was 14.0 ksi. For this site, data were available for Shelby tube samples as well as the NCHRP data set. As presented in Figure 38, the results from the PavementME analyses indicated that the results from the Shelby tube and NCHRP data set were somewhat similar and both had values lower than the FWD data set. The overall average of the subgrade M_R was 7.9 and 8.3 ksi for the NCHRP and Shelby tube data set, respectively. The difference between the overall subgrade M_R between the FWD and PavementME (NCHRP-Shelby tube) data sets was approximately 5.9 ksi. It is the authors' opinions that this was significantly different from an engineering standpoint.

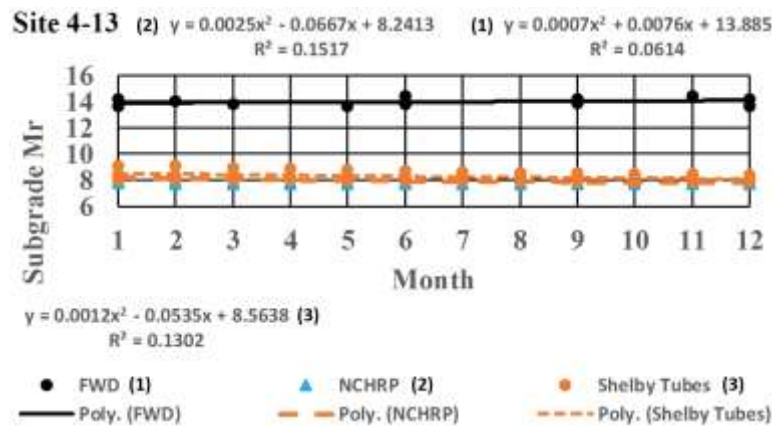


Figure 38
Seasonal variation in subgrade M_R from FWD and PavementME for Site 4-13

Figure 39 presents the results for Site 4-14. As with the previously discussed sites, there was minimal seasonal variation in the subgrade M_R from the FWD tests. The yearly overall subgrade M_R average was 7.0 ksi. On this site, soil data was only available from the NCHRP soil unit data. There was a significant difference between the FWD data set and PavementME data set and the PavementME data set had values higher than the FWD data set. The overall subgrade M_R average for the PavementME data set was 10.6 ksi. The difference between the overall average for the FWD and PavementME data set was approximately 3.6 ksi, which in the authors' opinions is significant.

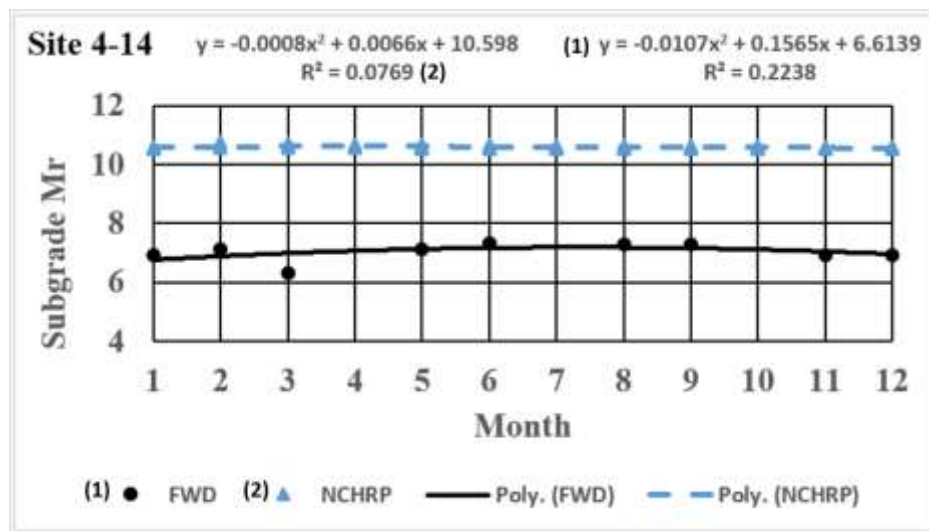


Figure 39
Seasonal variation in subgrade M_R from FWD and PavementME for Site 4-14

Summary of Subgrade M_R Results from FWD Testing and PavementME Analyses

Table 8 presents a summary of the subgrade M_R test results from FWD testing and the PavementME analyses using soil types from the NCHRP soil units and Shelby tube samples. For the comparisons, the FWD test results for the subgrade M_R were used as the control. Based upon the results, 43 percent of the PavementME results where the soil types and depths were taken from the NCHRP soil units were similar to the results from FWD testing. Regarding the PavementME results using soil types and depths from the Shelby tube samples, only 43 percent were similar to the results from FWD testing. Therefore, based upon the locations of testing within Louisiana, soil types with associated strata depths, and number of samples used in the analyses, the NCHRP soil unit and Shelby tube samples equally matched the FWD test results. This implies that the NCHRP soil unit samples may be used with confidence.

Table 9 presents the comparison of the NCHRP soil unit samples with Shelby tube samples from the PavementME analysis. Based upon the results, 86 percent of the samples were

similar. Regarding PavementME analyses, NCHRP soil unit samples may be confidently used as a substitute for soil samples acquired from the field.

Table 8
Summary of comparisons between FWD and PavementME data sets

Site	FWD	PavementME (NCHRP soil unit data set)	PavementME (Shelby tube data set)
1-1	Control	Similar	Similar
1-2	Control	Similar	Similar
1-3	Control	Similar	N/A
2-4	Control	Different	Different
2-5	Control	Similar	Different
2-6	Control	Different	N/A
3-7	Control	Similar	N/A
3-8	Control	Different	Different
3-9	Control	Different	N/A
3-10	Control	Different	N/A
4-11	Control	Different	N/A
4-12	Control	Similar	Similar
4-13	Control	Different	Different
4-14	Control	Different	N/A

Table 9
Summary of comparisons for subgrade M_R from PavementME analyses

Site	PavementME (NCHRP soil unit data set)	PavementME (Shelby tube data set)
1-1	Similar	Control
1-2	Similar	Control
2-4	Similar	Control
2-5	Different	Control
3-8	Similar	Control
4-12	Similar	Control
4-13	Similar	Control

Summary of FWD Test Results when Grouped by Soil Type

Table 10 presents the groups of sites per soil type. The grouping occurred by determining the predominate soil type and strata depth for each soil type in the top 5 ft. to 7 ft. of the subgrade based upon information from the NCHRP soil unit data in Appendix B.

Table 10
Groups of sites per soil type

A-4 sites	A-6 sites	A-7 sites
1-3	1-1	2-4
2-6	1-2	2-5
4-11	3-10	3-7
---	4-13	3-8
---	4-14	3-9
---	---	4-12

Figures 40 to 42 presents the graphs for each soil type. The points shown in each graph represents the average subgrade M_R value obtained from FWD testing for each month of the year. For the A-4 soil type, the curve fitted to the data had an r^2 value of 0.2067 and the equation is presented in Figure 40. Figure 41 presents the results for the A-6 soil type. The curve obtained had an r^2 value of 0.1243. Regarding the A-7 soil type, the curve fitted had an r^2 value of 0.0709, as presented in Figure 42.

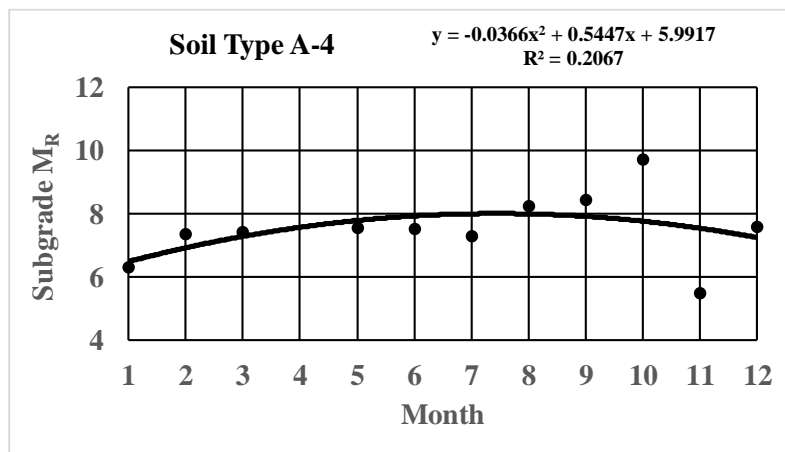


Figure 40
Subgrade M_R values for A-4 soils

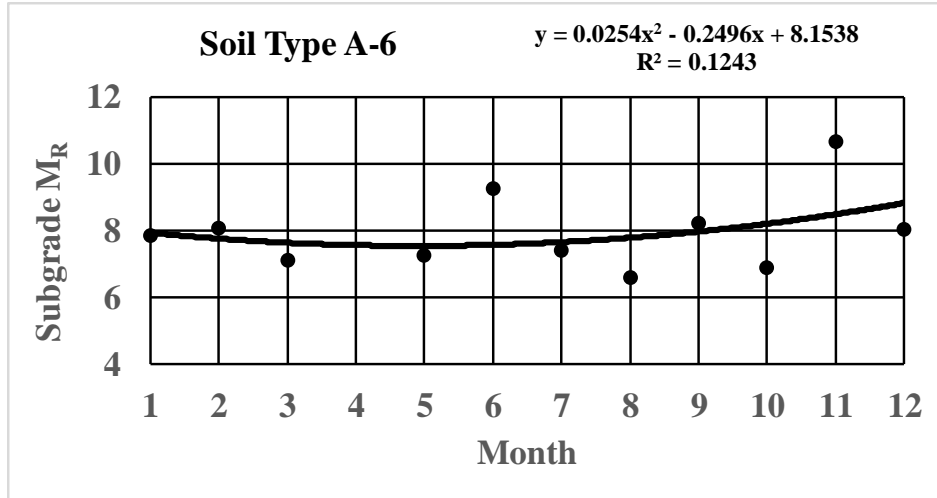


Figure 41
Subgrade M_R values for A-6 soils

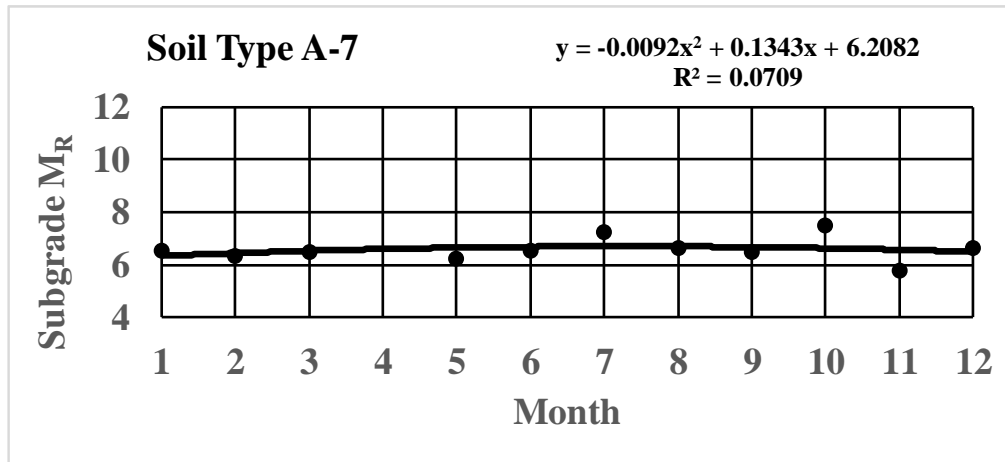


Figure 42
Subgrade M_R values for A-7 soils

Comparison of FWD Subgrade M_R Data to NCHRP Subgrade M_R Data

Table 11 presents a comparison of subgrade M_R data from FWD tests and NCHRP soil unit data. The data from the FWD was obtained by taking the yearly average of the subgrade M_R as previously discussed. Subgrade M_R data presented in Table 11 for the NCHRP soil unit data was obtained by taking the weighted average of the M_R data. For example, using data for Site 1-1 from Appendix B, the weighted average subgrade M_R (10.2 ksi) equals $\{(22,365*9.1+10,711*26.8+6,648*34.3)/70.2\}/1000$, as presented in Table 11.

Values in the difference column (Table 11) were obtained by subtracting the FWD M_R from the NCHRP M_R . If the difference values were less than 1.5 ksi, then the subgrade M_R obtained from FWD tests and NCHRP soil unit data were considered similar; otherwise they were considered different. Using that criteria, only 14.3 percent of the NCHRP soil unit values were similar to the FWD test values.

Table 11
FWD subgrade M_R versus NCHRP subgrade M_R

Site	FWD M_R (ksi)	NCHRP M_R (ksi)	Difference (ksi)	Comment
1-1	7.0	10.2	3.2	Different
1-2	6.1	10.2	4.1	Different
1-3	7.4	14.4	7.0	Different
2-4	9.6	10.6	1.0	Similar
2-5	6.5	15.7	9.2	Different
2-6	10.5	15.1	4.6	Different
2-7	5.9	14.0	8.1	Different
3-8	5.2	8.0	2.8	Different
3-9	5.1	5.0	-0.1	Similar
3-10	5.6	8.7	3.1	Different
4-11	5.2	13.8	8.6	Different
4-12	7.0	9.6	2.6	Different
4-13	14.0	10.5	-3.5	Different
4-14	7.0	14.7	7.7	Different

CONCLUSIONS

LTRC has conducted an extensive research project to determine the seasonal variation in the subgrade M_R from 14 sites throughout Louisiana. Each of these sites were on high volume roads and all tests were conducted on their shoulders. The study (1) conducted FWD testing on the 14 sites seasonal for a period of at least 3 years, (2) developed an online web application to determine the soil types throughout Louisiana based upon NCHRP soil units, (3) obtained Shelby tube samples from seven of the 14 sites and conducted soil classifications on the samples, and (4) conducted an assessment of the 14 sites with PavementME using soil data from both Shelby tube samples and NCHRP soil units when available.

FWD tests were conducted on the 14 research test sites and equations were developed for each site. The FWD tests were then grouped together based upon the predominate soil type at each site which were, A-4, A-6, and A-7. The corresponding equations for the A-4, A-6, and A-7 soil types had R^2 values 0.2067, 0.1243, and 0.0709, respectively.

Software was developed to interface with the NCHRP soil units for Louisiana and databases from DOTD such as LRS ID, control section GIS route maps, and LaGov DB2 database. The software was used to determine the soil type and soil strata present at each of the 14 research sites. Shelby tube sampling occurred at the seven of the 14 research sites. The soil types and strata were plotted for all 14 sites using data from both NCHRP soil units and Shelby tube sampling. Where data was available from both, comparisons were made. Only three strata were compared since that was the maximum amount of strata present in the NCHRP soil unit samples. In the first and second soil strata, 43 percent of the sites had similar soil types while the third strata 67 percent similar soil types. The overall average of the similar soil types in the strata were 50 percent. Considering the high variability in soil types that can be found in anyone location, the soil types from the NCHRP soil unit samples may be considered to provide a reasonable estimate of the soils present for the purpose of pavement design.

PavementME was used to conduct an analysis of the seasonal changes in the subgrade M_R from the 14 sites using soils data from both the NCHRP soil units and Shelby tube samples. These results were compared with the results from FWD tests, which was also used as the control. Based upon the results, 43 percent of the PavementME results where the soil types and depths were taken from the NCHRP soil units and Shelby tube samples were similar to the results from FWD testing. Therefore, based upon the locations of testing within

Louisiana, soil types with associated strata depths, and number of samples used in the analyses, the NCHRP soil unit samples matched the FWD test results as well as the Shelby tube samples. Comparisons of the subgrade M_R values produced by PavementME for the Shelby tube and NCHRP soil unit data indicated that they were similar 86 percent of the time. Therefore, based upon the comparisons in this research, it is reasonable to use NCHRP soil unit data as a substitute for Shelby tube samples when Shelby tube samples are not available.

RECOMMENDATIONS

In this study, all FWD testing was conducted on the shoulders of high volume roadways. It would be beneficial if additional testing were conducted on the roadway pavement itself to determine if similar variations occur there as well. FWD testing should also be conducted on lower volume roads to further refine the models developed in this study.

Based upon the assessment methods and comparisons between samples from NCHRP soil units and Shelby tube sampling, it is recommended that soil data from NCHRP soils units be used whenever soil samples are unavailable from either Shelby tube samples or subgrade soil surveys.

ACRONYMS, ABBREVIATIONS, AND SYMBOLS

AASHTO	American Association of State Highway and Transportation
AC	Asphaltic concrete
ASU	Arizona State University
CMS	climatic material structures
CRCP	continuously reinforced concrete pavement
CRREL	cold regions research and engineering laboratory
DOTD	Louisiana Department of Transportation and Development
EICM	enhanced intergrated climatic model
F_{env}	factor to adjust environmental conditions
FHWA	Federal Highway Administration
ft.	foot (feet)
FWD	falling weight deflectometer
G_s	specific gravity of solids
h	matric suction
ICM	intergrated climatic model
IDModel	infiltration and drainage model
in.	inch(es)
JPCP	jointed plain concrete pavement
K	thermal conductivity
K_{sat}	saturated hydraulic conductivity
LL	liquid limit
LTPP	long term pavement performance
LTRC	Louisiana Transportation Research Center
MEPDG	Mechanistic Empirical Design Guide
M_R	resilient modulus
M_{ROPT}	resilient modulus at optimum moisture content
NCHRP	National Cooperative Highway Research Program
OPT	optimum
PCC	Portland cement concrete
pdf	printable document file
PI	plasticity index
PI	placticity index
Q	heat or thermal capacity
SN_{eff}	in place structural number
S_{opt}	degree of saturation at optimum
SWCC	soil water characteristic curve
TMI	Thorwaite moisture index
w_{opt}	optimum gravimetric moisture content

γ

unit weight

θ

volumetric moisture content

REFERENCES

1. Lekarp, F., Isacsson, U. and Dawson, A. "State of the Art I: Resilient Response of Unbound Aggregates. *Journal of Transportation Engineering*, ASCE, Vol. 126, No. 1, 2000, pp. 76-83.
2. Dempsey, B., W. Herlach, A., and Patel, A. *The Climatic-Material-Structural Pavement Analysis Program*. Publication FHWA-RD-84/115, Vol.3, Final Report. FHWA, U.S. Department of Transportation. Washington D.C, 1985.
3. Lytton, R. L., Pufahl, D., Michalak, C., Liang, H., and Dempsey, K. *An Integrated Model of the Climatic Effects on Pavement*. Report No. FHWA-RD-90-033. Federal Highway Administration, Texas Transportation Institute, Texas A&M University McLean, VA, 1990.
4. Guymon, G. L., Berg, R. and Johnson, T. *Mathematical Model of Frost Heave and Thaw Settlement in Pavement*. Final Report, U. S. Army Cold Region Research and Engineering Laboratory, 1986.
5. Larson, G., and Dempsey, B. *Integrated Climatic Model*, Version 2.0. Report No. DTFA MN/DOT 72114, Newmark Civil Engineering Laboratory, University of Illinois at Urbana-Champaign, IL, 1997.
6. Witczak, M. W., Houston, W., Zapata, C., Richter, C., Larson, G., and Walsh, K. *Improvement of the Integrated Climatic Model for Moisture Content Predictions. Development of the 2002 Guide for the Development of New and Rehabilitated Pavement Structures*, NCHRP 1-37 A, Inter Team Technical Report (Seasonal 4), Tempe, AZ, 2000.
7. Witczak, M. W., Andrei, D., and Houston, W. *Resilient Modulus as Function of Soil Moisture – Summary of Predictive Models. Development of the 2002 Guide for the Development of New and Rehabilitated Pavement Structures*, NCHRP 1-37 A, Inter Team Technical Report (Seasonal 1), Tempe, AZ, 2000.
8. Witczak, M. W., Houston, W., and Andrei, D. *Resilient Modulus as Function of Soil Moisture – A Study of the Expected Changes in Resilient Modulus of the Unbound Layers with Changes in Moisture for 10 LTPP Sites*. Development of the 2002 Guide for the Development of New and Rehabilitated Pavement Structures, NCHRP 1-37 A, Inter Team Technical Report (Seasonal 2), Tempe, AZ, 2000.
9. Witczak, M. W., Houston, W. and Andrei, D. *Selection of Resilient Moduli for Frozen/Thawed Unbound Materials. Development of the 2002 Guide for the Development of New and Rehabilitated Pavement Structures*, NCHRP 1-37 A, Inter Team Technical Report (Seasonal 3), Tempe, AZ, 2000.
10. Houston, W. N., Mirza, M., and Zapata, C. *Environmental Effects in Pavement*

- Mix and Structural Design Systems. Calibration and Validation of the ICM Version 2.6.* NCHRP 9-23 project, Final Report - Part 2, National Cooperative Highway Research Program, 2006.
11. Perera, Y. Y. “Moisture Equilibria Beneath Paved Areas.” Ph.D. Dissertation, Arizona State University, Arizona, U.S.A., May 2003.
 12. Witczak, M. W., Zapata, C. and Houston, W. *Models Incorporated into the Current Enhanced Integrated Climatic Model: NCHRP 9-23 Project Findings and Additional Changes after Version 0.7.* Project NCHRP 1-40D, Final Report, 2006.
 13. Zapata, C.E., Andrei, D., Witczak, M., and Houston, W. “Incorporation of Environmental Effects in Pavement Design.” *International Journal of Road Materials and Pavement Design*, Vol. 8, No. 4, 2007, pp. 667-693.
 14. Schoeneberger, P.J., Wysocki, D., Benham, C. and Broderson, W. *Field Book for Describing and Sampling Soils (Version 1.1, refined, revised, and compiled).* National Soil Survey Center, Natural Resources Conservation Service, U.S. Department of Agriculture, Lincoln, NE., 1998.
 15. US Geological Survey. National Water Information System: Web Interface. <http://nwis.waterdata.usgs.gov/usa/nwis/gw>. Accessed April 24, 2019
 16. Lambe, T. W. and Whitman, R. *Soil Mechanics*, SI Version. Massachusetts Institute of Technology. John Wiley & Sons, 1979.
 17. Cernica, J.N. *Geotechnical Engineering: Soil Mechanics*. John Wiley & Sons, Inc., 1995.
 18. Fredlund, D.G., Xing, A., Fredlund, M., and Barbour, S. “The Relationship of the Unsaturated Shear Strength to the Soil-Water Characteristic Curve.” *Canadian Geotechnical Journal*, Vol. 32, 1995, pp. 440-448.
 19. Williams, P.J. *The Surface of the Earth, An Introduction to Geotechnical Science.* Longman, Inc., New York, 1982.
 20. Leong, E. C., and Rahardjo, H. “A Review on Soil-Water Characteristic Curve Equations.” Geotechnical Research Report, NTU/GT/96-5, Nanyang Technological University, NTU-PWD Geotechnical Research Center, Singapore, 1996.
 21. Zapata, C. E. “Uncertainty in Soil-Water Characteristic Curve and Impacts on Unsaturated Shear Strength Predictions.” Ph.D. Dissertation, Arizona State University, Tempe, AZ. September 1999.
 22. Fredlund, D. G., and Xing, A. “Equations for the Soil-Water Characteristic Curve.” *Canadian Geotechnical Journal*, Volume 31, No. 4, 1994, pp 521-532.
 23. Zapata, C. E., Houston, W., Houston, W., and Walsh, K. “Soil-Water Characteristic Curve Variability”. In C. D. Shackelford, S. L. Houston, and N-Y Chang (eds). *Advances in Unsaturated Geotechnics*. ASCE – GEO Institute

- Geotechnical Special Publication No. 99. Also Proceedings of Sessions of Geo-Denver, Denver, CO, 2000, pp. 84-124.
24. Li, D., and Selig, E. "Resilient Modulus for Fine Grained Subgrade Soils." *ASCE Journal of Geotechnical Engineering*, Vol. 120, No. 6, 1994, pp. 939-957.
 25. Drumm, E. C., Reeves, J., Madgett, M., and Trolinger, W. "Subgrade Resilient Modulus Correction for Saturation Effects." *ASCE Journal of Geotechnical and Geoenvironmental Engineering*, Vol. 123, No. 7, 1997, pp. 663-670.
 26. Rada, G., and Witczak, M. "Comprehensive Evaluation of Laboratory Resilient Moduli Results for Granular Material." In *Transportation Research Record: Journal of the Transportation Research Board*, No. 810, Transportation Research Board of the National Academies, Washington, D.C., 1981, pp. 23-33.
 27. Santha, B. L. "Resilient Modulus of Subgrade Soils: Comparison of Two Constitutive Equations." In *Transportation Research Record: Journal of the Transportation Research Board*, No. 1462, Transportation Research Board of the National Academies, Washington, D.C., 1980, pp. 79-90.
 28. Scott, R.F. *Heat Exchange at the Ground Surface*. U. S. Army Material Command, Cold Regions Research and Engineering Laboratory, Hanover, N. H., 1964.
 29. Berg, R.L. *Energy Balance on Paved Surface*. U. S. Army Terrestrial Sciences Center, Hanover, N.H., 1968.
 30. Baker, D. G., and Haines, D. "Solar Radiation and Sunshine Duration Relationship in the North-Central Region and Alaska." Experiment Station, University of Minnesota, Minneapolis, MN, Technical Bulletin 262, 1969.
 31. Vehrencamp, J. E. "Experimental Investigation of Heat Transfer at Air-Earth Interface." *Transportation*, American Geophysical Union, Washington, D.C., Vol. 34, No. 1, 1953.
 32. Zapata, C. E. *A National Catalog of Subgrade Soil-Water Characteristic Curve (SWCC) Default Inputs and Selected Soil Properties for Use with the MEPDG*. NCHRP 9-23A project, Final Report, National Cooperative Highway Research Program, 2010.
 33. Zapata, C. E., and Cary, C. *Integrating the National Database of Subgrade Soil Water Characteristic-Curves and Soil Index Properties with the MEPDG*. NCHRP 9-23B project, Final Report, National Cooperative Highway Research Program, 2012.
 34. Torres, G. "Estimating the Soil-Water Characteristic Curve Using Grain Size Analysis and Plasticity Index." M.S. Thesis, Arizona State University, Tempe, AZ. May 2011.
 35. Hazen, A. "Discussion of Dams on Sand Foundation." *A.C. Koenig Transactions, ASCE*, Vol. 73, 1911, pp. 199-203.

36. Cary, C. E., and Zapata, C. "Enhanced Model for Resilient Response of Soils Resulting from Seasonal Changes as Implemented in "Mechanistic–Empirical Pavement Design Guide." *In Transportation Research Record: Journal of the Transportation Research Board*, No 2170, Transportation Research Board of the National Academies, Washington, D.C., 2010, pp. 36-44.
37. Cary, C. "Resilient Modulus Testing for Unsaturated Unbound Materials." Master thesis. Arizona State University, Tempe, Arizona, 2008.
38. Cary, C. E., and Zapata, C. "Resilient Modulus Testing for Unsaturated Unbound Materials." *In The Transportation Research Board-Annual Meeting*, Washington, D.C., January 2010. Accepted for presentation in the TRB Annual meeting and for publication in the Annual Meeting DVD.
39. Cary, C. E., and Zapata, C. "Resilient Modulus for Unsaturated Unbound Materials. *International Journal of Road Materials and Pavement Design*," Vol. 12, No 3, Lavoisier, Paris, 2011, pp. 615-638.
40. Witczak M. W., and Uzan, J. "The Universal Airport Design System. Report I of IV: Granular Material Characterization," *Department of Civil Engineering, University of Maryland*, College Park, 1988.
41. Zaghoul, S. N., Gucunski, N., Jackson, H., and Hadidi, R. *Material Characterization and Seasonal Variation in Material Properties*. Report No. FHWANJ-2005-024, New Jersey Department of Transportation, Trenton, NJ, 2006.
42. Li, Q., Wang, K., and Hall, K. "Verification of Virtual Climatic Data in M-EPDG Using the LTPP Database." *In International Journal of Pavement Research and Technology*, Vol. 1, No. 1, Chinese Society of Pavement Engineering, Taiwan, 2010, pp. 10-15.
43. Breakah, T. M., Williams, R., Herzmann, D., and Takle, E. "Effects of Using Accurate Climatic Conditions for Mechanistic-Empirical Pavement Design." *ASCE Journal of Transportation Engineering*, Vol. 137, No. 1, 2011, pp. 84-90.
44. Rabab'ah, S., and Liang, R. "Field and Laboratory Evaluation of Cement Treated Permeable Base". *In The Transportation Research Board-Annual Meeting*, Washington, D.C., January 2007. Annual Meeting CD-Room.
45. Kim, D., Nantung, T., Siddiki, N., and Kim, J. "Implementation of the New Mechanistic-Empirical Design for Subgrade Materials – Indiana Experience." *In The Transportation Research Board-Annual Meeting*, Washington, D.C., January 2007. Annual Meeting CD-Room.
46. Lee, A. and Gaspard, K. NCHRP Soil Properties of Louisiana GIS Web Application, Louisiana Transportation Research Center,
<http://ladotd.maps.arcgis.com/apps/webappviewer/index.html?id=55c09f56253045e4>

- 9c36f99c41409add%20, Accessed: April 24, 2019.
47. AASHTO T307-99, "Standard Method of Test for Determining the Resilient Modulus of Soils and Aggregate Materials." American Association of State Highway and Transportation Officials, Washington DC. 2003.
 48. Witczak, M. "Harmonized Test Methods for Laboratory Determination of Resilient Modulus for Flexible Pavement Design," NCHRP 1-28A, 2003.
 49. Dynatest ELMOD 6, <https://www.dynatest.com/elmod-software>, 2016.
 50. Mohammad, L., Gaspard, K., Herath, A., and Nazzal, M. "Comparative Evaluation of Subgrade Resilient Modulus from Non-destructive, In-situ, and Laboratory Methods," Louisiana Transportation Research Center, Report FHWA/LA/06/417, 2016.
 51. Gaspard, K., Zhang, Z., Abufarsakh, M., Gautreau, G., Hanifa, K., and Zapata, C. "Modeling the In-situ Seasonal Variation Potential of Resilient Modulus in Subgrade Soils," *Advances in Civil Engineering*, <https://doi.org/10.1155/2019/1793601>, Accessed March 20, 2019.
 52. Abu-Farsakh, M., Mehrotra, A., Mohammad, L., and Gaspard, K. "Incorporating the Effect of Moisture Variation on Resilient Modulus for Unsaturated Fine-Grain Subgrade Soils," *Transportation Research Record: Journal of the Transportation Research Board*, 2015.

APPENDIX A

Table 12
Shelby tube soil data for LA 1; Site 1-1

Depth (ft.)	% passing # 200 sieve	Opt. MC %	Max. density (pcf)	LL	PL	PI	AASHTO Class.	USCS Class.
0-3	60	14.8	112.0	31	19	12	A-2-6	(CL)
3-6	98	25.0	97.0	84	30	54	A-7-5	(OH)
6-9	97	22.0	97.0	67	20	47	A-7-6	(OH)
9-12	79	17.0	110.0	34	19	15	A-6	(CL)
12-15	91	16.2	109.0	34	20	14	A-6	(CL)
15-18	98	24.0	97.2	63	19	44	A-7-6	(CH)
18-21	98	23.5	91.7	81	34	47	A-7-5	(CH)
21-24	99	31.0	87.0	87	26	61	A-7-5	(CH)

Table 13
Shelby tube soil data for US 171; Site 1-2

Depth (ft.)	% passing # 200 sieve	Opt. MC %	Max. density (pcf)	LL	PL	PI	AASHTO Class.	USCS Class.
0-3	62	N/A	N/A	19	15	4	A-4(0)	(CL-ML)
3-6	63	N/A	N/A	32	15	17	A-6(8)	(CL)
6-9	95	N/A	N/A	52	17	34	A-7-6(35)	(CH)
9-12	99	N/A	N/A	65	24	41	A-7-6(47)	(CH)
12-15	98	N/A	N/A	71	24	47	A-7-6(53)	(CH)
15-18	88	N/A	N/A	49	10	39	A-7-6(34)	(CL)
18-21	83	N/A	N/A	52	20	32	A-7-6(27)	(CH)
21-24	75	N/A	N/A	50	22	28	A-7-6(21)	(CH)

Table 14
Shelby tube soil data for LA 2, Site 2-4

Depth (ft.)	% passing # 200 sieve	Opt. MC %	Max. density (pcf)	LL	PL	PI	AASHTO Class.	USCS Class.
0-3	32	15.6	112.60	26	18	8	A-4(0)	(SC)
3-6	88	24.0	99.40	86	28	58	A-7-6(16)	(CH)
6-9	N/A	N/A	N/A	N/A	N/A	N/A	N/A	N/A
9-12	98	32.0	93.20	94.00	32.00	62.00	A-7-6(16)	(OH)
12-15	N/A	N/A	N/A	N/A	N/A	N/A	N/A	N/A
15-18	N/A	N/A	N/A	N/A	N/A	N/A	N/A	N/A
18-21	92	29.0	93.60	100.00	31.00	69.00	A-7-5(53)	(OH)
21-24	91	29.4	96.40	94.00	28.00	66.00	A-7-6(32)	(OH)

Table 15
Shelby tube soil data for US 165; Site 2-5

Depth (ft.)	% passing # 200 sieve	Opt. MC %	Max. density (pcf)	LL	PL	PI	AASHTO Class.	USCS Class.
0-3	64	12.0	120.5	22	14	8	A-4(2)	(CL)
3-6	55	12.N/A0	121.5	20	15	5	A-4(0)	(CL-ML)
6-9	10	N/A	N/A	N/A	N/A	N/A	N/A	N/A
9-12	61	16.5	123.0	26	15	11	A-6(4)	(CL)
12-15	51	19.2	111.5	38	15	23	A-6(8)	(CL)
15-18	72	17.5	108.2	35	16	19	A-6(12)	(CL)
18-21	83	24.0	104.0	48	17	31	A-7-6(26)	(CL)
21-24	70	10	N/A	27	15	12	A-6(6)	(CL)

Table 16
Shelby tube soil data for US 84; Site 3-8

Depth (ft.)	% passing # 200 sieve	Opt. MC %	Max. density (pcf)	LL	PL	PI	AASHTO Class.	USCS Class.
0-3	63	13.3	115.5	35	20	15	A-6(7)	(CL)
3-6	87	N/A	N/A	51	21	30	A-7-6(28)	(CH)
6-9	68	14.8	111.7	32	18	14	A-6(7)	(CL)
9-12	90	22.4	98.8	52	18	34	A-7-6(32)	(CH)
12-15	99	29.7	90.0	86	27	59	A-7-6(69)	(CH)
15-18	97	30.1	89.4	85	29	56	A-7-6(64)	(CH)
18-21	98	31.2	88.2	92	30	62	A-7-5(72)	(OH)
21-24	99	30.7	87.6	97	45	52	A-7-6(66)	(OH)

Table 17
Shelby tube soil sample from LA 13; Site 4-12

Depth (ft.)	% passing # 200 sieve	Opt. MC %	Max. density (pcf)	LL	PL	PI	AASHTO Class.	USCS Class.
0-3	63	16.00	111.0	27	24	3	A-4(0)	(OL)
3-6	68	13.60	115.9	44	18	26	A-7-6(16)	(CL)
6-9	98	17.60	106.6	46	17	29	A-7-6(30)	(OL)
9-12	94	21.00	106.0	45	18	27	A-7-6(27)	(CL)
12-15	94	22.00	102.0	47	19	28	A-7-6(28)	(OL)
15-18	95	20.10	105.4	55	21	34	A-7-6(36)	(OH)
18-21	93	24.00	99.5	53	22	31	A-7-6(32)	(OH)
21-24	99	21.10	103%	36	23	13	A-6(4)	(OL)

Table 18
Shelby tube soil data for US 61; Site 4-13

Depth (ft.)	% passing # 200 sieve	Opt. MC %	Max. density (pcf)	LL	PL	PI	AASHTO Class.	USCS Class.
0-3	93	17.1	108.5	34	22	12	A-6(11)	(CL)
3-6	83	15.2	112.2	29	19	10	A-4(7)	(CL)
6-9	83	16.0	110.5	35	18	17	A-6(13)	(CL)
9-12	59	13.7	106.0	29	14	15	A-6(6)	(CL)
12-15	46	N/A	N/A	20	12	8	A-4(0)	(SC)
15-18	36	N/A	N/A	28	13	15	A-6(1)	(SC)
18-21	10	N/A	N/A	23	13	10	A-2-4(0)	(SP-SC)
21-24	12	N/A	N/A	14	14	0	A-1-b(0)	(SP-SM)

APPENDIX B

Table 19
NCHRP soil unit data for LA 1; Site 1-1

	Top Layer	Layer 2	Layer 3
AASHTO Classification:	A-4	A-6	A-7-6
AASHTO Group Index:	0	8	22
Top Depth (in):	0.0	9.1	35.8
Bottom Depth (in):	9.1	35.8	70.1
Thickness (in):	9.1	26.8	34.3
% Component:	35	35	35
Water Table Depth (ft):	2.00	2.00	2.00
Depth of Bedrock (ft):	N/A	N/A	N/A
CBR	29.7	9.4	4.5
M_R (psi)	22,365	10,711	6,648
Passing #4 %	100.0	100.0	100.0
Passing #10 %	100.0	100.0	100.0
Passing #40%	92.5	95.0	90.0
Passing #200 %	70.0	80.0	72.5
Passing 0.002 mm	15.0	26.5	50.0
LL	20.0	30.0	53.5
PI	3.0	12.0	30.0
Saturated volumetric Moisture content (%)	41	40	45
Saturated hydraulic conductivity (ft/hr.)	0.09169	0.03334	0.00250

Table 20
NCHRP soil unit data for US 171; Site 1-2

	Top Layer	Layer 2	Layer 3
AASHTO Classification:	A-4	A-6	A-7-6
AASHTO Group Index:	0	8	22
Top Depth (in):	0.0	9.1	35.8
Bottom Depth (in):	9.1	35.8	70.1
Thickness (in):	9.1	26.8	34.3
% Component:	35	35	35
Water Table Depth (ft):	2.00	2.00	2.00
Depth of Bedrock (ft):	N/A	N/A	N/A
CBR	29.7	9.4	4.5
M _R (psi)	22,365	10,711	6,648
Passing #4 %	100.0	100.0	100.0
Passing #10 %	100.0	100.0	100.0
Passing #40%	92.5	95.0	90.0
Passing #200 %	70.0	80.0	72.5
Passing 0.002 mm	15.0	26.5	50.0
LL	20.0	30.0	53.5
PI	3.0	12.0	30.0
Saturated volumetric Moisture content (%)	41	40	45
Saturated hydraulic conductivity (ft/hr.)	0.09169	0.03334	0.00250

Table 21
NCHRP soil unit data for US 171; Site 1-3

	Top Layer	Layer 2	Layer 3
AASHTO Classification:	A-4	A-6	A-4
AASHTO Group Index:	0	9	5
Top Depth (in):	0.0	22.8	46.1
Bottom Depth (in):	22.8	46.1	79.9
Thickness (in):	22.8	23.2	33.9
% Component:	50	50	50
Water Table Depth (ft):	0.75	0.75	0.75
Depth of Bedrock (ft):	N/A	N/A	N/A
CBR	25.2	8.9	13.0
Mr (psi)	20,157	10,353	13,220
Passing #4 %	100.0	100.0	100.0
Passing #10 %	100.0	100.0	100.0
Passing #40%	97.5	97.0	97.5
Passing #200 %	77.5	85.0	72.5
Passing 0.002 mm	16.0	27.5	27.5
LL	21.0	31.0	27.5
PI	3.5	12.0	9.0
Saturated volumetric Moisture content (%)	40	40	40
Saturated hydraulic conductivity (ft/hr.)	0.10836	0.01084	0.01084

Table 22
NCHRP soil unit data for LA 2; Site 2-4

	Top Layer	Layer 2	Layer 3	Layer 4
AASHTO Classification:	A-4	A-4	A-7-6	A-6
AASHTO Group Index:	0	0	20	8
Top Depth (in):	0.0	5.1	9.1	40.9
Bottom Depth (in):	5.1	9.1	40.9	79.9
Thickness (in):	5.1	3.9	31.9	39.0
% Component:	37	37	37	37
Water Table Depth (ft):	3.00	3.02	3.02	3.02
Depth of Bedrock (ft):	N/A	N/A	N/A	N/A
CBR	38.4	29.0	4.8	8.8
Mr (psi)	26,365	22,061	6,939	10,289
Passing #4 %	87.5	87.5	92.5	92.5
Passing #10 %	87.5	87.5	92.5	92.5
Passing #40%	65.0	67.5	85.0	82.5
Passing #200 %	37.5	43.5	67.5	62.5
Passing 0.002 mm	12.5	13.5	47.5	27.5
LL	20.0	22.5	57.5	36.5
PI	3.5	5.0	30.0	16.5
Saturated volumetric Moisture content (%)	41	38	45	43
Saturated hydraulic conductivity (ft/hr.)	0.10836	0.10836	0.01084	0.03334

Table 23
NCHRP soil unit data for US 165; Site 2-5

	Top Layer	Layer 2	Layer 3	Layer 4
AASHTO Classification:	A-1-b	A-7-6	A-7-6	A-6
AASHTO Group Index:	0	6	5	2
Top Depth (in):	0.0	14.2	35.0	59.8
Bottom Depth (in):	14.2	35.0	59.8	81.1
Thickness (in):	14.2	20.9	24.8	21.3
% Component:	17	17	17	17
Water Table Depth (ft):	N/A	N/A	N/A	N/A
Depth of Bedrock (ft):	N/A	N/A	N/A	N/A
CBR	55.0	8.8	9.7	15.4
Mr (psi)	33,201	10,268	10,969	14,708
Passing #4 %	67.5	77.5	55.0	87.5
Passing #10 %	55.0	70.0	47.5	82.5
Passing #40%	50.0	62.5	45.0	77.5
Passing #200 %	20.0	45.0	40.0	42.5
Passing 0.002 mm	8.5	47.5	47.5	25.0
LL	15.0	50.0	50.0	25.5
PI	2.5	23.0	23.0	12.5
Saturated volumetric Moisture content (%)	26	39	29	35
Saturated hydraulic conductivity (ft/hr.)	1.08358	0.10836	0.0334	0.0334

Table 24
NCHRP soil unit data for LA 34; Site 2-6

	Top Layer	Layer 2	Layer 3
AASHTO Classification:	A-4	A-6	A-4
AASHTO Group Index:	0	5	5
Top Depth (in):	0.0	11.0	28.0
Bottom Depth (in):	11.0	28.0	68.1
Thickness (in):	11.0	16.9	40.2
% Component:	55	55	55
Water Table Depth (ft):	1.74	1.74	1.74
Depth of Bedrock (ft):	N/A	N/A	N/A
CBR	44.3	11.2	
Mr (psi)	28,928	12,013	12,591
Passing #4 %	99.0	99.0	97.0
Passing #10 %	95.0	95.0	95.0
Passing #40%	80.0	90.0	80.0
Passing #200 %	47.5	60.0	55.0
Passing 0.002 mm	9.5	25.0	25.0
LL	20.0	31.5	33.0
PI	2.0	13.0	13.0
Saturated volumetric Moisture content (%)	37	N/A	N/A
Saturated hydraulic conductivity (ft/hr.)	0.10836	0.10836	0.03334

Table 25
NCHRP soil unit data for US 65; Site 3-7

	Top Layer	Layer 2	Layer 3
AASHTO Classification:	A-7-6	A-7-5	A-7-6
AASHTO Group Index:	42	47	35
Top Depth (in):	0.0	9.1	42.1
Bottom Depth (in):	9.1	42.1	59.8
Thickness (in):	9.1	33.1	17.7
% Component:	97	97	97
Water Table Depth (ft):	1.02	1.02	1.02
Depth of Bedrock (ft):	N/A	N/A	N/A
CBR	2.8	10.3	32.1
Mr (psi)	4,966	11,385	23,518
Passing #4 %	100.0	100.0	100.0
Passing #10 %	100.0	100.0	100.0
Passing #40%	100.0	100.0	100.0
Passing #200 %	97.5	97.5	97.5
Passing 0.002 mm	50.0	75.0	57.5
LL	65.5	70.5	58.5
PI	36	40.0	30.5
Saturated volumetric Moisture content (%)	46	46	43
Saturated hydraulic conductivity (ft/hr.)	0.00250	0.10836	0.01084

Table 26
NCHRP soil unit data for US 84; Site 3-8

	Top Layer	Layer 2	Layer 3	Layer 4
AASHTO Classification:	A-7-6	A-7-6	A-7-6	A-6
AASHTO Group Index:	24	6	0	6
Top Depth (in):	0.0	9.1	18.1	39.0
Bottom Depth (in):	9.1	18.1	39.0	85.0
Thickness (in):	9.1	9.0	20.9	46.1
% Component:	39	40	40	40
Water Table Depth (ft):	1.02	1.02	1.02	1.02
Depth of Bedrock (ft):	N/A	N/A	N/A	N/A
CBR	4.6	10.3	4.1	5.6
Mr (psi)	6,797	11,385	6,304	7,735
Passing #4 %	100.0	97.5	97.5	97.5
Passing #10 %	100.0	97.5	97.5	97.5
Passing #40%	100.0	97.5	97.5	95.0
Passing #200 %	97.5	95.0	41.0	75.0
Passing 0.002 mm	33.0	47.5	50.0	34.0
LL	45.0	63.0	25.0	40.0
PI	21.5	35.0	25.0	22.5
Saturated volumetric Moisture content (%)	40	44	43	43
Saturated hydraulic conductivity (ft/hr.)	0.01084	0.00250	0.01084	0.010836

Table 27
NCHRP soil unit data for US 71; Site 3-9

	Top Layer	Layer 2	Layer 3
AASHTO Classification:	A-7-6	A-7-5	A-7-6
AASHTO Group Index:	42	47	35
Top Depth (in):	0.0	9.1	42.1
Bottom Depth (in):	9.1	42.1	59.8
Thickness (in):	9.1	33.1	17.7
% Component:	42	42	42
Water Table Depth (ft):	1.02	1.02	1.02
Depth of Bedrock (ft):	N/A	N/A	N/A
CBR	2.8	2.6	3.3
Mr (psi)	4,966	4,653	5,498
Passing #4 %	100.0	100.0	100.0
Passing #10 %	100.0	100.0	100.0
Passing #40%	100.0	100.0	100.0
Passing #200 %	97.5	97.5	97.5
Passing 0.002 mm	50.0	75.0	57.5
LL	65.5	70.5	58.5
PI	36.0	40.0	30.5
Saturated volumetric Moisture content (%)	46	46	43
Saturated hydraulic conductivity (ft/hr.)	0.00250	0.00250	0.01084

Table 28
NCHRP soil unit data for LA 1; Site 3-10

	Top Layer	Layer 2	Layer 3
AASHTO Classification:	A-7-6	A-6	A-6
AASHTO Group Index:	19	16	11
Top Depth (in):	0.0	9.8	35.8
Bottom Depth (in):	9.8	35.8	59.8
Thickness (in):	9.8	26.0	24.0
% Component:	39	39	39
Water Table Depth (ft):	2.76	2.76	2.76
Depth of Bedrock (ft):	N/A	N/A	N/A
CBR	5.6	6.0	8.1
Mr (psi)	7,675	8,064	9,731
Passing #4 %	100.0	100.0	100.0
Passing #10 %	100.0	100.0	100.0
Passing #40%	100.0	100.0	100.0
Passing #200 %	95.0	92.5	87.5
Passing 0.002 mm	33.0	26.5	26.5
LL	41.0	38.5	34.0
PI	18.0	17.0	13.0
Saturated volumetric Moisture content (%)	40	41	41
Saturated hydraulic conductivity (ft/hr.)	0.03334	0.03334	0.09169

Table 29
NCHRP soil unit data for US 171; Site 4-11

	Top Layer	Layer 2
AASHTO Classification:	A-4	A-6
AASHTO Group Index:	1	9
Top Depth (in):	0.0	29.9
Bottom Depth (in):	29.9	79.9
Thickness (in):	29.9	50.0
% Component:	33	33
Water Table Depth (ft):	1.02	1.02
Depth of Bedrock (ft):	N/A	N/A
CBR	24.2	8.9
Mr (psi)	19,623	10,381
Passing #4 %	100.0	100.0
Passing #10 %	100.0	100.0
Passing #40%	97.5	92.5
Passing #200 %	82.5	70.0
Passing 0.002 mm	20.5	26.5
LL	21.0	35.0
PI	3.5	14.5
Saturated volumetric Moisture content (%)	40	40
Saturated hydraulic conductivity (ft/hr.)	0.10836	0.01084

Table 30
NCHRP soil unit data for LA 13; Site 4-12

	Top Layer	Layer 2	Layer 3
AASHTO Classification:	A-4	A-7-6	A-6
AASHTO Group Index:	3	19	13
Top Depth (in):	0.0	16.9	48.8
Bottom Depth (in):	16.9	48.8	72.0
Thickness (in):	16.9	31.9	23.2
% Component:	42	42	42
Water Table Depth (ft):	1.02	1.02	1.02
Depth of Bedrock (ft):	N/A	N/A	N/A
CBR	14.9	5.6	6.9
Mr (psi)	14,416	7,702	8,775
Passing #4 %	100.0	100.0	100.0
Passing #10 %	97.5	100.0	97.5
Passing #40%	95.0	97.5	95.0
Passing #200 %	85.0	85.0	82.5
Passing 0.002 mm	17.5	45.0	32.5
LL	22.5	49.5	37.5
PI	6.5	20.0	16.5
Saturated volumetric Moisture content (%)	44	47	46
Saturated hydraulic conductivity (ft/hr.)	0.03334	0.00250	0.00250

Table 31
NCHRP soil unit data for US 61; Site 4-13

	Top Layer	Layer 2	Layer 3
AASHTO Classification:	A-4	A-7-6	A-6
AASHTO Group Index:	3	20	11
Top Depth (in):	0.0	9.1	22.8
Bottom Depth (in):	9.1	22.8	77.2
Thickness (in):	9.1	13.8	54.3
% Component:	42	42	42
Water Table Depth (ft):	N/A	N/A	N/A
Depth of Bedrock (ft):	N/A	N/A	N/A
CBR	16.8	5.1	9.1
Mr (psi)	15,559	7,209	10,483
Passing #4 %	100.0	100.0	100.0
Passing #10 %	100.0	100.0	100.0
Passing #40%	100.0	100.0	100.0
Passing #200 %	95.0	95.0	95.0
Passing 0.002 mm	15.0	27.5	18.5
LL	22.5	41.5	35.0
PI	5.0	20.0	10.5
Saturated volumetric Moisture content (%)	44	N/A	N/A
Saturated hydraulic conductivity (ft/hr.)	0.10836	0.10836	0.10836

Table 32
NCHRP soil unit data for LA 21; Site 4-14

	Top Layer	Layer 2	Layer 3
AASHTO Classification:	A-5	A-6	A-2-5
AASHTO Group Index:	0	4	0
Top Depth (in):	0.0	9.1	53.1
Bottom Depth (in):	9.1	53.1	79.9
Thickness (in):	9.1	44.1	26.8
% Component:	27	27	27
Water Table Depth (ft):	2.00	2.00	2.00
Depth of Bedrock (ft):	N/A	N/A	N/A
CBR	17.6	12.9	19.0
Mr (psi)	16,028	13,127	16,842
Passing #4 %	97.5	95.0	97.5
Passing #10 %	97.5	90.0	95.0
Passing #40%	77.5	82.5	72.5
Passing #200 %	37.5	57.5	22.5
Passing 0.002 mm	12.0	26.5	12.0
LL	N/A	28.5	N/A
PI	0.0	11.5	0.0
Saturated volumetric Moisture content (%)	41	N/A	N/A
Saturated hydraulic conductivity (ft/hr.)	0.33341	0.10836	0.91688

This public document is published at a total cost of \$250. 42 copies of this public document were published in this first printing at a cost of \$250. The total cost of all printings of this document including reprints is \$250. This document was published by Louisiana Transportation Research Center to report and publish research findings as required in R.S. 48:105. This material was duplicated in accordance with standards for printing by state agencies established pursuant to R.S. 43:31. Printing of this material was purchased in accordance with the provisions of Title 43 of the Louisiana Revised Statutes.